

FMH606 Master's Thesis 2018

Process Technology

Pyrolysis of plastic waste into green fuels – experimental study

Alireza Hassani

Faculty of Technology, Natural sciences and Maritime Sciences
Campus Porsgrunn

Course: FMH606 Master's Thesis, 2018

Title: Pyrolysis of plastic waste into green fuels – experimental study

Number of pages: 86

Keywords: Catalytic pyrolysis, waste plastic, LDPE, Gasoline-range hydrocarbons, ZSM-5 catalyst, Experimental design, Process development

Student: Alireza Hassani

Supervisor: Prof. Lars-Andre Tokheim

External partner: Norner AS (Dr. Siw Fredriksen, Dr. Muhammad Bashir and Kai Arne Sætre)

Availability: <Open/Confidential>

Summary:

Recycling of plastic waste in more environmental friendly ways is under great attention. Catalytic pyrolysis of plastic waste is among the sustainable methods that can recover valuable products from plastics. However, this method faces challenges due to complex nature of plastics and complex catalytic kinetics. Therefore, this experimental work aimed at utilization of an improved semi-batch reactor to evaluate recovery of valuable products from LDPE through catalytic pyrolysis over ZSM-5 catalyst. Experimental design employed to evaluate the improved set-up and yield of resulted gases and liquids at different catalyst loadings and temperature. TGA used to simulate polymer degradation in presence and absence of catalyst and catalyst screening. The obtained product further analyzed by gas chromatography and FTIR to identify different groups of hydrocarbons in products. Thermal pyrolysis resulted mostly waxes that contained heavy olefinic C_{20+} . Addition of ZSM-5 significantly improved the gas yield which was containing noticeable amount of olefin monomers (ethylene and propylene). On the other hand, ZSM-5 upgraded the liquid product to gasoline ranged fuel (C_5-C_{12}) rich in aromatic. Both increasing temperature and increasing ratio of catalyst was associated with production of light gases. At the same time effect of catalyst loading was more sensible at lower temperature. However, utilization of semi-batch reactor is not a good option as there is no proper control on residence time of products, and therefore, less contact between reactant and catalyst resulted.

Preface

This thesis work title:” *Pyrolysis of plastic waste to environmental friendly fuel - experimental study*” is done to fulfill a master’s degree in process Technology at University of South-Eastern Norway. The thesis is part of four-year research program that investigates the efficient and sustainable recovery of plastic waste based on circular economy leading by Norner AS.

Experimental work shaped foundation of this thesis which have been performed in lab facilities at Norner AS to evaluate a dedicated set-up for pyrolysis and assess catalytic pyrolysis of LDPE over ZSM-5. For me it was a unique experience to be part of this research institute with many knowledgeable and experienced researchers which taught me valuable lessons.

I would like to thank my supervisor Prof. Lars-Andre Tokheim for his great support and guidance thought my work. I would like also to express my appreciation to Dr. Fredriksen, Dr. Muhammad Bashir and Kai Arne sætre for their never-ending help, consultation and encouragement. This thesis would not have been a proceeded without the help of Norner staffs at NornerAS. I extend my gratitude to Knut Fosse, Kjærsti Lindvig, Ingeborg Wik, Charlotte Waag, Steffen Anfinsen, Svein Nenseth, Tore Dreng and Jostein Mathiessen. Thank you all for guidance and training on the use of all the equipment provided by Norner AS for this thesis. In the end, I sincerely wish to appreciate my parents for their infinite love and support at all stages of my life.

Porsgrunn, 13 May 2018

Alireza Hassani

Contents

1	Introduction	7
2	Literature review	11
2.1	Overview of polyolefin waste	11
2.2	Overview of pyrolysis of plastic waste	12
2.2.1	<i>Main operating factor: Temperature</i>	<i>14</i>
2.2.2	<i>Overview of polymer degradation mechanism</i>	<i>15</i>
2.2.3	<i>Kinetic study of degradation using thermogravimetric analysis.....</i>	<i>17</i>
2.3	Identification of catalysts used in pyrolysis	19
2.3.1	<i>Overview of catalytic cracking.....</i>	<i>19</i>
2.3.2	<i>Heterogeneous zeolite acid catalyst.....</i>	<i>21</i>
2.3.3	<i>Mesoporous and nano-zeolite catalyst.....</i>	<i>23</i>
2.3.4	<i>Other notable catalysts utilized for pyrolysis</i>	<i>24</i>
2.3.5	<i>Deactivation and regeneration of catalyst.....</i>	<i>24</i>
2.4	Recovery of valuable hydrocarbons from catalytic pyrolysis of polyolefins.....	25
2.4.1	<i>Upgrading of PtL to specific range of fuels</i>	<i>25</i>
2.4.2	<i>Recovery of olefin monomer.....</i>	<i>27</i>
2.4.3	<i>Thermo-catalytic recovery of post-consumer packaging waste.....</i>	<i>29</i>
3	Development of bench-scale apparatus and experimental procedure.....	31
3.1	Material	31
3.2	Semi-batch reactor for in-situ catalytic pyrolysis	32
3.2.1	<i>Heating method</i>	<i>33</i>
3.2.2	<i>Preliminary evaluation of temperature measurement.....</i>	<i>34</i>
3.3	Methods	36
3.3.1	<i>Experimental procedure.....</i>	<i>36</i>
3.3.2	<i>Experimental design and procedure.....</i>	<i>37</i>
3.3.3	<i>Thermogravimetric analysis of LDPE degradation at various conditions</i>	<i>38</i>
3.3.4	<i>Gas chromatography analysis.....</i>	<i>39</i>
3.3.5	<i>Fourier-transform infrared spectroscopy.....</i>	<i>40</i>
4	Result and discussion of pyrolysis	41
4.1	TGA analysis	41
4.1.1	<i>Effect of heating rate on thermal degradation and catalytic degradation</i>	<i>41</i>
4.1.2	<i>Effect of processing and appearance on LDPE degradation</i>	<i>44</i>
4.1.3	<i>Effect of catalyst loading on degradation of LDPE</i>	<i>45</i>
4.1.4	<i>Screening activated and spent catalysts.....</i>	<i>46</i>
4.2	Experimental design and optimization of products	49
4.2.1	<i>Effect of process conditions on yield of products</i>	<i>50</i>
4.2.2	<i>Effect of process conditions on coke deposition.....</i>	<i>53</i>
4.3	Effect of temperature and catalyst ratio on product distribution	54
4.3.1	<i>Analysis of liquid products.....</i>	<i>54</i>
4.3.2	<i>Analysis of gaseous products.....</i>	<i>56</i>
4.3.3	<i>Identification of functional groups in liquid products</i>	<i>57</i>
4.4	Reproducibility of result and sources of error	59
5	Conclusion and proposal for future experimental work.....	62

Nomenclature

LDPE	Low density polyethylene
MPW	Municipal plastic waste
MSW	Municipal solid waste
PP	Polypropylene
PE	Polyethylene
NRC	Research council of Norway
FTIR	Fourier-transform infrared spectroscopy
DOE	Design of experiment
GC	Gas chromatography
MS	Mass spectrometer
HDPE	High-density polyethylene
PVC	Polyvinyl chloride
PET	Polyethylene terephthalate
PS	Polystyrene
AC	Alternating electric current
P/C	Polymer to catalyst ratio
TG	Thermogravimetric weight loss curve
DTG	Weight loss derivative curve
LHV	Low heating value

1 Introduction

In this chapter background, problem statement, objectives of study, and organization of report is discussed.

1.1 Background

Consumption of plastics have been increased dramatically from their early commercialization in the 1930s and 1940s. The worldwide production of plastic resins increased by 620% from 1975 to 2012. The reported rate of plastic resins production was 335 million tons in 2016. Presence of municipal plastic wastes (MPW) in municipal solid wastes (MSW) is approximately 10-15% globally. In Europe 39% of produced plastics is converted to products with short life span in packaging sector. Accordingly, 50.9 % of total plastic wastes accounted for packaging wastes in 2015. Various types of polypropylene (PP) and polyethylene (PE), regarded as polyolefins, are dominant materials in all plastic waste stream, specially packaging waste [1-4].

Plastics are still having high value at the end of their life span. Taking this fact into account, The European Commission adopted an EU Action Plan for a circular economy in December 2015. The plan sets plastics as a key priority and committed to ensure that all post consumed plastic packaging will be recycled and reused by 2030. It targets a new plastic economy which determine the design and production of plastics and plastic products with respect to reuse and recycling in a more sustainable way [2].

Figure 1.1 illustrates pathway for recycling of plastic material by considering circular economy. Sustainable recycling pathways are based on converting packaging plastic wastes to feedstock through thermochemical routes including pyrolysis and gasification. Alternatively, mechanical pathways can generate new raw materials by re-granulating of clean waste. If it is not possible to re-use or recycle the plastic wastes, energy can be recovered from wastes by using their high calorific value through incineration. Landfilling should be avoided at all costs as a nonefficient method which have numerous environmental disadvantages [5].

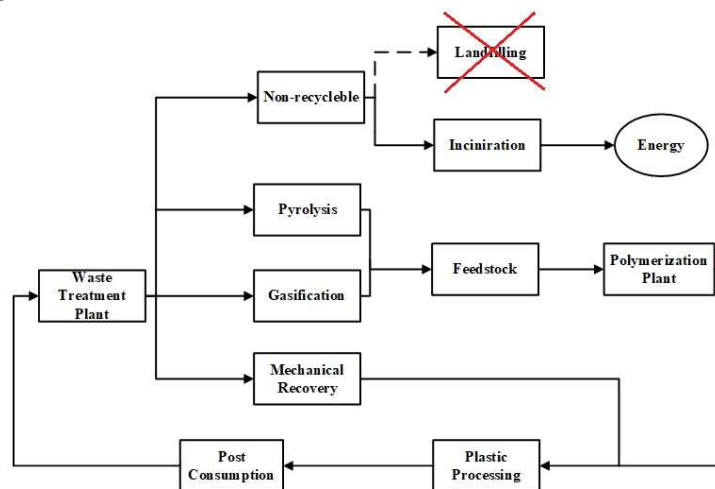


Figure 1.1: Suggested pathway for recovery of plastic waste with respect to principle of circular economy

Pyrolysis is an efficient process which can directly degrade plastic materials to various viable products such as monomer, diesel, gasoline and intermediate products as a feed for petrochemical industry. Unlike biomass, no oxygen exists in the molecular structure of PE and PP which are the most dominant components in waste stream. On the other hand, pyrolysis process degrades long chain molecules in the absence of oxygen to smaller molecules.[6] Therefore, the carbon efficiency significantly arises through this thermochemical path. Additionally, in pyrolysis process there is no emission of toxic and environmentally harmful substances. It is gaining popularity in recent years as an alternative technique to convert wastes rather than incineration and landfilling.

Current work is part of Norwegian research program called “FuturePack” which is being conducted by Norner company. The project is funded by the research council of Norway (NRC) and 13 industrial partners. The general agenda of project is to establish sustainable plastic packaging design through utilizing more bio-based and recycled material with focus on circular economy. Building blocks of polymers which is regarded as monomers can be recycled by using pyrolysis. Accordingly, one of the sub-objectives of this project is to recover green fuel and/or raw feedstock for polymerization from packaging wastes through pyrolysis process.

1.2 Problem statement

Pyrolysis process is gaining attention as promising technique for treatment of MPW. Yet implementation of pyrolysis in large scale faces many challenges that should be addressed by researchers. Plastic-derived pyrolytic product is very complex which make it challenging to consume as fuel for transportation proposes and as a feed for petrochemical industry. Hence desirable products can be obtained through use of catalyst to modify reaction courses.

Catalytic pyrolysis process is an efficient way of converting polymeric waste to valuable products. It has synergic effect which can considerably decrease cost of establishing a future continues pyrolysis process. However, adding catalyst to the process change the route of degradation of macromolecules compared to only thermal process. Also, different types of catalysts result in selectivity of specific range of hydrocarbons presented in products. Additionally, each type of catalyst and their ratio to feed, contributes to both different ranges of products at different process conditions. Due to wide range of molecular weight of both fed polymers and various products, it is quite challenging to develop a kinetics model for catalytic pyrolysis. The costs that is associated with supply, pre-treatment and regeneration of catalyst is high. Many researches have been conducted globally to overcome this challenge both for scale-up proposes and making pyrolysis process feasible.

Most of the plastic pyrolysis research have been conducted in bench-scale with focus on mapping yields of desired products at various operational conditions. There is lack of considering life cycle assessment measures in their process development. Power consumption is a considerable operational cost of pyrolysis process as plastics undergo degradation at elevated temperatures. This fact becomes more critical when it comes to degradation of PE and PP due to their low heat conductivity. Accordingly, utilization of novel heating methods and their evaluation in new established set-up should also be considered.

Similarly, Norner met similar challenge in development of a new pyrolysis experimental set-up. They used muffle oven technology as heating source for pyrolysis process. Outcome showed a significant uncertainty regarding measuring the pyrolysis temperature as there was uneven temperature distribution in oven medium. On the other hand, eight different feeds compositions along with three different catalyst, have been tested at fixed temperature during previous work. It is almost impossible to judge the maturity and reproducibility of process as different results, due to different feeds, are expected. Hence the pyrolysis experiment conducted only with one grade of polymer and solely one catalyst in present work.

1.3 Objectives of the study

The Principle objective of this report is “**Utilization of improved bench-scale pyrolysis process to assess recovery of valuable products from LDPE through thermal and catalytic paths.**” The main objective can be fulfilled by giving answers to a number of key questions that are of either theoretical or experimental nature:

Theoretical:

- What are the advantageous of using catalytic pyrolysis over thermal pyrolysis?
- How catalytic pyrolysis upgrade products obtained from thermal pyrolysis?
- What are the catalysts that have been utilized for catalytic pyrolysis of plastic waste?
- What are the main challenges associated with use of catalyst in pyrolysis?
- How pyrolytic products can be upgraded by using Catalyst?

Experimental:

- How induction heating can benefit pyrolysis process?
- What is the most accurate way of measuring the melt temperature of polymers inside reactor?
- What is the challenges in collection of pyrolysis product in both catalytic and thermal pyrolysis?
- What is the improvement new semi-batch pyrolysis set-up compared to the one previously used by Norner?
- What are the challenges in using new set-up that should be considered in future process development?
- How product of pyrolysis can be collected conveniently
- How temperature affect the total yield of wax/oil and gas during thermal pyrolysis of LDPE
- How to recognize the various groups of functional hydrocarbons by using Fourier-transform infrared spectroscopy (FTIR)
- How carbon distribution of products changes at different temperatures during thermal and catalytic pyrolysis by referring to results from Gas Chromatography Analysis (GC)

- How Thermogravimetric Analysis (TGA) can reveal the impact of plastic processing on LDPE by comparing degradation behavior of processed polymers with virgin
- How TGA instrument can be used to investigate the kinetic of LDPE degradation?
- How different polymer to catalyst ratio (P/C) and temperature affect the products in catalytic pyrolysis experiment
- How the yields of light olefin gaseous components change?
- How the TGA can be used for assessment of activation and deactivation of catalyst
- Can design of experiment helps with qualifying the reproducibility of process in first place and with mapping the optimum operational range in second place?
- How Thermogravimetric Analysis (TGA) can reveal the impact of plastic processing on LDPE by comparing degradation behavior of processed polymers with virgin
- How TGA instrument can be used to investigate the kinetic of LDPE degradation?
- How different polymer to catalyst ratio (P/C) and temperature affect the products in catalytic pyrolysis experiment
- How the yields of light olefin gaseous components change?
- How the TGA can be used for assessment of activation and deactivation of catalyst
- Can design of experiment helps with qualifying the reproducibility of process in first place and with mapping the optimum operational range in second place?

1.4 organization of the report

This report is based on five chapters. Chapter 1 introduce the basis and objectives of this study, Chapter 2 give an overview on polymers and pyrolysis along review of relevant studies on catalytic pyrolysis of plastic waste. Chapter 3 shares details regarding the developed set-up, heating method used in batch reactor, temperature measurement and methods established for implementation of experimental part. Chapter 4 presented and discussed the result that obtained from TGA analysis, outcome of experimental work and analytical analysis that implemented on pyrolytic products. In Chapter 5 the conclusion and proposal for future experimental work is presented.

2 Literature review

2.1 Overview of polyolefin waste

Olefin or alkene are group of unsaturated hydrocarbons with minimum one carbon to carbon double bond in molecular structure. The simplest olefin begins with two carbon number which is called ethylene or ethene. Propylene or propene is next molecule in the olefin group consists of three carbon molecules (See Figure 2.1). Due to their unsaturation they have potential for synthesis of polymer chain through establishment of C-C linkages. The process is regarded as polymerization of olefin monomer (ethylene or propylene) and the resultant polymer is regarded as polyolefins. Polyolefins includes low-density polyethylene (LDPE), linear low-density polyethylene (LLDPE), high-density polyethylene (HDPE) and polypropylene (PP) [7].

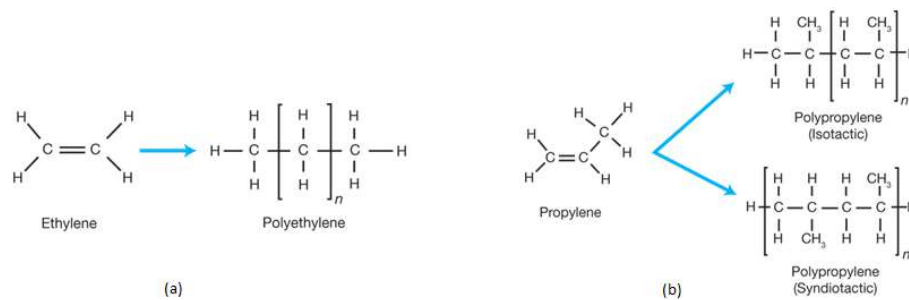


Figure 2.1: A schematic of most consumed olefin monomers and polyolefins molecules [8]

Nowadays polyolefins are accounted for 50% of raw materials that is being consumed in plastic industry [3]. Their low cost, high chemical resistivity, physical performance, excellent processability and good recyclability have made them a preference than other commercial polymers [9].

Moreover, polyolefins can be effectively separated from the MPW stream because of their similar chemical and physical properties. Flotation or float-sink method is a density-based separation that divides plastics based on their flowability (as shown in Figure 2.2) in water (flotation agent). Polyolefins have density below 1 g/cm^3 so they can be effectively separated from the rest of MPW containing polyvinyl chloride (PVC), polyethylene terephthalate (PET) and polystyrene (PS) as they have higher density than water ($>1 \text{ g/cm}^3$) [5].

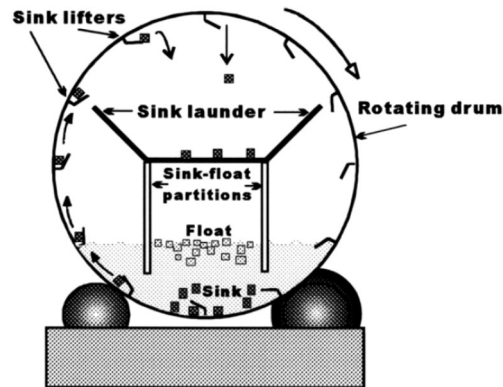
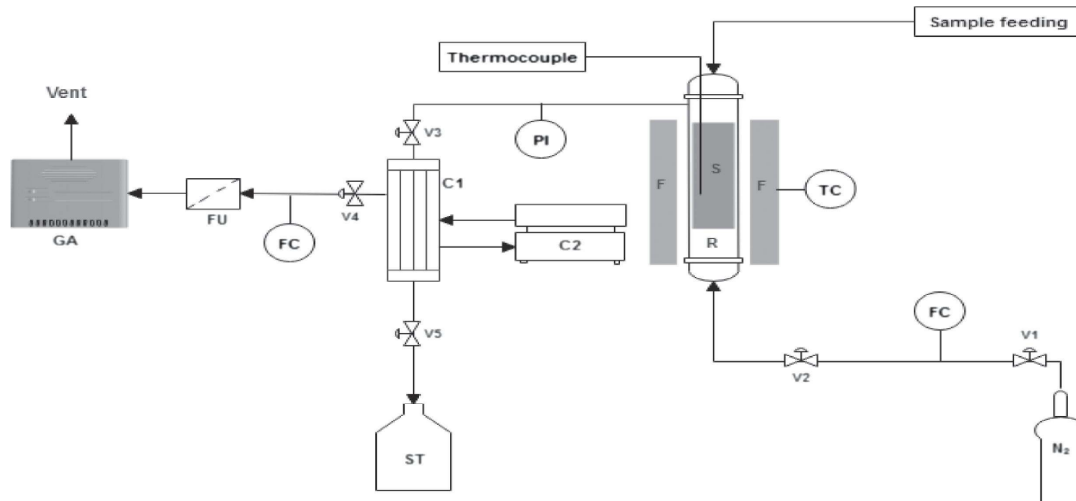


Figure 2.2: A schematic of rotating drum system designed for separation of MPW in water based on their density [10]

2.2 Overview of pyrolysis of plastic waste

Pyrolysis is thermal degradation of long organic molecules to shorter ones in oxygen starving atmosphere. Figure 2.3 shows a pyrolysis unit with all necessary element in order to have successful pyrolysis and collection of products. The pyrolysis medium is traditionally purged with an inert gas which does not participate in pyrolysis reaction. In most of the pyrolysis practices, nitrogen has been used to purge the reactor medium and conveying system that transport the feed to the body of reactor. The furnace heats up the reactor body and controller maintain the temperature at set point. After completion of pyrolysis reactions, formed products which are mostly in form of gas, due to high temperature of reactor, leaves the reactor. The volatile vapors passed through a condenser and are cooled down to room temperature to separate liquid and gas fraction from the output stream. liquid product can be stored for further utilization or analysis. Similarly, the separated gas stream passes through a filtering unit to remove solid particles and ashes which existed as contaminants in waste stream [11, 12].

**Legend:**

F: Furnace, R: Reactor, S: Sample, TC: Temperature controller, FC: Flow controller, V: Valve, C1: Condenser, C2: Chiller, ST: Storage tank, FU: Filter unit, GA: Gas analyzer

Figure 2.3: Schematic overview of pyrolysis unit [11]

Operational temperature in pyrolysis is between range of 300 to 850 °C [13]. The products of pyrolysis are non-condensable gas fraction, pyrolytic liquid (PtL), wax, char and ash. PtL consists of different group of functional hydrocarbons; paraffins, olefins, naphthenes and aromatics. On the other hand, PtL can be further processed for separation of hydrocarbons in range of gasoline (C₄-C₁₂), diesel (C₁₂-C₂₃), kerosene (C₁₀-C₁₈), wax(C₁₈-C₅₀) and lubricating oil (C₁₄-C₅₀) [14, 15]. The reported lower heating value (LHV) of PtL obtained from real MPW is 38 (MJ/kg) which is less than diesel (42 MJ/kg) and considerably higher than fuels obtained from biomass (~17 MJ/kg) [16, 17]. Ahmad et al. conduct a comparative study between PtL obtained from PP and HDPE with commercial diesel and gasoline [18]. The outcome of this work is presented in Table 2.1. The heating value of liquid obtained from pyrolysis of HDPE and PP is slightly less than gasoline and diesel fuels. As result a PtL is a potential alternative to be consumed as fuel in transportation market.

Table 2.1: Comparison between chemical and physical properties of standard fuels and liquid derived from PP and HDPE pyrolysis [18]

Properties	HDPE PtL	PP PtL	Gasoline	Diesel
Heating value (MJ/kg)	40.5	40.8	42.5	43
Viscosity at 40 °C (mm ² /s)	5.08	4.09	1.17	1.9-4.1
Density at 15 °C (g/cm ³)	0.89	0.86	0.78	0.870
Research octane number	85.3	87.6	81-85	-

Motor octane number	95.3	97.8	91-95	-
Diesel index	31.05	34.35	-	40

Parameters affecting pyrolysis is listed and shown in Table 2.2. Quality and yield of products are mainly affected by different process variables including resident time, temperature and presence of catalyst [19].

Table 2.2: Process variables that affect pyrolytic products [20]

Parameter	Influence
Composition of feed	Primary products are directly related to type and composition of feed
Temperature/ heating rate	Enhancement of molecular scission and favoring formation of small molecules for increased temperature and increase heating rate
Resident time	Higher residence time increases the conversion rate of primary products to secondary
Reactor type	Different type of heat transfer, resident time of liquid, resident time of primary product, mixing, batch/continues operation
Use of catalyst	Considerably affect the kinetics and distribution of products

2.2.1 Main operating factor: Temperature

Polyolefins (PP and PE) undergo degradation at ~ 400 °C [21]. Temperature has the most significant influence on pyrolysis process as it affects kinetics of all primary and secondary reactions. As result yield and mixture of products are directly affected by temperature [22].

Three different ranges of temperature below 600 °C, 600-800 °C, and above 800 °C define states of pyrolysis which are regarded as low, medium and high [23]. High temperature will improve the breakage of carbon bonds and favors production of short molecules. Hence, presence of more gaseous products ($C_2 - C_4$ hydrocarbons) and less liquid is expected. Higher temperature also results higher yield of thermodynamically stable products such as coke, tar, char [13, 24, 25]. The effect of heating rate is analogous to the effect of temperature as higher rates enhance the cracking of molecules [19].

Depending on heating rate, pyrolysis has been classified into two main modes: Fast, slow [26]. Table 2.3 shows the main operating conditions for fast and slow pyrolysis that proposed for biomass. In practice, no standard measure that define the edge between slow and fast pyrolysis exists.

Table 2.3: categories of pyrolysis based on resident time and heating rate [13, 27]

Mode	Residence time (s) of products	Heating rate (°C/s)
Slow	450 - 550	0.1 - 1

2 Literature review

Fast	0.5 – 10	10 – 200
Flash	Below 0.5	Above 100

However slow heating rate and long resident time, in scale of minutes or hours, for formed vapors in reactor are identical for slow pyrolysis. In contrast short resident time of products inside pyrolysis medium along with high heating rates is considered as fast pyrolysis. Hence resident time is the most significant factor defines whether the pyrolysis is fast or slow. Deposition of coke on reactor wall and production of char increases during slow pyrolysis [13, 28, 29].

Onwudili et al. investigated pyrolysis of virgin LDPE in a closed batched reactor purged with nitrogen at different temperatures and resident times. Operating temperature has chosen to be between 300 to 500 °C. Yield of the obtained products with respect to temperature is listed in Table 2.4. Pyrolysis reactor initially heated up to target temperature and kept constant for 60 min. Since the experiment conducted in a closed system, it is noteworthy that the temperature and resident time were the most effective process variables and effect of heating rate can be neglected. At 410 °C pyrolysis run, complete conversion occurred with waxy products ranged between C₅ to C₄₀. Temperature had huge impact as the aromatics components take up 65-70% of oil fraction at 500 °C [30].

Table 2.4: Effect of temperature on pyrolysis of LDPE in closed batch reactor [30]

Temperature (°C)	Char (%w/w)	Liquid (%w/w)	Gas (%w/w)	Unreacted polymer (% w/w)	Notes
350	-	-	-	100	<ul style="list-style-type: none"> No cracking occurred
400	-	-	0.7	99.3	<ul style="list-style-type: none"> White hard unreacted polymer
410	-	94.7	-	-	<ul style="list-style-type: none"> Whitish brown wax Optimum yield of oil/wax
425	-	89.5	10	-	<ul style="list-style-type: none"> Dark-brown oil with minor wax
450	1.75	72.4	25	-	<ul style="list-style-type: none"> Appearance of char in product
500	15.5	47	-	-	<ul style="list-style-type: none"> Noticeable char

2.2.2 Overview of polymer degradation mechanism

The kinetics of the degradation is one the most important aspects of pyrolysis process due its high level of complexity, and because of complicated molecular structure of polymers. Establishment of a kinetics model is a necessity both for comprehension of process itself and

simulation and optimal design of future plant Addition of catalyst can also change the route of degradation and therefore studies trying to establish diverse models for different types of polymer combined with effect of catalyst on kinetics [31, 32].

In general, first order reaction equation combined with Arrhenius law is employed to model the degradation (equation (2.1) [31]:

$$\frac{d\alpha}{dt} = A_0 \cdot \exp\left(-\frac{E_a}{RT}\right) \cdot (1 - \alpha) \quad (2.1)$$

α is concentration of reactant explained by $\frac{(m_0-m)}{m_0}$ (m_0 [mg] is initial mass of reactant and m [mg] is reactant mass at certain time), t is time [min], A_0 is pre-exponential factor [K^{-1}], E_a is apparent activation energy [$kJ \cdot mol^{-1}$], R is gas constant [$kJ \cdot mol^{-1} \cdot K^{-1}$] and T is reaction temperature, respectively. Nevertheless, more complicated models should be considered as MPW pyrolysis is degradation of more than one pure component.

For non-isothermal runs degradation, effect of heating rate on kinetics should be taken into account. Therefore, considering the constant heating rate, $\beta = dT/dt$ equation 2.1 is modified to equation 2.2.

$$\beta \frac{d\alpha}{dT} = A_0 \cdot \exp\left(-\frac{E_a}{RT}\right) \cdot (1 - \alpha) \quad (2.2)$$

Table 2.5 listed and explained numbers of more advanced non-isothermal models that are used to predict the kinetics of MPW degradation [31, 33].

Table 2.5: Suggested kinetic model for prediction of polymer degradation adopted from Khedri et al. [31]

Method	Expression
Friedman	$\ln\left(\beta \frac{d\alpha}{dt}\right) = \ln(A_0) + \ln(1 - \alpha) - \frac{E_a}{R} \frac{1}{T}$ (2.3)
Ozawa	$\ln(\beta) = -\ln\left(\frac{d\alpha}{dt}\right) + \ln(A_0) + \ln(1 - \alpha) - \frac{E_a}{R} \frac{1}{T}$ (2.4)
FWO	$\ln(\beta) = \ln\left(\frac{A_0 E_a}{R \ln(1 - \alpha)}\right) - 5.331 - 1.052 \frac{E_a}{R} \frac{1}{T}$ (2.5)
KAS	$\ln\left(\frac{\beta}{T^2}\right) = \ln\left(-\frac{A_0 R}{E_a \ln(1 - \alpha)}\right) - \frac{E_a}{R} \frac{1}{T}$ (2.6)

2.2.3 Kinetic study of degradation using thermogravimetric analysis

TGA is well-known technique that is being used to investigate kinetics of polymers decomposition. Figure 2.4 represent an overview of major elements in TGA system. The sample is initially placed in a pan posed inside the furnace which is purged with nitrogen. The degradation can be implanted under controlled nitrogen flow with accurate control of temperature. Weight loss of sample is main quantity that is being monitored accurately during each TGA experiment. Very low amount of sample degrades in this test in a perfectly controlled condition. As result the heat and mass transfer barrier is neglected and only kinetics have impact on course of degradation [34].

Heating of medium can be operated either isothermally or non-isothermally. During isothermal experiment, temperature should be ramped up rapidly to desired temperature and keep constant for the rest of experiment. thermogravimetric weight loss curve (TG) and the weight loss derivative curve (DTG) can be graphed with respect to time or temperature. For non-isothermal operation the sample heats up repeatedly as long as degradation take place. Non-isothermal heating gives a valuable data for simulating semi-batch operation. However, fast pyrolysis can be simulated through isothermal process. The obtained data can be effectively used to calculate parameters in kinetic equations [35].

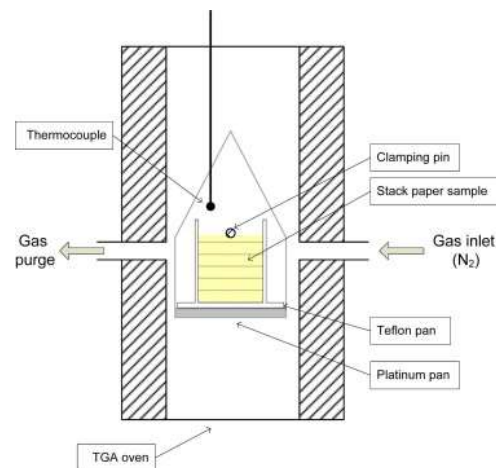


Figure 2.4: A schematic diagram of laboratory TGA furnace consisting the essential components [34]

In more advanced configurations, TGA is coupled with FTIR and mass spectrometer (MS) to analysis the composition of vapor products formed inside the furnace. Figure 2.5 shows an experimental configuration of TGA-FTIR and TGA-MS [36, 37].



Figure 2.5: A schematic diagram of TGA-FTIR and TGA-MS system [36]

2 Literature review

Khedri et al. studied isothermal and non-isothermal decomposition of HDPE under nitrogen atmosphere. Furnace heated up 25 and 50 °C/min to desired temperatures at 390, 400, 410, 420 and 430 °C for isothermal investigation. For non-isothermal TGA runs the different heating rates of 40, 45, 50 and 55 °C/min used for ramping from 40 to 575 °C. For isothermal TGAs, degradation rate significantly raised by increasing temperature. Hence, decomposition was less dependent on initial ramping. Non-isothermal ramping at high rate delays degradation onset, however, it is associated with higher decomposition rate. As author conclude, isothermal heating is more accurate to investigate kinetics as decomposition mechanism vary with changing temperature [31].

Miteva et al. investigated the kinetic of thermal and catalytic degradation of plastic mixture (70% HDPE, 30% PP) using FWO and KAS models. The experiment conducted using TGA instrument at different heating rates of 3, 5, 7, 10 and 20 °C/ min. The work discovered that increasing heating rate is directly proportional to increase of polymer degradation onset temperature. The E_a value calculated for this mixture were 267.34 and 269.07 kJ/mol using FWO and KAW kinetics models. Addition of 5 wt.% ZSM-5 acid catalyst to mixture lowered the activation energy by 100 kJ/mol [38].

Elordi et al. concludes that kinetics models based on weight loss of polymer are limited. Primary and secondary reactions should be considered in kinetic models in order to investigate the effect of process conditions on yield of specific group of products [39].

Jing et al. established a lumped scheme for mild cracking of polyolefins to liquid hydrocarbons in a closed batch reactor (See Figure 2.6). The polymers initially melted at temperatures between 100-200 °C (1). Molten polymer decomposes to intermediate products (P1) around 300 ~ 330 °C. At 370 ~ 420 °C further degradation of intermediate to wax, oil and gas can be realized through path 3-7. Products presented in mentioned phases are olefins. However, as they are thermodynamically unstable products, thus further increase in temperature and residence of products in pyrolysis medium, favors their conversion to naphthene ((8) ~ (10)). Further increase in temperature triggers dehydrogenation reaction and facilitate production of aromatics and char ((11) ~ (12)) [40].

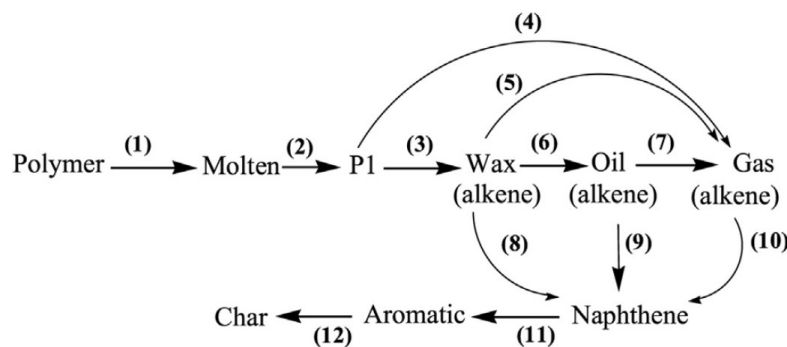


Figure 2.6: A schematic diagram of lump model for polyolefins predicted by Jing et. al [40]

2.3 Identification of catalysts used in pyrolysis

2.3.1 Overview of catalytic cracking

The products obtained from thermal process have large spectrum within C_5 - C_{80} . Hence, their commercial value is limited and they must be upgraded to narrower range of carbon number [41]. On the other hand, to obtain less waxy products, higher temperatures above $500\text{ }^\circ\text{C}$ is necessary. The catalytic cracking can satisfy this wish by both lowering the pyrolysis temperature and significantly increasing the yield of desirable products [42]. Solid acid catalysts have been extensively utilized to improve cracking, isomerization, oligomerization, cyclisation and aromatization reactions in pyrolysis of polyolefins. Moreover, there are numerous advantages in catalytic cracking compared to thermal decomposition[42, 43]:

- By reducing the activation energy, catalytic process decreases required cracking temperature. Activity of catalyst is inversely proportional to cracking temperature.
- Selectivity of each group of products can be tailored by selecting catalyst with appropriate acidity, pore size, pore structure.
- Polyolefin PtL can be effectively upgraded to cyclic, branched and aromatic hydrocarbons which are suitable to be used as diesel and gasoline fuels by enhancing their cetane and octane number.

Catalytic cracking can be implemented directly in reactor (in-situ) or outside pyrolysis reactor (ex-situ) to crack vaporized products obtained from thermal cracking in second step (see Figure 2.7)[44]. Staged cracking brings more versatility for optimizing the pyrolysis process. The mass transfer between catalyst and reactants increases significantly in second stage. Moreover, the deactivation effect that waste contaminations have on catalyst can be eliminated. Simultaneously, higher energy efficiency can be achieved with lower temperature for subsequent catalytic reactor compared to thermal unit [45].

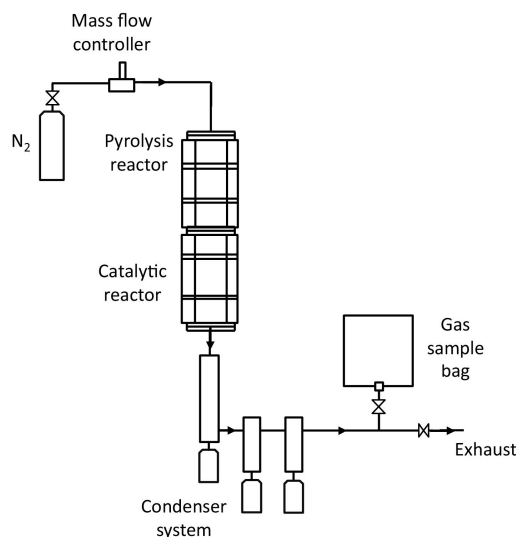


Figure 2.7: Process diagram of ex-situ catalytic cracking after thermal cracking reactor [45]

Table 2.6 shows an overview of literature that utilized catalyst in decomposition of polyolefins with respect to obtained optimum operating point proposed by each research.

2 Literature review

Table 2.6: Overview of literature that performed catalytic cracking at different process conditions

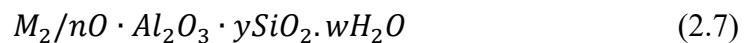
Author	Feed	Reactor and process variables	Outcomes
Mastral et al. [46]	HDPE HZSM-5 Si/Al ratio: 35 Pore size: $0.53 \times 0.56/0.51 \times 0.55$ nm	Fluidized-bed In range 350 – 550 °C P/C = 0.93 – 9.2	<ul style="list-style-type: none"> • Optimum Gas yield of 80 at 0.93 • Gas yield considerably decrease at low temperatures or high P/C ratio • Temperature above 500 °C and high P/C ratio increase presence of olefin oil/wax products
Elordi et al. [47]	HDPE HY Si/Al ratio = 30 Pore size = 0.74×0.74 nm	Conical spouted bed reactor At 500 °C 20 g cat in bed material polymer feeding rate: 1 g/min	<ul style="list-style-type: none"> • Optimum yield of 47 wt.% for non-aromatic C₅ – C₁₁ after 2.5 h reaction time • Deactivation of catalyst by coke, increased the total yield of wax from 1 wt.% to 23 wt.% after 2.5 h from the start of experiment
Marcilla et al. [48]	HDPE HUSY Si/Al = 6.0 Pore size = 0.74 nm	Semi-batch reactor P/C = 10	<ul style="list-style-type: none"> • Dominant oil/wax yield (61.6 wt.%) with 1.9 wt.% coke on catalyst • Presence of olefins (64 wt.%) and paraffins (26.9 wt.%) were noticeable in gases • The total yield of aromatics (31.3 wt.% exceeded from other components)
Serrano [49]	LDPE (46.5 wt.%), HDPE (25 wt.%) and PP (28.5 wt.%) H β Si/Al = 39 Pore size = 0.64 nm BET surface area (m ² /g) = 613	Semi-batch reactor Initially ramping from room temperature to 400 °C with rate of 25 °C/min and resident time of 30 min 0.032 g of catalyst in 1.6 g of polymer	<ul style="list-style-type: none"> • Production of oil/wax products (~75 wt.%) exceed than gaseous hydrocarbons • Liquid products ranged between C₅ – C₁₁ accounted for 60 wt.% of total yield • In gas phase C₂ – C₄ was dominant species (~71 wt.%)
Grieken et al. [50]	LDPE HMCM-41 Si/Al = 76	Stirred semi-batch Three various temperatures of 380, 400 and 420 °C during different resident time (0 – 360	<ul style="list-style-type: none"> • Almost 50 wt.% of liquid products obtained at 420 °C while the wax yield reached to the lowest point (40 wt.%) • Evolution of gaseous products had mean value of around 5 wt.% for all runs

2 Literature review

	BET surface area (m ² /g) = 1275	min) under flow of nitrogen were studied	<ul style="list-style-type: none"> The catalyst represented a high activity
Olazar et al. [51]	HDPE FCC BET surface area (m ² /g) = 338	Conical spouted bed Experiment conducted with severely steamed FCC catalyst at 500 °C 30 g of catalyst placed in bed with continues feed of polymer (0.5 g/min) for 6 – 7 h	<ul style="list-style-type: none"> The products categorized in three different range ranges: < C₅, C₅ – C₉, > C₉ with yield of around 55, 35 and 10 wt.% respectively Low yield of diesel-fuel as it was only 13 wt.%

2.3.2 Heterogeneous zeolite acid catalyst

Heterogeneous catalysts have been used widely in pyrolysis of polyolefins. This type of catalyst are characterized by their microporous crystalline structure formed with mainly aluminosilicates and first elemental group in periodic table (M = lithium (*Li*), sodium (*Na*), potassium (*K*), magnesium (*Mg*), calcium (*Ca*), barium (*Ba*))[15]. A general chemical formula of the zeolite composition can be presented by:



y represents *Si/Al*, *n* is valence of the cation and *w* is amount of structural water. Primary structural unit is based on *SiO₄*, *AlO₄* tetrahedral which are linked together through oxygen atoms. Each oxygen is bonded with two *Si* and *Al* atom and this linkage develop a three-dimensional microporous structure. Different ratio and configuration of *SiO₄* to *AlO₄* establish interconnected pores with different forms and sizes [15]. Major difference in morphology are main catalyst in zeolite family is shown in Figure 2.8.

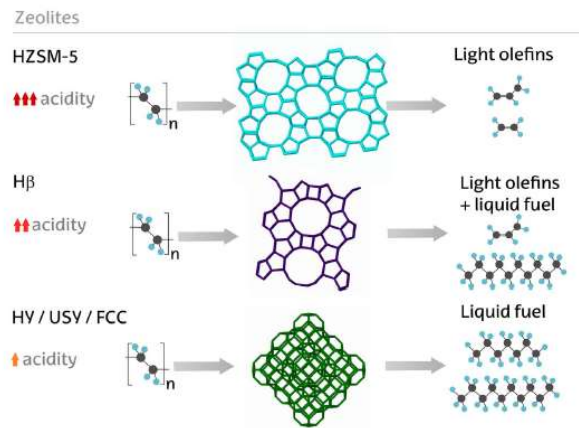


Figure 2.8: A schematic representation of crystal structure of ZSM-5, H β , HY, HUSY and FCC catalyst [52]

The imbalances in charge between the silicon and aluminum atoms in catalyst structure causes the formation of acid sites. The acid sites in zeolite is recognized by two different types: Brønsted acid site (proton donors) and Lewis acid site (electron acceptor) as shown in Figure 2.9. Activity of catalyst is recognized by amount of acid sites presented in structure.

Formation of Carbocations on Acid Sites of Catalysts

Brønsted acid sites – donate protons

Lewis acid sites – accept electrons

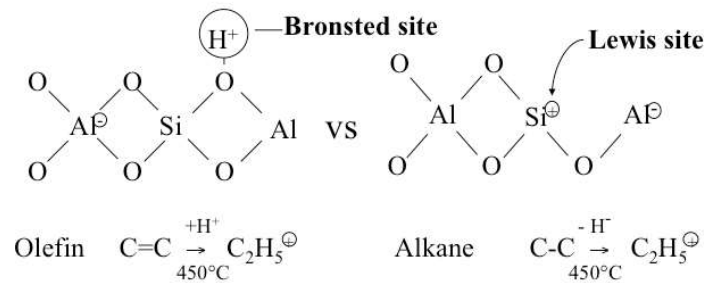


Figure 2.9: Location of Brønsted and Lewis site in crystal structure of zeolites [53]

High thermal stability, high surface area along with high acidity makes zeolites an ideal choice to expedite cracking of polyolefins [15]. Breakage of backbone of polyolefins initiates on outer surface of catalyst as polymer chain is initially longer than pore size of catalyst by carbenium ion mechanism. Firstly, abstraction of the hydride ion (Lewis acid sites) or addition of proton (Brønsted acid sites) in the C-C bonds leads to initial cracking of macromolecules. Structured pores in catalyst is like molecular sieve which large molecules cannot diffuse through it and molecules can be separated based on their size and shape. Thus, pore size and structure are important factors that define the spectrum of final molecules [15]. ZSM-5 is the most used catalyst among zeolites in catalytic pyrolysis of waste polyolefins. HY, HUSY and H β are also widely used. Table 2.7 represents main structural characteristics of zeolites. Most noticeable distinction between these catalysts are different acidity caused by various Si/Al ratio and their pore size.

Table 2.7: Structural features of common zeolites used in degradation of plastic waste [41]

Zeolite	Pore size (nm)	Si/Al ratio
HZSM-5	0.53 × 0.56, 0.51 × 0.55	10 – 1000
HY	0.74	1.5 – 3
H β	0.64 × 0.76, 0.55 × 0.55	8 – 1000

Monas et al. studied the catalyst pyrolysis of HDPE for same process condition and same polymer to catalyst ratio (P/C) using HZSM-5, H β , HY and HUSY. Narrow spectrum of C₃-C₁₅ products resulted for all catalysts. Alkene were the most dominant group in products with mordenite and HZSM-5. In contrast presence of alkane in products was higher than alkene. However, in all products considerable amount of isoparaffinic products observed which makes it suitable to be used as high-octane fuels. Outcome of work revealed that order of saturation and molecular weight of products obtained are as follow [54]:

(light products) HZSM-5 < mordenite < H β < HY < HUSY (heavy products)

(more alkanes) HUSY > HY > H β > mordenite > HZSM-5 (more alkenes)

Higher pore size results in production of more liquid products, as long molecules can diffuse through the internal channels. HZM-5 (smallest pore size) favors the production of light C₁-C₄ gases with considerable presence of light olefins. Larger pores in HY catalyst is identical to production of more liquid in products. H β introduces an intermediate pore size between HZSM-5 and HY which makes it suitable for producing a mixture of liquid and gas. However larger pores lead to rapid condensation, and thus deactivation of catalyst [52].

2.3.3 Mesoporous and nano-zeolite catalyst

Despite high acidity of zeolites, their low surface area and small pore size limit access of long hydrocarbon to acid site located in internal channel. Accordingly more accessible acid site on external surface or larger pore sizes have been considered in design and development of mesoporous MCM-41, amorphous SiO_2/Al_2O_3 , nano-zeolites (n-HZSM-5) [41].

Aguado et al. studied the catalytic cracking of polyolefin mixture over HMCM-41 and n-HZSM-5 for temperatures ranged between 375 to 450°C and P/C between 4 to 200. Both catalyst showed complete conversion of polymeric feed at P/C of 4 during 400°C pyrolysis. However, n-HZSM-5 overall conversion was higher than HMCM-41 for P/C ratios above 4. In fact, higher Aluminum ratio resulted improved catalytic activity of n-ZSM-5. In case of n-ZSM-5 presence of C₃-C₆ reaches to highest value of 85 wt.% with considerable production of aromatic species close to 23% at 400 °C and P/C = 4. Pyrolysis of HMCM-41 yielded noticeable C₅-C₁₂ (gasoline fraction), C₁₃-C₂₂ (gasoil fraction) of 90 wt.% at P/C = 100 and temperature between 375 to 450°C [55].

2.3.4 Other notable catalysts utilized for pyrolysis

Most of the catalytic pyrolysis processes are implemented at high polymer to catalyst ratios to crack polyolefins effectively. It is mainly due to the fact that heterogenous catalysts are insoluble in viscous polymer melts. Low solubility results in low contact between catalyst and reactants. Thus, evolution of secondary reaction leading to branched hydrocarbons and aromatics will be limited during pyrolysis of polyolefins. To eliminate this effect Kaminsky et al. proposed utilization of only AlCl_3 or mixture with TiCl_4 for degradation of macromolecules. This texture is soluble in polyolefin melt, and therefore, the consumption of catalyst can be reduced to low concentrations of 0.1 wt.% or 1 wt.%. The catalyst successfully tested both in batch and continues fluidized-bed reactor. Compared to thermal run at 500 °C, addition of only 0.1% AlCl_3 lowered the pyrolysis temperature to 400 °C while gave same result [42].

In similar study Donaj et al. examined the possibility of cracking polyolefins with commercial Ziegler-Natta (Z – N) catalyst. The advantage of using commercial Z – N catalyst was that TiCl_4 is supported on MgCl_2 . This composition increases thermal stability of catalyst as MgCl_2 protect active site (TiCl_4) from destruction at high temperatures. The amount of catalyst utilized was only 1 wt.% of total feed. Moreover only 5 – 16 wt.% of Z – N catalyst is consisted of active site [56]. Outcome of this work will be further discussed in section 2.4.2.

2.3.5 Deactivation and regeneration of catalyst

Lopez et al. [57] studied the deactivation of HZSM-5 during pyrolysis of mixed plastics containing HDPE (40 wt.%), PP (35 wt.%), PS (18 wt.%), PET (4 wt.%) and PVC (3 wt.%). The catalyst utilized for this research was commercial ZSM-5 with Si/Al ratio of 50 and total acidity of 0.17 mmol NH_3/g . Catalyst presumed to be active and therefore no activation method implemented on catalyst sample. The pyrolysis implemented in a semi-batch reactor at 440 °C for 30 min with fresh, spent and regenerated catalyst. Their textural properties represented in Table 2.8. High Bet surface area and micropore corresponds to high porosity of catalyst structure. Lowered micro pores volume of spent ZSM-5 compared to fresh catalyst indicated the carbon deposition inside the internal surface area of catalyst. Compared to fresh catalyst, higher external surface area of spent catalyst was caused by blockage of pores with coke on catalyst surface.

This outcome further confirmed as BET surface area of catalyst returned to almost same value as fresh catalyst, after burning the coke in air stream at 550°C. However, higher external surface area of regenerated ZSM-5 accounted for changes in crystal structure of catalyst. Moreover, char formation during regeneration process was responsible for amount of coke left in regenerated catalyst. The quick deactivation of catalyst resulted same yield of oil, gas and solids compared to thermal pyrolysis. In contrast the regeneration efficiently improved the product yields similar to fresh catalyst [57].

Table 2.8: Physical and textural properties of catalyst utilized in Lopez et al. research [57]

Property	Fresh ZSM-5	Spent ZSM-5	Regenerated ZSM-5
BET surface area (m^2/g)	412	291.6	411.1
External surface area (m^2/g)	65.9	288.6	124.3

Micropore volume (cm ³ /g)	0.1	10 ⁻³	0.1
Total pore volume (cm ³ /g)	0.4	0.6	0.4
Micropore area (m ² /g)	346.1	3.0	286.8
Carbon (% w/w)	-	23.0	0.7

Serrano et al. subjected three different catalysts of n-HZMS-5, HMCM-41 and H β , to a cycle of reaction/regeneration/reaction. First reaction was pyrolysis of HDPE at 400°C and resident time of 30 min with P/C of 4 under flow of nitrogen in a semi-batch reactor. The regeneration process for spent catalyst carried out in quiescent air at 500°C and 5 h. The second reaction performed at same process conditions, but at P/C of 50. The activity of regenerated catalysts with respect to fresh n-HZM-5, HMCM-41 and H β were 89.2, 81.5 and 73.4 wt.%, respectively. However, the product distribution after pyrolysis with each catalyst remained intact [49].

2.4 Recovery of valuable hydrocarbons from catalytic pyrolysis of polyolefins

2.4.1 Upgrading of PtL to specific range of fuels

Akubo et al. [58] studied catalytic pyrolysis of HDPE for production of oil rich in aromatic. The feed initially cracked in thermal reactor at 600°C. Subsequently, generated volatile products passed through a fixed bed reactor filled with HY catalyst (BET surface area of 421 m²/g) and heated to 600°C. To further realize the impact of modified catalyst on yield of aromatics, the catalyst impregnated with 1 wt.% and 5 wt.% of Ni, Fe, Mo, Ga, Ru and Co. During non-catalysis pyrolysis the evolved products are only consisted of aliphatic hydrocarbons.

Catalytic pyrolysis with non-modified HY increased the yield of aromatics to 80% which are rich in single and double ring aromatic components. Toluene, ethylbenzene and xylene along with naphthalene and alkylated naphthalene were the most of compounds presented in oil. After impregnation, except Co-HY, all catalysts that have been modified with 1% metal promoter improved aromatic yield by 5 – 15 % w/w. In contrast the total liquid yield slightly lowered from 45% to mean value of 35% after modification. Introducing 5% metal promoters slightly decrease the yield of aromatic for Ni-, Fe- and Ru-HY catalyst. However, the performance of Mo-, Ga and Co-HY considerably decrease in producing aromatic hydrocarbon. Moreover, addition of metal to HY structure contribute to faster deactivation of catalyst.

Zhang et al. [59] have studied catalytic pyrolysis of LDPE using microwave-induced heating. Feed initially polysized for 10 min at 480 °C and then passed through second packed-bed reactor filled with ZSM-5 zeolite catalyst (Zeolyst International, USA; SiO₂/Al₂O₃ = 50) in temperature ranged between 300 to 500 °C and P/C between 1.32 – 4.68. In only thermal pyrolysis 62.57 wt.% of products was C₂₁₊ waxes along with 35.38 wt.% gas. However,

2 Literature review

ZSM-5 assisted cracking efficiently favored production of gasoline ranged monoaromatics ($C_8 - C_{12}$) in liquid phase (74.73 – 88.49 wt.%). The maximum yield of mono aromatic hydrocarbons (88.49 wt.%) achieved at 450 °C and catalyst to reactant ratio of 4. The dominant species were xylenes, ethyltoluene, trimethylbenzene, indene, diethylbenzene. Presence of double-ring aromatics varied from 11.51 to 25.27 wt.% in liquid at all runs. Naphthalene, methylnaphthalene, dimethyl naphthalene were major double-ring aromatics observed in liquid. Presence of Ethylene is considerable in gas phase (65 – 80 wt.%) after catalytic cracking compared to thermal pyrolysis which is only 35 wt.%.

In another study, Zhang et al. [60] further investigated the upgrading of unsaturated hydrocarbons (alkene and aromatics) to jet fuel (by promotion of more cycloalkane species in PtL) by sequential hydrogenation in closed batch reactor. Figure 2.10 represent set-up utilized by author for both catalytic cracking and hydrogenation. The feed for hydrogenation reaction obtained from thermal cracking of LDPE at 500°C followed by ex-situ catalytic cracking using HZSM-5 at 375°C for catalyst loading of 10-20 wt.%. From this process conditions 50-64 wt.% oil recovered with presence of 30-40 wt.% single ring aromatics. Afterwards, 2g of resulted organic products mixed with 6 g of n-heptane were fed in a close reactor for hydrogenation using Raney Ni 4200 catalysts. Reactor were purged and supplied with hydrogen to assure the presence of reactant for saturation process. Hydrogenation reactions conducted at temperatures between 150 - 250°C, initial pressure ranged 500 -900 psi, 1- 4 h reaction time and catalyst to reactant ratio between 0.05-0.2. The research discovered that up to 84.32% of cycloalkane can be produced at 200°C, 900 psi initial pressure, with 10 wt.% Raney Ni 4200 in hydrogenation reactor [60].

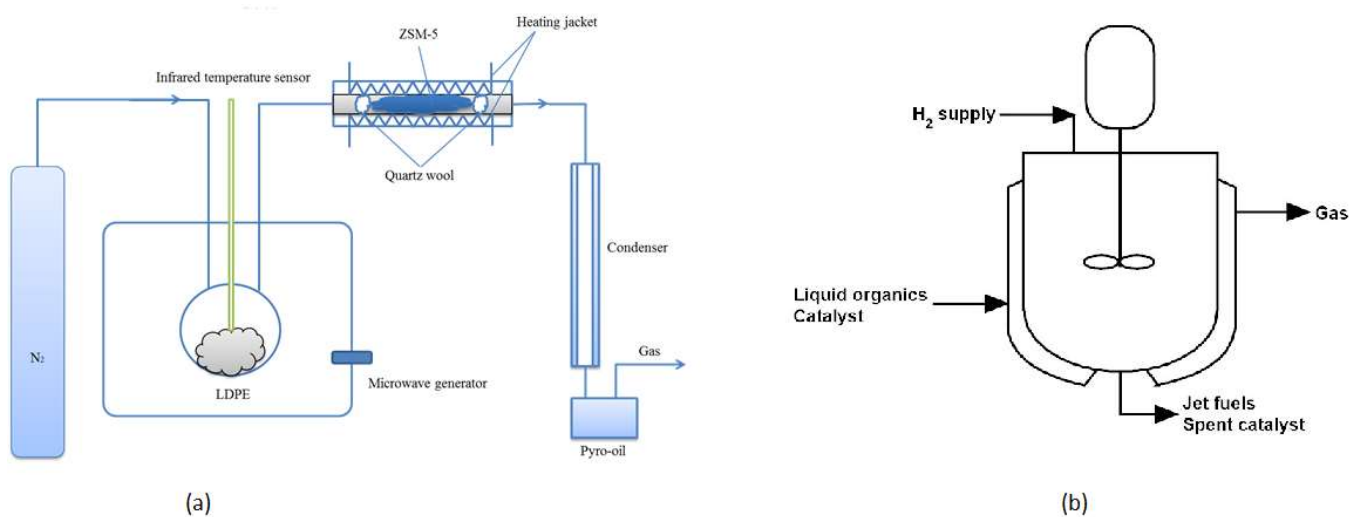


Figure 2.10: a) ex-situ microwave induced catalytic cracking of LDPE followed by b) hydrogenation processes in a close batch reactor using Raney Ni 4200 catalyst

Ratnasari et al. [45] studied recovery of gasoline range (C_8-C_{12}) hydrocarbon through ex-situ catalytic cracking of HDPE. For thermal cracking, first reactor heated to 500 °C with heating rate

of 10 °C/min. Yield of products produced in this research is illustrated in

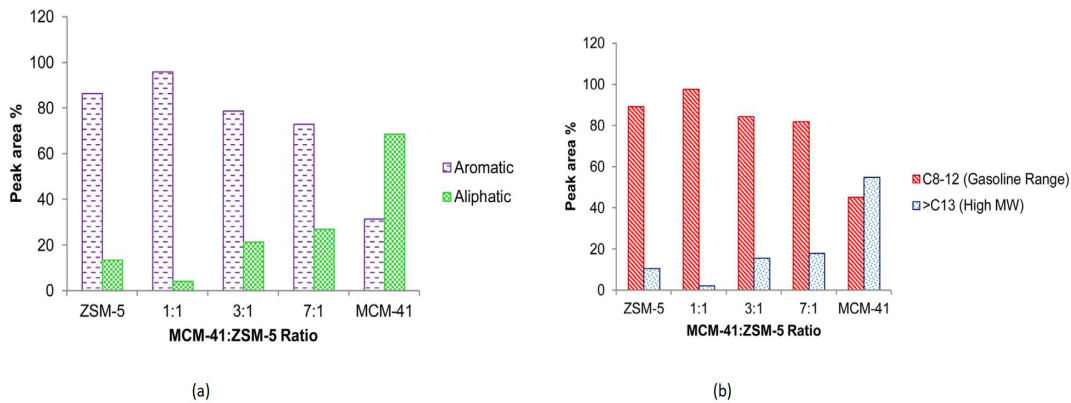


Figure 2.11. Pyrolysis products from thermal process passed through fixed bed pre-heated to 500°C that was filled with catalyst. Second reactor, packed with MCM-41 (Si/Al = 4 and S_{BET} (m^2/g) = 799), ZSM-5 (Si/Al = 20 and S_{BET} (m^2/g) = 266) or at various MCM-41 to ZSM-5 ratio of 1, 3 and 7. The mass ratio between total weight of catalyst and polymer kept 2 for all experiments. Total yield of oil had a mean value of 80%wt. for all tests. However, ZSM-5 resulted above 80% aromatics while MCM-41 produce around 60% aliphatic. MCM-41:ZSM-5 ratio of 1 optimized the production of aromatics to 95.85%wt. containing gasoline range hydrocarbons.

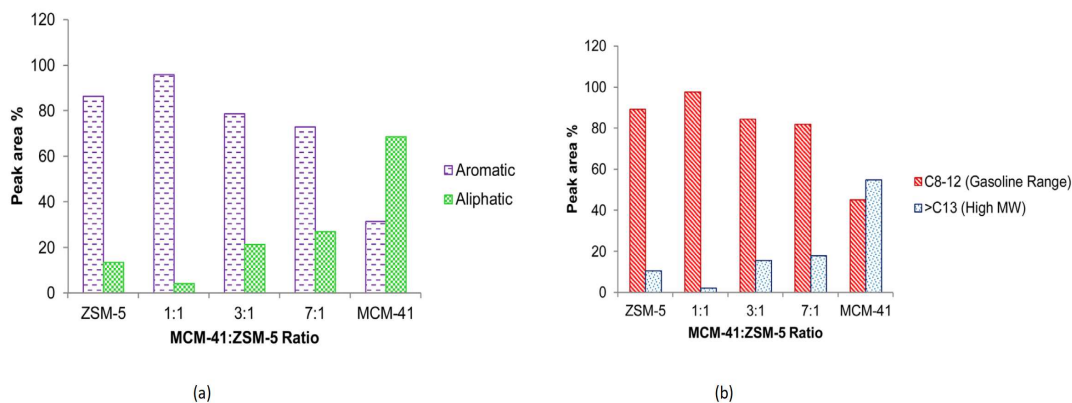


Figure 2.11: a) total yield of aromatic and aliphatic hydrocarbons along with b) total yield of C₈-C₁₂ and C₁₃+ carbon ranges after pyrolysis of HDPE at 500°C using various ratios of MCM-41:ZSM-5 [45]

2.4.2 Recovery of olefin monomer

Traditionally, olefins are produced through steam cracking of naphtha in petrochemical units. Therefore, a two-step monomer recovery from plastic can be realized by thermally crack polymers to oil in first place, and further cracking of products to light olefin at more intense temperatures as shown in Figure 2.12 [61].

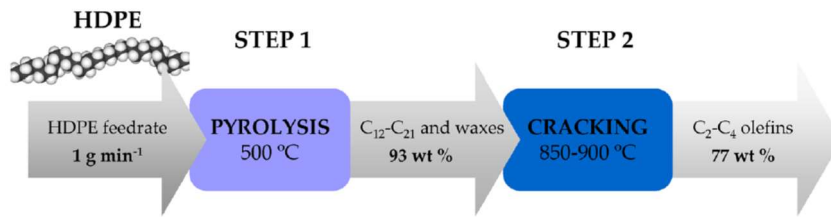


Figure 2.12: Step-wise recovery of C_2 - C_4 olefin monomers from thermal cracking of HDPE [61]

Artetxe et al. [61] carried out two-stage pyrolysis HDPE in conical spouted bed reactor (CSBR) reactor. Plastic materials, thermally pyrolyzed at 500 °C, and formed volatile products cracked in a subsequent tubular reactor at temperature range of 800-900 °C with short resident times between 0.016-0.032s. In this configuration, optimum yield of light olefins (C_2 - C_4) which was 77 wt.% obtained at 900 °C. Ethene was dominant species with yield of 40.4 wt.% while propene and butene were 19.5 and 17.5 wt.% respectively.

Jing et al. [62] followed this approach by micro-wave assist steam cracking of PtL obtained from thermal cracking of PP, LDPE and their mixture, at 1000 °C. Considerable amount of light olefins (C_2 - C_4) which accounted for 50.62-68.64 wt.% of total products obtained. At optimum steam cracking conditions, ethylene and propylene yields were 47 and 22.83 wt.%, respectively.

According to Ren et al. [63] the most energy consuming process in chemical industry is steam cracking. Thus, researches try to study more energy efficient alternative processes for recovery of light olefins from naphtha-like feed. Conversion of catalytic steam cracking of feed ranged in C_4 - C_9 to propylene have been already commercialized. Another approach which have been investigated in bench-scale is conversion of heavy crude oil through pyrolysis over acid catalysts. This method can be operated at moderate temperatures ranged in between 600 – 700°C with overall yield of light olefins (C_2 - C_4) ranged between 30 – 40 wt.%.

Elordi et al. [64] studied in-situ catalytic pyrolysis of HDPE for recovery of olefin monomers over CSBR reactor. The experiment carrier out at temperatures ranged between 450 – 570°C. The catalyst used for this research was HZSM-5 with Si/Al ratio of 30 and pore diameter of 0.84 nm. The pyrolysis implemented in continues mode with feeding rate of 1 g/min while 30 g of catalyst placed inside reactor bed. Light olefin fraction (C_2 - C_4) was dominant in product composition during HDPE pyrolysis. However, by increasing temperature the total yield of light olefin declined from 57.8 wt.% at 450 °C to 50.3% at 570°C. simultaneously total yield of ethylene in gas phase increased, from 7 wt.% at 450 °C to 10 wt.% at 570 °C, while total amount of propylene and butene began to decline with increasing temperature, from 49 wt.% at 450 °C to 39 wt.% 570 °C.

Donaj et al. [56] studied catalytic pyrolysis of polyolefin mixture (46 wt.% LDPE, 30 wt.% HDPE, and 24 wt.% isotactic PP wt.%) in a fluidized-bed reactor. They utilized commercial Z-N for the first time as a catalyst during pyrolysis experiment at temperature between 500-750 °C. The experiment performed at a very low amount of catalyst in feed (1 wt.%) Catalytic pyrolysis at 650°C gave 20 wt.% higher gas yield than thermal cracking. By increasing thermal pyrolysis temperature to 728°C, the gas yield reached to 42 wt.% and was still less than catalytic run at 650°C (54 wt.%). Light olefin recovered from this work is listed in Table 2.9. Higher pyrolysis temperature or addition of catalyst did not improve ethylene yield, however higher

temperature had negative effect on propylene production. As author concluded propylene has tendency to decompose to more thermodynamically stable products, and fast quenching of product with steam can prevent propylene degradation. According to author suggestion, optimum range for olefin monomer recovery is between 600-750°C.

Table 2.9: Yield of olefin monomers obtained in gas phase during both catalytic and thermal runs [56]

Temperature (°C)	650	650	728
Catalytic run	Yes	No	No
Total Gas yield (% wt.)	54.3	36.9	42.4
Ethylene (% wt.)	22.3	21.4	24.4
Propylene (% wt.)	21.1	19.4	11.6

2.4.3 Thermo-catalytic recovery of post-consumer packaging waste

Exposure of polyethene films to sunlight for greenhouse application, expedite photocatalytic degradation and oxidation of PE material. As result presence of Ethylene-vinyl acetate (EVA) is abundant in greenhouse film waste as common additive.

Serrano et al. [65] studied thermal and catalytic pyrolysis of LDPE-EVA copolymer mixture at 400 and 420 °C. The research aimed at utilization of mesoporous Al-SBA-15 and Al-MCM-41 along with nanocrystalline HZSM-5 zeolite. The feed mixture consisted of 86% pure LDPE as well as 14% EVA copolymer (33% vinyl acetate). Acidity of n-HZSM-5 was dominant as the catalyst completely cracked the mixture at 420°C. The product yields obtained from this work is illustrated in Figure 2.13. Presence of Al-SBA-15 and Al-MCM-41 did not present any effect as they resulted same conversion as thermal runs at 400 °C.

Their performance improved at 420 °C but was considerably less than n-HZSM-5. Author concluded that this fact is due to acetic acid released from EVA which enhance production of aromatic and coke precursors and mainly causes deactivation of Al-MCM-41 and Al-SBA-15 due their mesopores structure. However, release of acetic acid results in noticeable amounts of aromatics both in thermal pyrolysis (~15 wt.%), and catalytic pyrolysis with value higher than 20 wt.% regardless of catalyst type. Mesoporous catalysts yielded high amount of gasoline hydrocarbon (C₆-C₁₂) between 40-54 wt.%. At the same time n-HZSM-5 shifted products toward gaseous C₁-C₅ range with mostly valuable C₃-C₅ olefins (C₄>30 wt.%) [65].

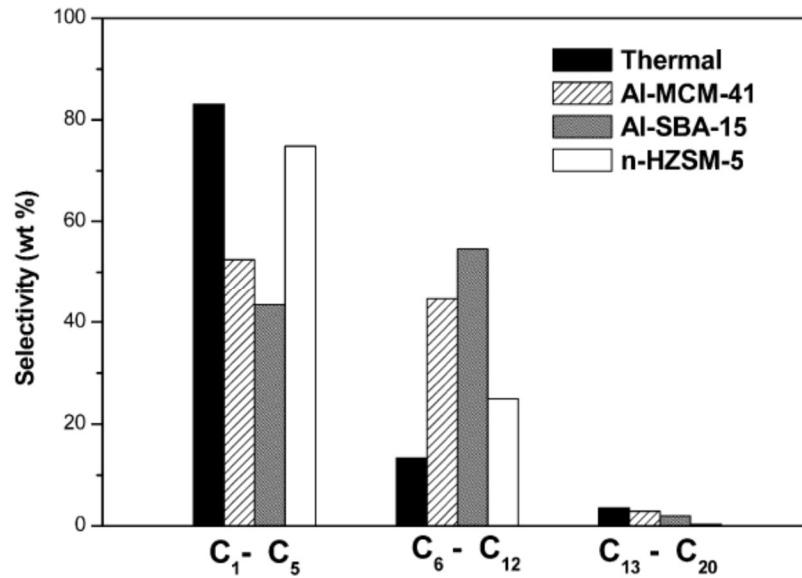


Figure 2.13: Product distribution of catalytic pyrolysis LDPE/EVA mixture over different catalysts [65]

Adrados et al. [66] studied thermal and catalytic pyrolysis of real MPW obtained from MSW recovery facility in Bizkaia (Spain). Major identified plastic types in waste were PE (35 wt.%), PP (40 wt.%), PS (19 wt.%), PET (5 wt.%) and PVC (1 wt.%). Two set of thermal catalytic pyrolysis containing 10 wt.% red mud (by product of alumina production) implemented for pure polymer with composition close to real waste. The degradation performed in a semi-batch reactor under nitrogen flow of 1 dm³/min at 500°C with heating rate of 20°C/min. The pyrolysis temperature maintained for 30 min. Due to presence of –OH and =O groups in real waste 5.3 wt.% of products contained char, while the char yield was below 1 wt.% for simulated plastic. Liquid samples from real waste was less viscous because of their lower molecular weight. Aromatic species in all samples was remarkably high with value above 70 wt.%. The fact was due to dehydrogenation reactions induced by catalytic effect of metals and glasses for real waste and red mud in pure polymers. Moreover, around 50 wt.% (14.6-18.8 wt.% ethylene) of gas phase contained valuable C₂-C₄ hydrocarbons for all runs.

3 Development of bench-scale apparatus and experimental procedure

3.1 Material

Linear low-density polyethylene (LLDPE) (Borstar FB2310) was purchased in form of pellets from Borealis (Vienna, Austria). The polymer grade is high molecular low-density polyethylene that has good and flexible processability. This grade is containing anti-oxidants and is specially designed for applications including food packaging, frozen food packaging, agricultural films and protective film. From now on, this material which this polymer will be called only LDPE. The physical properties of polymer are listed in Table 3.1.

Table 3.1: Physical and properties of FB2310 (LLDPE) measured by standard methods

Property	Typical Value	Test Method
Density	931 kg/m ³	ISO 1183
Melt flow rate (190 °C, 2.16 kg)	0.2 g/10 min	ISO 1133
Melting temperature	127 °C	ISO 11357-3

The catalyst used for this experimental work was ZSM-5 (Product Name: CBV 3024E) supplied by Zeolyst International (Conshohocken, PA, USA). The main properties of utilized catalyst are listed in Table 3.2. After delivery the catalyst calcined in a fluidized-bed reactor under flow of dried air which was placed inside furnace. The catalyst initially dried at 130 °C for 2h to assure desorption of moisture and carbon dioxide from acid sites. Afterwards, to avoid hot spot on catalyst and not affecting crystal structure, the catalyst heated up slowly (2 °C/min) to 550 °C. To assure completed calcination furnace temperature kept at 550 °C for 5 h. The activated catalyst, sampled in glass bottles and to avoid absorption of unwanted components on acid sites (H₂O, CO₂), it stored inside glove box under inert nitrogen atmosphere. Standard sample of C₇-C₄₀ saturated hydrocarbons (Product number: 49452-U SUPELCO) dissolved in n-hexane purchased from sigma-Aldrich (St. Louis, MO, USA).

Table 3.2: Physical and acid properties of ZSM-5

Catalyst property	
SiO ₂ /Al ₂ O ₃ Mole Ratio	30
Na ₂ O Weight	0.05 %wt.
Surface Area	405 m ² /g

3.2 Semi-batch reactor for in-situ catalytic pyrolysis

Experimental research shaped foundation of presented work. As result, a bench-scale set-up fabricated and modified based on previous experience [67] with development of a pyrolysis set-up. A schematic overview of set-up presented in Figure 3.1.

The nitrogen flow is supplied and adjusted by using a needle valve. Nitrogen pressure can be monitored through pressure gage places in nitrogen stream. However, it is not possible to measure the exact flow of nitrogen flowing into reactor as no flow measurement device was installed.

In total absence of oxygen, pyrolysis products appear in gaseous hydrocarbon as reactor temperature is relatively high. As result over pressurization of reactor is expected, and it can cause hazard. To avoid this problem, a semi-batch reactor with open outflow used to allow vapors leave the reactor. Moreover, the reactor is equipped with high-purity 10 bar rupture disk supplied by Swagelok (Stavanger, Norway). Fixed amount of 15 g LDPE decided to be used for each pyrolysis test without considering the catalyst amount.

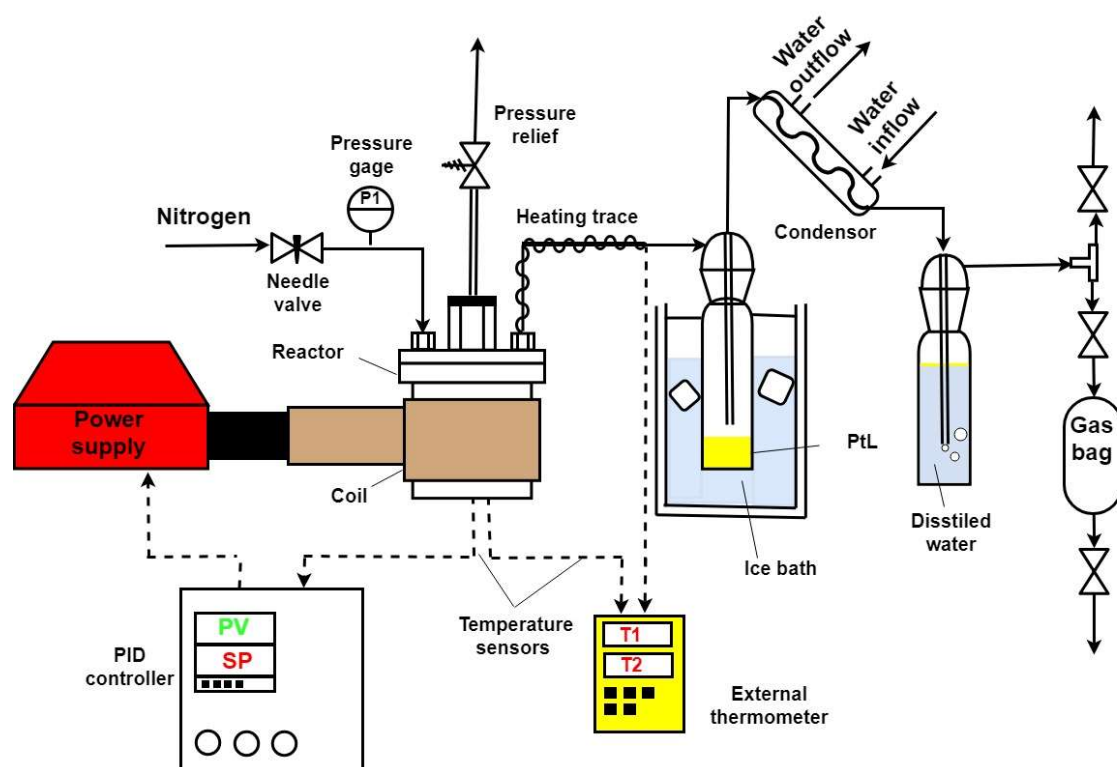


Figure 3.1: A schematic diagram of newly established process for present experimental work

The reactor is vertical cylindrical shaped with internal diameter of 60 mm and external diameter of 72 mm made of Sandvik 253 MA stainless steel (UNS: S30815). This type of steel has a good structural stability at high temperature and is operable to temperature up to 1150°C. The reactor heat-up up using induction as heating source (Product name: Minac 18/25 SM) supplied by EFD-induction (Skien, Norway). The heating method was easy to implement as the only required device to induce heat in reactor was a coil connected to power supply. Desired heating procedure can be done by programming the single loop PID

3 Development of bench-scale apparatus and experimental procedure

controller (product: Pro-16) which was supplied from West Control Solutions (Gurnee, IL, USA).

Some operational problems experienced in previous work regarding the fast condensation of waxy products in the outlet pipe. Subsequently outlet pipe blocked and due to pressurization of reactor, the wax was knocked out to collection bottle. As result, a heating trace embedded around the outlet pipe to avoid any solidification of waxes. Heating source was not subjected to any control and its input signal were adjusted manually through experiments. However, the product temperature at inlet of first washing bottle was being monitored constantly to assure temperature above 100 °C. Therefore, an external thermometer (FLUKE 54 II; Fluke, Everett, WA, USA) used for monitoring and logging of both reactor temperature and products temperature at heating trace outlet using K-type thermocouple (with accuracy of $\pm 2.2^\circ\text{C}$).

The PtL products collected in first washing bottle which was placed in 0°C ice bath. The products stream then passed through a condenser which were further cooled down by water (fluctuating between 10 to 20°C), and second washing bottle filled with deionized water. The main reason for this staged-cooling was to separate volatile hydrocarbons from gaseous products. The gas collection could be done by opening the inlet valve upstream of gas at any time during experiment.

Beside all of the improvement that made from previous set-up, yet addition of a stirring system to reactor was not possible. The two options that were taken into account were as follow:

- **Magnetic stirrer:** The maximum temperature that spin bar can withstand is around 225°C. Aimed pyrolysis temperatures in this work ranged between 400-550°C.
- **Mechanical driven stirrer:** There was not much space in reactor cap to house stirrer shaft in the the reactor.

For further prospective improvement, it is vital to fix this issue as mixing can assure efficient constant of reactants in the reactor medium and avoid side reactions that could occur due to uneven distribution of reactant and temperature.

3.2.1 Heating method

In previous pyrolysis experiments, Norner used a muffle oven to supply heat for the reactor. Two reactors filled with reactant were pyrolysis simultaneously in muffle oven. Temperature distribution inside the oven was high as measurement showed 80 °C difference between external temperature sensors inside reactors and process value measured by oven controller. Hence, the first available alternative to overcome this challenge was to utilize induction heating. Main principle of induction heating is shown in Figure 3.2. The metal body is wounded with coil connected to high frequency alternating electric current (AC). High frequency AC current in coil induces and alternates magnetic flux through the reactor body. The magnetic flux induces eddy current that cause Joule heat effect in piecework located in coil, which increase the temperature of reactor [68].

3 Development of bench-scale apparatus and experimental procedure

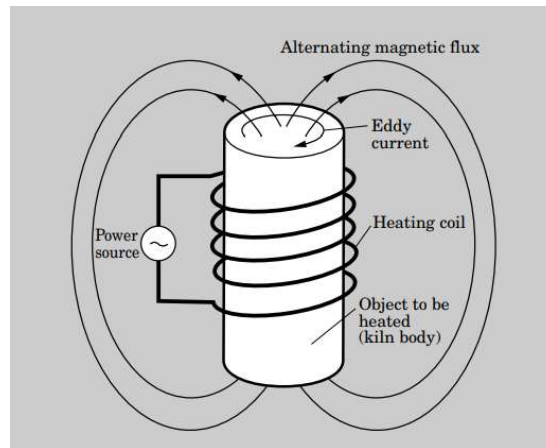


Figure 3.2: An illustration of metal magnetic alternating magnetic flux that passes through metal body in coil and generates heat [68]

The method was appropriate way of heating up metal body to desired temperature as power source was relatively small and immediately available to use. Compared to other oven heating and resistant heating, the method has energy efficiency of 85 wt.% as directly transmits power to the work piece. It is a very noticeable advantage as it lowered the energy cost by increasing the energy efficiency. The required start up for other conventional heating methods are normally in order of hours. By using the induction heating, desired temperature can be achieved in order of minutes[68, 69]. Technical details of power source used for this work are listed in Table 3.3.

Table 3.3: Characteristics of power source used for heating the reactor in present work

Model	Minac 18/25 SM
Max output power	25 kW
Frequency range	10-25 kHz
Output power regulation range	2-100%
Supplier	EFD-induction

3.2.2 Preliminary evaluation of temperature measurement

Unfortunately, as no string implemented in reactor design, a preliminary test both with empty reactor and reactor filled with 7.4 g of only LDPE tested. The main objective of these two tests were to find out the best spot on reactor body for temperature measurement as the best indicator for melt temperature inside reactor. Therefore, as the controller P, I and D terms were tuned for the sensor on external side-body of reactor, temperature at this point was chosen as input temperature signal for controller (TC). Two temperature sensors (T1 and T2) were placed on middle point at bottom of reactor, on internal and external surface respectively (see Figure 3.3). Controller programmed to initially heat up the reactor at 10 °C/min to 200°C and kept at 200°C for 10 min. This stepwise ramping was to make sure that

3 Development of bench-scale apparatus and experimental procedure

polymer would be completely melt and reactor body will have enough time to heat up uniformly. After isothermal heating, the temperature increased with rate of $10^{\circ}\text{C}/\text{min}$ to 450°C .

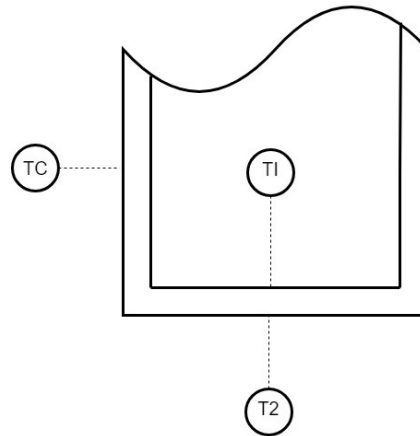


Figure 3.3: Location of temperature sensors which were used to logging the temperature of reactor as part of preliminary temperature measurement evaluation

Results obtained from temperature test for empty reactor is shown in Figure 3.4. T1 is always higher than T2 which is mainly due to high cooling rate of reactor external surface where the T2 is located. External thermometer was highly vulnerable to noise produced by coil due to high frequency current. As soon as the run started, the measurement value in external thermocouple jumped for 10°C . This effect is not reflected in graph as temperature recorded for every single minute. However, in addition to false rise at beginning of run, some sharp fluctuations for temperature observed, specifically at the end of experiment. At the same time, the controller showed better performance than external thermometer, as its measurement was completely stable without getting affected by noise. When the process measurement (TC) reached to set-point, value for TC, T1 and T2 were 450 , 439 and 414°C respectively. By offsetting the effect of noise from temperature, the values for T1 and T2 can be corrected to 429 and 399°C , respectively.

The main reason for this temperature difference is due to skin effect during induction heating. The phenomena caused by high current density at the external surface of piece work closed to induction coil. Moreover, regardless of skin effect, due to low conductivity of reactor material ($20\text{-}23 \text{ W/m}\cdot^{\circ}\text{C}$ at $400\text{-}600^{\circ}\text{C}$) and relatively high thickness of reactor wall (6 mm), high temperature gradient between external and internal surface of reactor wall is expected.

3 Development of bench-scale apparatus and experimental procedure

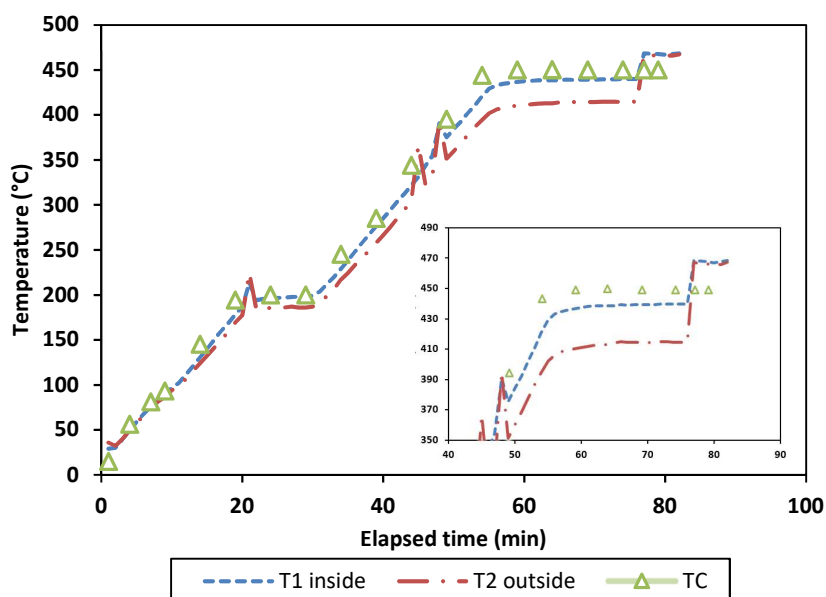


Figure 3.4: Temperature profiles for three different temperature sensors at three different locations on reactor body

At the same time the test repeated for same ramping program to test reactor filled with 7.4 g of LDPE. The appearance of products obtained from this test is shown in Appendix B. Only 8 wt.% white wax obtained at first washing bottle and the rest was unreacted brownish polymer that left inside reactor after it cooled down to ambient temperature. The expected onset temperature at for LDPE degradation is about 423°C for heating rate of 10°C/min. The result from this experiment confirmed that temperature measurement at reactor wall is not appropriate as it does not indicate melt temperature inside reactor properly. It is also clear that recording the temperature at midpoint, bottom and inside reactor gives best result. Therefore, all pyrolysis runs in present work, performed by using input signal from temperature measurement on center point at the bottom and external surface of reactor.

3.3 Methods

3.3.1 Experimental procedure

The experimental procedure for both catalytic pyrolysis and thermal cracking is explained here. For both thermal and catalytic series, the reactor initially heated-up to 200°C and stayed for 10 min. The reactor further heated up to pyrolysis temperature in 5 and 25 min for catalyst and thermal pyrolysis, respectively, and stayed at pyrolysis temperature for 30 min. Before experiment, first washing bottle were cleaned and dried in 130°C oven. Second washing bottle was filled with 100 ml of water. Both Washing bottles were weighted before experiment.

The reactor filled up with 15 g of LDPE and required amount of ZSM-5 based on decided P/C ratio, for each pyrolysis test. After sealing and tightening the reactor cap, it placed in the rig for continues purging of nitrogen through the system. At the same time the inlet and outlet valves of gas bag kept open to assure flow of nitrogen through gas bag as well.

3 Development of bench-scale apparatus and experimental procedure

After 15 min the controller started, and pyrolysis experiment began. The nitrogen flow stopped, and gas bag inlet valve closed. 30 min left to the end of pyrolysis experiment, gas collection in the gas bag performed for 30s. After completion of degradation and 5 min left to end of experiment time, low flow of nitrogen (unknown value) used to empty out the remained volatile products that stayed in reactor. The weight of liquid product calculated by comparing the weight of washing bottles after product collection and before experiment. The reactor was checked for any solid residue after each run. The weight of produced gas was calculated using following equations:

$$\text{Weight of gas} = \text{initial LDPE mass} - \text{liquid mass} - \text{solid residue} \quad 3.1$$

$$\text{Liquid yield} = \frac{\text{liquid mass}}{\text{initial LDPE mass}} \times 100 \quad 3.2$$

$$\text{gas yield} = \frac{\text{Weight of gas}}{\text{initial LDPE mass}} \times 100 \quad 3.3$$

To calculate the yield of coke on catalyst, the catalyst heated up from ambient temperature to 1000°C at presence of dried air. The weight difference between 400 and 1000°C selected as indicator for amount of coke deposited on catalyst.

3.3.2 Experimental design and procedure

As previously mentioned, two series of experiments planned in this work; thermal and catalytic. The thermal pyrolysis performed for three different levels of temperatures: 450, 500 and 550°C. Figure 3.5 represents an overview of DOE design used for planning catalytic series. The 2^k factorial design was employed to plan presented experimental work at first place, investigating robustness of the developed process and its tolerance to sources of variability, and simultaneously evaluating sensitivity of product yields to main operating variables. The pyrolysis temperature (x_1 , °C) and amount of catalyst in feed (x_2 , %) were picked as main operating variables (factors).

3 Development of bench-scale apparatus and experimental procedure

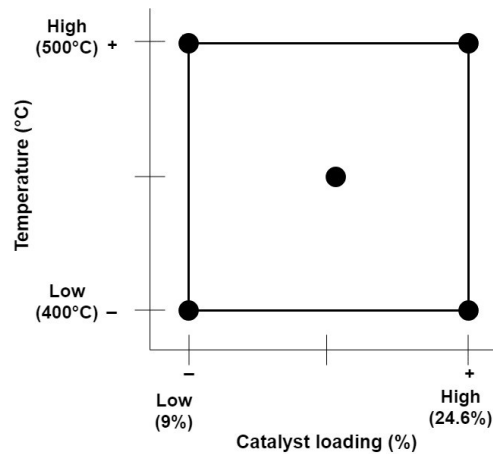


Figure 3.5: Schematic of experimental design used for this experimental work

The catalysis temperature was between 400 and 500°C. Amount of LDPE in feed was 15 g and catalyst loading differed from 9 wt.% to 24.6 wt.% of total feed. In total, 7 experiments performed with no replicate at corners, and adding 3 experiments at center point to investigate the reproducibility of results obtained from this experimental apparatus.

Dependent output responses are liquid yield (y_{oil}), gas yield (y_{gas}) and coke deposition on catalyst (y_{coke}) in current design. The post analysis and regression of predictive model done by using MODDE 12.1 (Umetrics AB, Malmö, Sweden). First-order regression equation containing interaction (x_1x_2) term is used to model the response as shown below:

$$y_i = \beta_0 + \beta_1x_1 + \beta_2x_2 + \beta_3x_1x_2 \quad 3.4$$

β_0, β_2 and β_3 are constant coefficients and they will be calculated.

3.3.3 Thermogravimetric analysis of LDPE degradation at various conditions

The TGA Q500 Thermogravimetric Analyzer with a platinum sample holder equipped with microbalance which is sensitive to changes as small as 0.1 μg in the sample weight used for TGA experiment. The instrument operates at atmospheric pressure and selectable nitrogen flow of 60 ml/min or air flow of 40 ml/min. Operable temperature range for instrument is from ambient temperature to 1000°C and all experiments conducted in mentioned range. A detailed overview of all runs and procedure performed in this work is listed in Table 3.4. As part of TGA test one powder sample and two different LDPE film produced to investigate the effect of plastic processing on polymer degradation behavior. The virgin LDPE pellets cryogenically milled to powder size below 0.1 mm. The extruded film is produced on a Varex 50/60/50 three-layer coextrusion film line from Windmüller & Hölscher, with a 200 x 1.2 mm die. The molded film produced using laboratory platen press (Product number: P200P, Dr.COLLIN GmbH, Ebersberg, Germany).

3 Development of bench-scale apparatus and experimental procedure

Table 3.4: Experimental scheme for TGA analysis at present work

Series A		
sample	form	specification
LDPE	Virgin granules	Non-isothermal runs at 5, 10, 20, 30, 60, 100°C/min.
	0.1 mm powder	Total sample weight of 10 mg (± 2) under N ₂ flow.
	Extruded film	
	Molded film	
Series B		
sample	specification	
10/90 ZSM-5/LDPE	Non-isothermal runs at 10, 20, 30, 60°C/min with total sample weight of 20 mg (± 2) under N ₂ flow. The LDPE was in form of 0.1 mm particles.	
20/80 ZSM-5/LDPE		
25/75 ZSM-5/LDPE		
Activated ZSM-5	Non-isothermal runs at 20°C/min with total sample weight of 10 mg (± 2). The experiment performed both under dry air and N ₂ atmosphere to evaluate the calculation of coke on catalyst and calcination process.	
Spent catalyst from catalytic pyrolysis experiments		

3.3.4 Gas chromatography analysis

Gas chromatograph coupled with flame ionization detector (FID) and thermal conductivity detector (TCD) (Agilent 7890B) used to detect main non-condensable gases: Ethane, ethene, propane and propene. Waxy products obtained from thermal experiment diluted in n-hexane with dilution ratio of 1:5 at 60°C. The liquid products diluted with ratio of 1:10 in same solvent before injection to GC device. To avoid crystallization of long chain hydrocarbons due to cooling, each sample immediately transferred to GC sample holder after preparation. Identification of both gaseous and liquid products performed by using ASTM D7833 and ISO 3924:2016 standard methods, respectively. The detailed description of methods is listed in Table 3.5.

Table 3.5: Main characteristic of GC method utilized for analysis of gas and liquid products obtained from pyrolysis

Method	ISO 3924:2016	ASTM D7833
	Determination of condensed hydrocarbon range distribution	Determination of non-condensable C ₁ -C ₅₊ hydrocarbons

3 Development of bench-scale apparatus and experimental procedure

GC	HP 6890 series	Agilent 7890B
Column	DB-1HT	CP 6968
Column length	15	
Column ID (mm)	0.32	
Stationary phase	0.1	
Carrier gas	Helium	Helium
Carrier gas low rate (mL/min)	30	150
Heating rat	10	15
Detector	FID	FID
Detector temperature	350	300
Injector temperature	340	250

3.3.5 Fourier-transform infrared spectroscopy

Liquid and wax analysis were subjected to FTIR spectrometer (product number: L16000A, PerkinElmer, USA). Each obtained IR spectrum further analysis for detection of different functional group of hydrocabons.

4 Result and discussion of pyrolysis

4.1 TGA analysis

4.1.1 Effect of heating rate on thermal degradation and catalytic degradation

Non-isothermal TG and DTG curves for LDPE degradation is shown in Figure 4.1 and Figure 4.2 at various heating rates: 5, 10, 20,30,60 and 100°C/min. Both curves represented same trend as degradation occurred only in one stage. Each curve is recognized by three characteristic temperatures: starting decomposition temperature (T_i), maximal degradation rate temperature (T_p) and completion temperature denoted by T_f . All these values for LDPE degradation are reported in Table 4.1.

Table 4.1: characteristic temperatures for LDPE degradation at different heating rate

Heating rate (°C/min)	5	10	20	30	60	100
T_i (°C)	350	350	350	350	350	350
T_p (°C)	456	456	477	483	501	508
T_f (°C)	479	492	505	517	534	549

Different heating rates did not have any impact on temperature at which the degradation of LDPE initiated. However, increasing heating rate from 5°C/min to 100°C/min delayed the maximum degradation rate, and end temperature of polymer degradation. This fact indicates that reaction temperature increasing by increasing heating rate with in contrast to the fact that higher rate enhances polymer cracking [20]. Khedri et al. [31] proposed that delayed degradation is due to the inaccuracy of sample temperature measurement by thermocouple. Aforementioned the thermocouple is located close to the pan in furnace and it is not in direct contact with sample. For isothermal run this error can be neglected as the temperature inside the furnace is stabilized. Another reason is that due to endothermic nature of plastic decomposition, more heat is required by sample and therefore, a temperature gradient between sample and thermocouple location will be generated. Faster heating can intensify instability and thus, result in more error on temperature measurement.

Accordingly, non-isothermal is a good way for qualitative analysis of degradation. However, for more advanced mathematical kinetic studies, specially to calculate kinetics parameters, it is better to implement TGA at low heating rates or isothermally.

After completion of degradation no residue stayed in pan and all polymer devolatilized and flushed out by nitrogen.

4 Result and discussion of pyrolysis

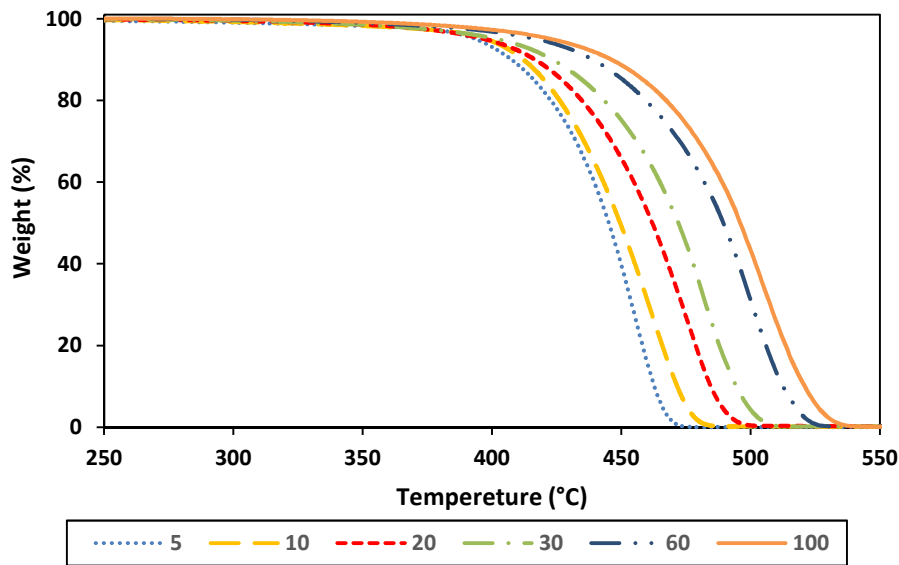


Figure 4.1: TG curve for degradation of LDPE at different heating rates: 5, 10, 20, 30, 60 and 100°C/min

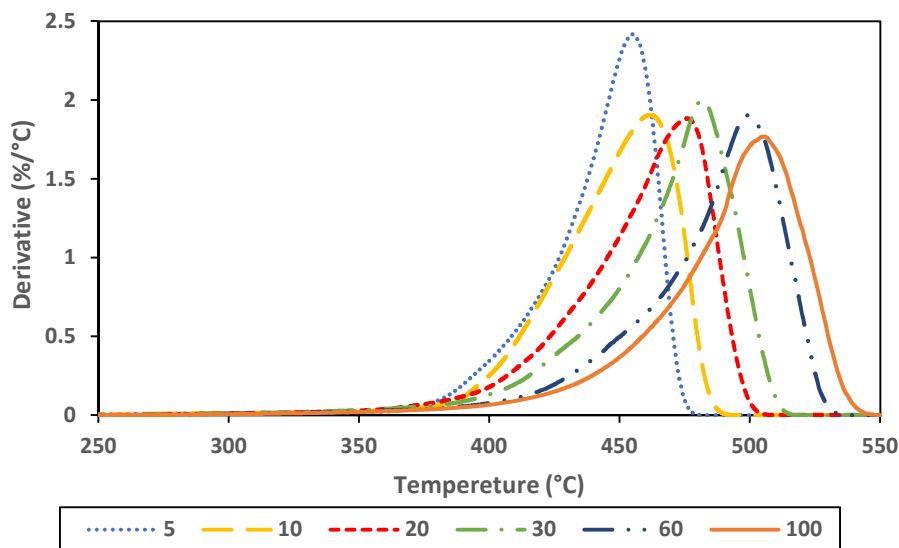


Figure 4.2: DTG curve for degradation of LDPE at different heating rates: 5, 10, 20, 30, 60 and 100°C/min

Error! Reference source not found. and **Error! Reference source not found.** illustrates the TG and DTG curves for degradation of LDPE using 10% ZSM-5 at heating rates of 10, 20, 30, 60 and 100°C/min. The starting degradation temperature during all catalytic degradations tests was equal for all runs (300°C). However, compared to non-catalytic TGA test, lowered T_i value (50°C less than non-catalytic degradation) illustrated considerable synergic effect of catalyst in decomposition of polymer molecules.

As expected, 10% residue monitored after completion of test which is accounted for the weight of catalyst. A comparison between maximum degradation rate temperature for catalytic and noncatalytic TGA run is arranged at Table 4.2. The difference between T_f during thermal and catalytic have a value between 60-70°C and is slightly higher than different between T_i .

4 Result and discussion of pyrolysis

Moreover, the catalytic cracking at 60°C/min is reaching to the thermal degradation at 10°C/min. This fact further confirms the inaccurate temperature measurement in furnace as ZSM-5 dominantly enhance cracking regardless of process parameter.

Table 4.2: comparison between maximum degradation temperature during catalytic and noncatalytic tests

Heating rate (°C/min)	10	20	30	60
T _p /°C (no catalyst)	456	477	483	501
T _p /°C (10% zsm-5)	389	407	422	445

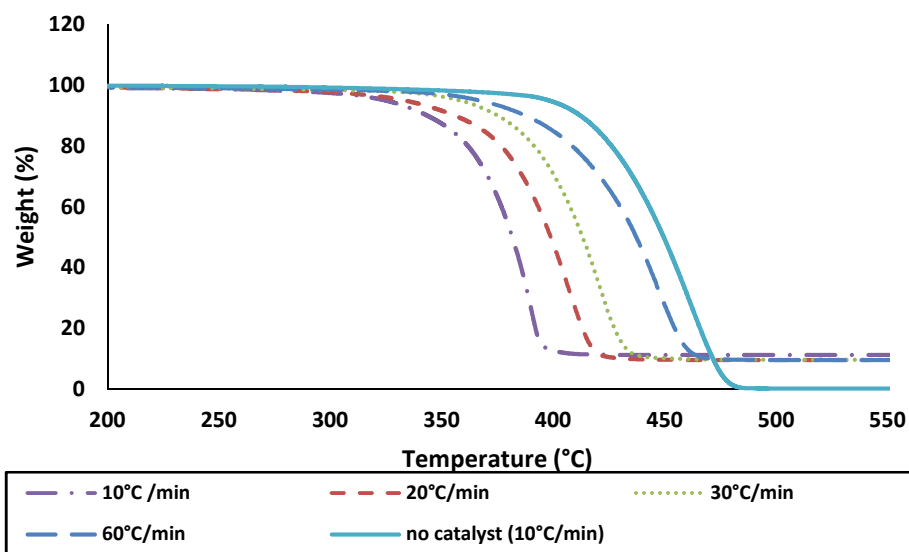


Figure 4.3 : TG curve for catalytic degradation of LDPE with presence of 10 wt.% ZSM-5 at different heating rates: 5, 10, 20, 30, 60 and 100°C/min

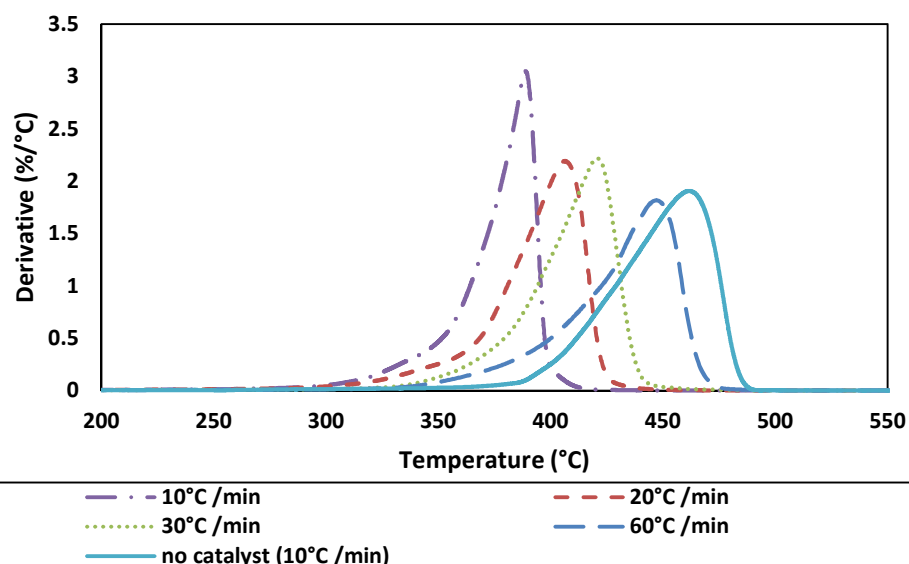


Figure 4.4: DTG curve for catalytic degradation of LDPE with presence of 10 wt.% ZSM-5 at different heating rates: 5, 10, 20, 30, 60 and 100°C/min

4.1.2 Effect of processing and appearance on LDPE degradation

Melting of solid polymers is the main step in polymer processing industry during production of plastic based goods. Therefore, during melt processing, the plastics are subjected to heating and high shear rates which causes thermomechanical degradation [5]. As result in this section thermal degradation of different forms of processed plastics are investigated.

Figure 4.5 and Figure 4.6 represent the TG and DTG curve of virgin pellet, extruded LDPE film, milled LDPE and molded LDPE at heating rate of 10°C/min for all sample. The virgin material is directly purchased from polymerization plant and was in form of pellet. The 80 µm blown film is made by extruding at temperature between 210-220°C and pressure between 318-385 bar. The molded film is produced with laboratory press molding device at temperature of 120°C far below the degradation temperature. Low temperature and no friction during processing, helps with assessing the effect of only physical size on degradation. The resultant graphs showed that all samples are almost have the same degradation behavior which is not affected by processing. Jing et al. [40] suggested that initial degradation of polyolefins to intermediate products occurs at 300-330°C. According to obtained graphs, it can be concluded that plastic process does not have any considerable effect on degradation behavior of LDPE as long as the melt processing temperature limit is considerably below starting degradation temperature (300-330°C). Moreover, the sample size, at least in small scales, is not a factor that affect degradation as molded film gave same result as other samples.

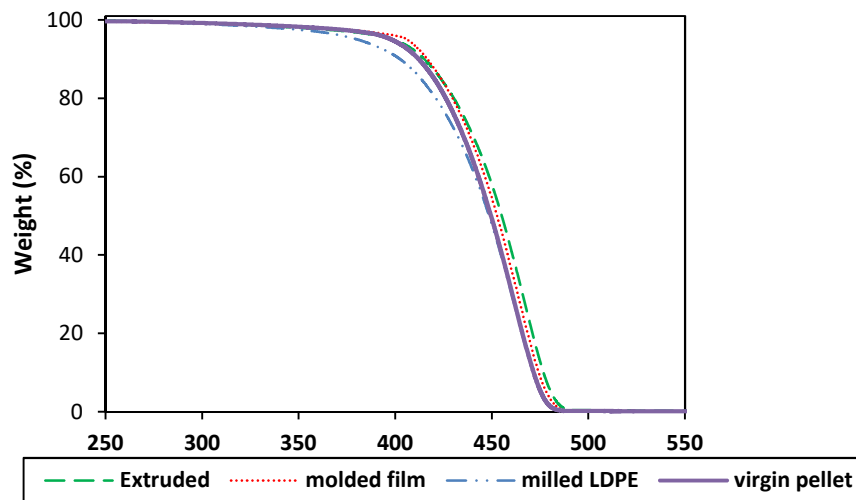


Figure 4.5: TG curve of different process LDPE samples (extruded film at 210-220°C, molded film at 120°C, 0.1 powder and virgin polymer) at heating ratio of 10°C/min

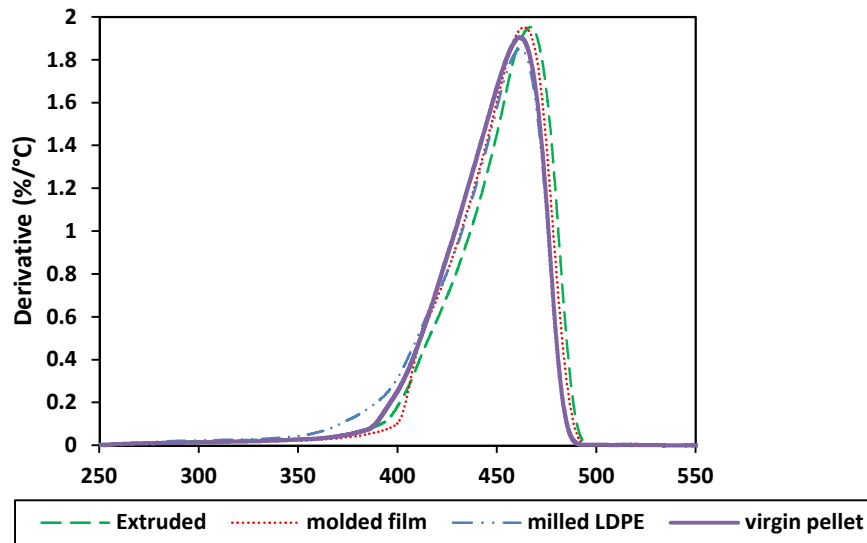


Figure 4.6: DTG curve of different process LDPE samples (extruded film at 210-220°C, molded film at 120°C, 0.1 powder and virgin polymer) at heating ratio of 10°C/min

4.1.3 Effect of catalyst loading on degradation of LDPE

Figure 4.7 represent TG and DTG curve LDPE degradation in absence of catalyst and various catalyst loading of 10%, 17.5% and 23% at heating rate of 20°C/min. It is noteworthy that addition of catalyst significantly boosts degradation process. The maximum degradation temperature all samples occurred around 412°C while it is 475°C for cracking of polyethylene.

The synergic effect of catalyst is evident here and the temperature difference is identical to value observed by comparing thermal and catalyst at different heating rates. Nevertheless, the amount of catalyst in the sample did not presented any significant effect of degradation. However, one should consider that TGA test is appropriate to investigate the evolution of primary products. At the same time all resulted solid, liquid and gaseous hydrocarbons devolatilizes after formation since furnace temperature is high.

4 Result and discussion of pyrolysis

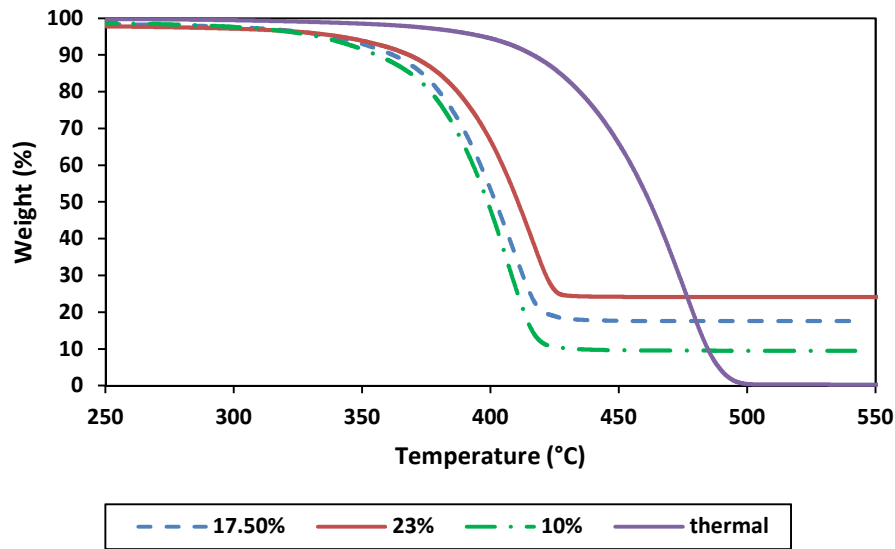


Figure 4.7: TG curve of catalytic degradation of LDPE with different ZSM-5 ratio: 24%,17.5%, 9% and 0% during TGA run at 20°C/min

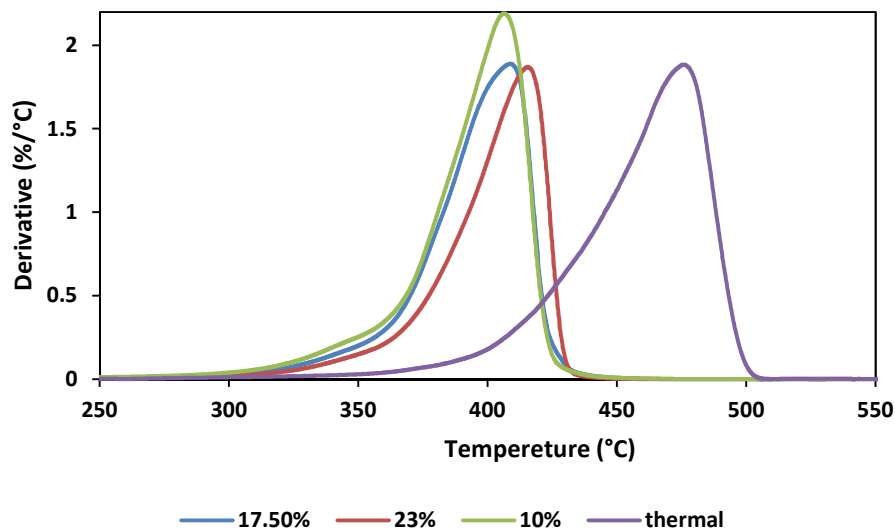


Figure 4.8: DTG curve of catalytic degradation of LDPE with different ZSM-5 ratio: 24%,17.5%, 9% and 0% during TGA run at 20°C/min

4.1.4 Screening activated and spent catalysts

Figure 4.10 and Figure 4.11 illustrate TG and DTG curve of activated catalyst and spent catalyst. Activated catalyst showed weight loss in two stages during entire run from ambient to 1000°C. First step initiated at room temperature and continued until 245°C and catalyst sharply lost its weight by 4 wt.%. During second stage, started after 245°C, catalyst lost its weight gradually until the end of experiment by 2 wt.%. The DTG curve showed that the weight loss rate in first stage was 5 times higher than second stage.

ZSM-5 is an inorganic material and no decomposition of structure is expected for temperatures below 1000°C. At the same time, no organic matter expected both on surface

4 Result and discussion of pyrolysis

and internal pore structure of catalyst as the catalyst have not been utilized before test. Numerous works observed the absorption of H₂O and CO₂ on zeolites [70-73]. Ohlin et al. [72] studied the desorption of CO₂ and H₂O from ZSM-5 structure. The outcome of this research revealed that increasing temperature expedite the desorption of these two components from zeolite. Hill et al. [73] concluded that adsorbed water forms a layer of film on catalyst external surface. The film poses a mass transfer barrier for molecules inside the internal pore structure of catalyst.

In present work, the activated catalyst has been exposed to air while transferring catalyst to TGA sample holder. Hence first stage of weight loss accounted for desorption of H₂O and CO₂ from external catalyst surface. After this process completed, the desorption of water and other components from internal surface became detectable (second stage of weight loss).

The spent catalyst used for TGA experiment, obtained from pyrolysis experiment at 450°C and catalyst to total feed ratio of 17.5 wt.%. During the TGA test, the sample once exposed to air and for another run it exposed to nitrogen. Similar to activated catalyst, both spent catalyst samples underwent weight loss in two stages. Desorption of adsorbed components from surrounding air by acid site observed in first stage of weight loss. By completion of this stage, the sample under air atmosphere resulted a sharp decline after 440°C, and catalyst lost its weight by 3%. The maximum weight loss rate observed at 550°C. No sharp weight fall observed for spent ZSM-5 in nitrogen, however the catalyst started to lose its weight gradually after 625°C until 1000°C and it did not reach to same weight as spent catalyst in air.

To interpret this meaningful difference at nitrogen and air atmosphere, it is worthwhile to know that coke is made of polyaromatic molecules [74, 75]. At the same time the spent catalyst was covered with a layer of coke. Hence the second stage of weight loss under nitrogen is due to degradation of organic matters deposit on cook, and combustion of this species on catalyst in air atmosphere led to weight change.

Figure 4.9 is a proof of this reasoning as appearance of spent catalyst after each run helps in realizing the effect of different carrier gas on decomposition of coke on catalyst. Activated unused ZSM-5 is white while the the spent catalyst had gray color due organic molecules deposited on its surface, and after calcination in air it became completely white. However, the color of catalyst after TGA test under nitrogen atmosphere is whitish-grey as result of incomplete degradation of coke.

Moreover, the effectiveness of calcination under air atmosphere is higher as its completion occurred at 625°C. On the other hand, 550°C can be confirmed as suitable temperature for regeneration to avoid destruction and deformation of ZSM-5 crystal structure.



Figure 4.9: From right to left: spent catalyst, catalyst sample subjected to air and catalyst subjected to nitrogen during TGA test

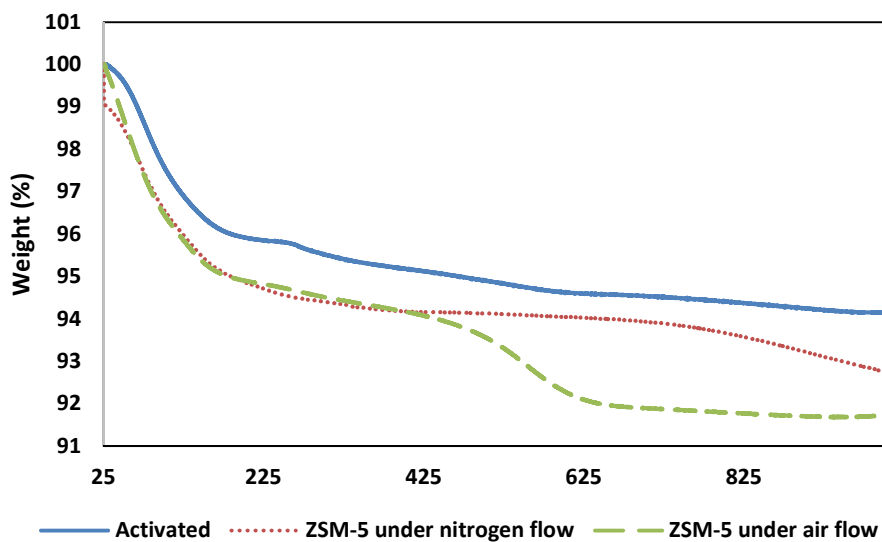


Figure 4.10: TG curve of activated ZSM-5 and spent ZSM-5 under different air and nitrogen flow

4 Result and discussion of pyrolysis

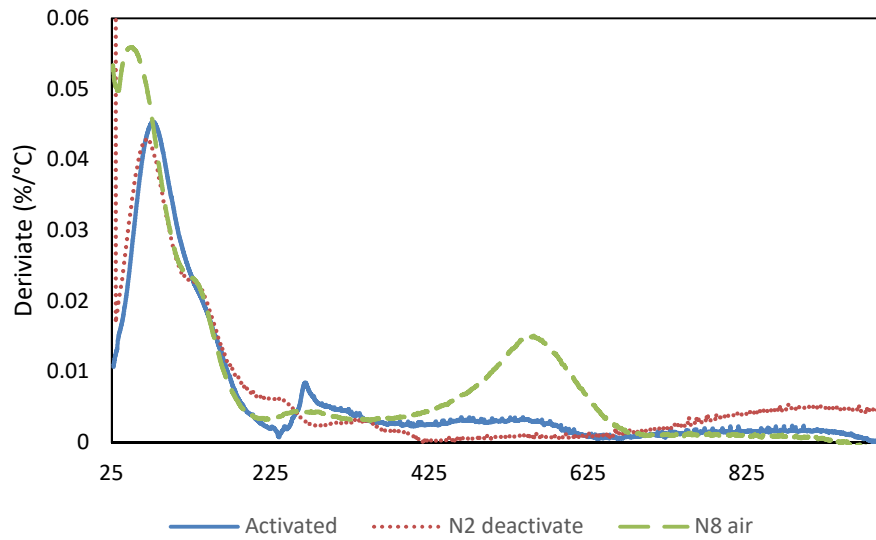


Figure 4.11: DTG curve of activated ZSM-5 and spent ZSM-5 under different air and nitrogen flow

4.2 Experimental design and optimization of products

The detailed outcome obtained from tailored experimental design is listed in Table 4.3. Appearance of obtained products from each experimental run can be find in Appendix C.

Table 4.3

Experiment Name	Temperature (°C)	Catalyst loading (%)	Liquid yield (%)	Gas yield (%)	Coke yield (%)	Residue (%)	
Thermal	N ₁	450	-	91.66	8.34	-	-
	N ₂	500	-	89.06	10.94	-	
	N ₃	550	-	90.46	9.64	-	
Catalytic	N ₄	450	17.5	29	71	2.16	
	N ₅	500	24.6	22.4	77.6	1.99	
	N ₆	400	9	54	46	4.12	
	N ₇	400	17.5	31.3	68.7	3.12	
	N ₈	400	24.6	33.56	63.24	3.92	3.2
	N ₉	500	9	21.46	78.54	2.49	
	N ₁₀	450	17.5	33	67	2.25	

4 Result and discussion of pyrolysis

4.2.1 Effect of process conditions on yield of products

Figure 4.12 represent the yield of major products obtained from thermal degradation of LDPE at 450, 500 and 550°C in a semi batch-reactor. All tests resulted a mean value of 90 wt.% waxes. Accordingly, total yield of gas was around 10% for all runs.

The low yield of gas resulted during almost 55 min, and therefore gas collection was not possible for further post analysis due to inappropriate gas bag. The thermal experiments were the first runs performed using this set-up. As result it was mostly part of a learning process to diagnose process-related issues and implementing necessary improvement. Thus, the experimental apparatus was equipped with an appropriate gas bag collection designed for low gas flow at the end of thermal series.

The products left the reactor in form of gas and all deposited in first washing bottle in form of solid. It was evident that they had high boiling point and their condensation can block outlet pipe. Luckily, in spite of inaccurate temperature control for the heating trace, no blockage or condensation of outlet pipe observed both during experiment and washing pipes afterwards.

After first run it is also observed that ramping time (25 min) from 200°C to set point during thermal pyrolysis is relatively high and feeds undergo degradation in relatively same heating rate (10-14°C/min) for all thermal test. Thus, temperature effect could not be investigated, and it can be concluded that all test experienced same process conditions. Therefore, same amount of liquid (waxy products) and gas observed after this experimental series. For that reason, rapid ramping to pyrolysis temperature (5 min) decided for catalyst series.

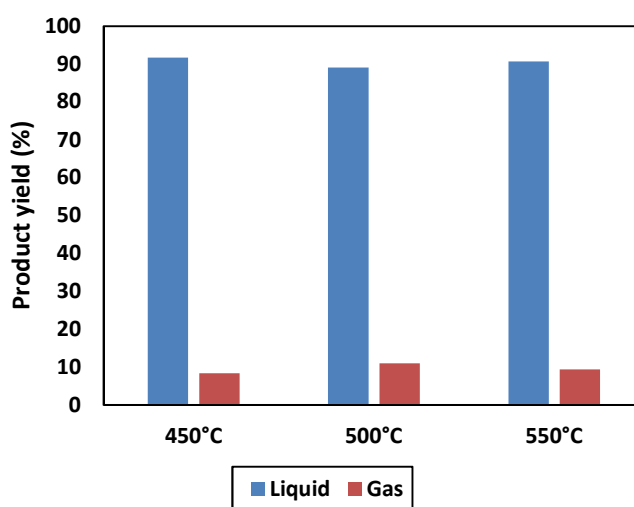


Figure 4.12: Yield of liquid and gaseous products after thermal pyrolysis series.

Figure 4.13 represent the yield of liquid products resulted after catalytic degradation of LDPE at two temperature levels of 400 and 500°C and high and low catalyst loading of 24 and 9 wt.%, respectively. It is noteworthy that catalytic pyrolysis had huge impact on lowering the total yield of liquid/wax products, compared to thermal run. Regardless of amount catalyst, liquid yield decreased by 70% to mean yield of 22 wt.% after using catalyst at 500°C. Low catalysis temperature at 400°C produced liquid between 33-54 wt.%. It is obvious that effect of temperature became dominant than catalyst ratio at high temperature, as both low and high catalyst ratio gave same yield of gas and oil. Effect of catalyst ratio was more considerable at

4 Result and discussion of pyrolysis

400°C as run with high amount of catalyst (24.9 wt.%) resulted 20% less oil than run at 400°C and 9 wt.% ZSM-5.

On the other hand, presence of gaseous product was almost dominant after all catalytic runs. The considerable gas yield in catalytic pyrolysis is due to strong acidity of ZSM-5 and its tendency to produce light C₂-C₄ gases. Therefore, more amounts of catalyst increase acid sites presented in polymer melt. At the same time higher temp boosted the catalyst performance for both catalyst ratios. These findings are in accordance with other researches that conducted pyrolysis of LDPE using ZSM-5 [59, 61, 76].

Therefore, it is evident that oil production for catalytic cracking is favored at low catalyst amount and low temperature. However lower temperature decreased the pace of reactions as continues bubbling in second washing bottle observed during experiments at 400°C. Therefore, resulted residue (3 wt.%) after experiment at 400°C and 24.6 wt.% of catalyst is explained by overproduction of intermediate products, due to high amount of acid sites, which could not degrade further as low temperature caused slower secondary reactions.

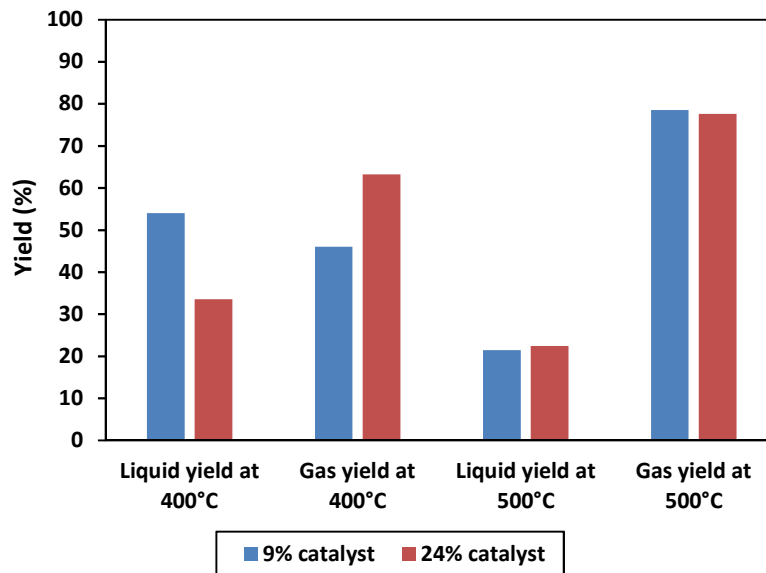


Figure 4.13: Yield of catalysis oil for high and low ratio of catalyst loading at 400 and 500°C.

The linear model equations for liquid yield, gas yield is expressed by equation 4.1 and 4.2. The model generated by using multiple linear regression (MLR) feature in software (MODDE).

$$y_{oil} = 32.1029 - 10.925x_1 - 4.87499x_2 + 5.345x_1x_2 \quad 4.1$$

$$y_{gas} = 67.44 - 11.725x_1 - 4.075x_2 - 4.545x_1x_2 \quad 4.2$$

Table 4.4 represent the main statistical indicators that suggests by MODDE 12.1 for evaluation of regressed models: oil and gas. The percent of variation of response from prediction and actual values is explained by R². A value close to 1 for R² is a necessity for a

4 Result and discussion of pyrolysis

good model, however it not the only parameter that should be considered for model validation. Q^2 represent the model prediction power for new data, and to having a valid model, Q^2 should be above 0.5. The model validity indicates the difference between model error than pure error in measurement of responses. Model validity higher than 0.5 is satisfactory and signify that the model error is in a same range as the pure error [77]. Reproducibility is also indicating the variation of responses for the same conditions (in this work it is the three experiments performed at 450°C and catalyst loading of 17.5%).

Table 4.4: statistical parameter that obtained from comparison of real response and response predicted by first-order model in MODDE 12.1

Model	Percent of variation	Prediction power	Model validity	Reproducibility
Liquid products	0.98	0.69	0.75	0.96
Gaseous products	0.97	0.39	0.64	0.96

The values represent a decent validity for model, however addition one more experiment would change the values as these models are only based on 7 experimental runs. In the other words, validation of process maturity through this statistical analysis is an ongoing process that should be realized by operation of more experiments.

Figure 4.14 represents visualized contour of regressed model (4.1)) for liquid yield as a function of catalyst loading and temperature. The counter mapped for predicted gas yield with respect to process condition can be found in Appendix D.

As it can be seen clearly, the optimum yield occurred at low level of both catalyst and temperature (400°C and 9 wt.% ZSM-5). Oil yield changes more rapidly at low temperature with changing catalyst amount. It further confirms the conclusion that made earlier regarding the more impact of catalyst ratio at lower temperature. Moreover, model predicts that pyrolysis with 24.6% catalyst at 425°C could results same oil as run with 9% ZSM-5 at 470°C. At the same time, point at 24.6% catalyst and 475°C is identical to pyrolysis with 9%

4 Result and discussion of pyrolysis

catalyst at 485°C. Therefore, it can be concluded from the model prediction that synergic effect of catalyst is lowered by increasing the pyrolysis temperature.

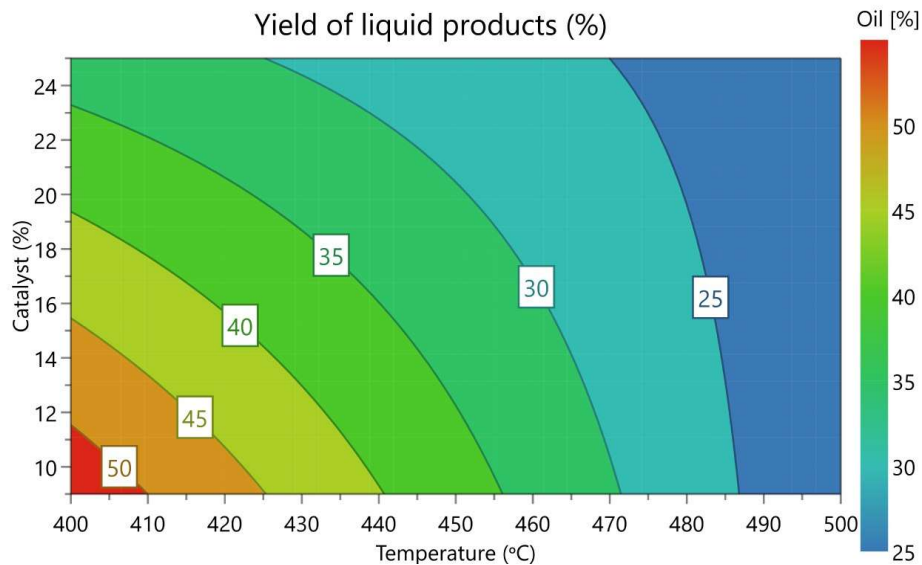


Figure 4.14: Visualized contour of liquid yield during catalytic cracking of LDPE at temperatures between 400 to 500°C and ZSM-5 (catalyst) loading of 9-24%

4.2.2 Effect of process conditions on coke deposition

The coke deposition is one of the most notable factors that should be considered in design and optimization, as the cost associated with regeneration of catalyst impose high energy and economical cost.

Figure 4.15 illustrate the coke yield resulted from catalytic cracking series in presented work. Increasing temperature decrease the amount of organic carbons formed on ZSM-5 internal and external surface. As mentioned earlier, ZSM-5 (heterogenous catalyst) is non-soluble in polyolefin melt. Also lack of appropriate stirring device causes uneven distribution of catalyst in reactor medium. Despite the mentioned fact, almost similar behavior for both catalyst ratio observed at each temperature. Therefore, this observation confirms dominate effect of temperature on coke yield in developed experimental apparatus.

4 Result and discussion of pyrolysis

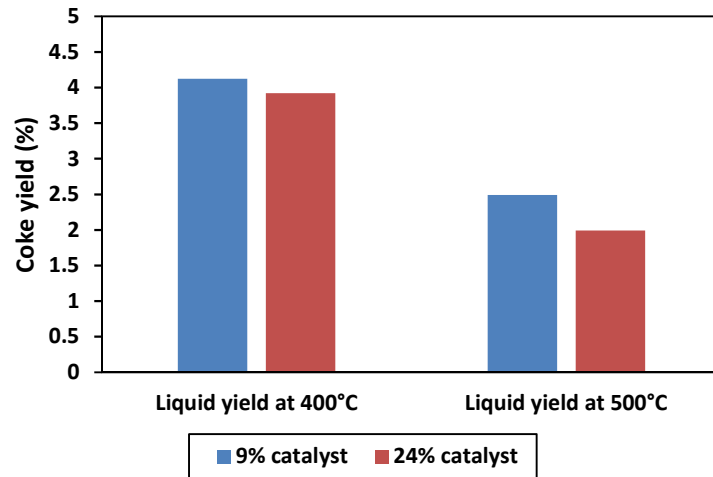


Figure 4.15: Weight percentage of coke which deposited on catalyst

The regressed first-order model for coke yield as a function of temperature, catalyst loading, and temperature-catalyst interaction is represented in equation 4.3:

$$y_{coke} = 2.86426 - 0.89x_1 - 0.175x_2 - 0.0750005x_1x_2 \quad 4.3$$

All factors in the model have negative sign in equation which explain that by increasing their value coke deposition will be attenuated. However, the effect of catalyst loading, and interaction is negligible in coke model as they have relatively low coefficient. Thus, the dominant effect of temperature on coke deposition can be further realized from the model. The visualized counter for coke response with respect to temperature and catalyst loading can be found in Appendix D.

4.3 Effect of temperature and catalyst ratio on product distribution

4.3.1 Analysis of liquid products

Figure 4.16 represents the carbon number distribution of products obtained from thermal pyrolysis at 450°C and catalytic pyrolysis using ZSM-5 at different catalytic loading of 9 and 24.6% and temperature between 400-500°C.

Thermal pyrolysis produced more than 75 wt.% of C₂₀₊ wax in condensable products. This fact explained the solid nature for products obtained through all thermal pyrolysis as they have relatively high melting and boiling point. However, around 25 wt.% of products are consisted of gasoline (C₅-C₁₂) and diesel range (C₁₂-C₂₀) which can be separated from the wax for further utilization as commercial fuels.

At the same time, the wax products obtained from plastic pyrolysis has characteristics identical to Fischer-Tropsch waxes with recognized commercial value to be used in

4 Result and discussion of pyrolysis

production of lubrication base oil [78]. Moreover, the wax can be further upgraded to valuable hydrocarbons with high yield of propylene by fluid catalytic cracking process [79].

Addition of catalyst significantly shifted the products toward C_5 - C_{12} , as all of products after catalytic series have consisted of above 88 wt.%. C_5 - C_{12} . During pyrolysis with low catalyst loading (9%) all intermediate products have been completely converted to C_5 - C_{12} spectrum. However, in case of high loading of catalyst, there is minor presence of C_{12+} hydrocarbons. Specially this shift was more intense at 500°C at which presence of C_{40+} observed. Zhang et al. [59] conducted ex-situ catalytic cracking of LDPE over ZSM-5 and fully achieved C_5 - C_{12} hydrocarbons in pyrolysis products rich in aromatics component which had a potential to be used as gasoline fuel.

To find out the reason for meaningful difference, one should notice that unlike ex-situ catalytic cracking, in-situ catalytic pyrolysis in semi-batch reactor used during this research work. Thus the intermediate products had less time to contact catalytic after their formation. This fact can be further realized as C_{20+} appeared in product at high level of catalytic loading while highest amount of acid sites presented in polymer melt. With no doubt, more acid sites expedited cracking reactions which resulted in higher amount of gas (above 63 wt.%) and caused pressurization of reactor. Subsequently higher outflow of formed volatile products occurred. The higher temperature intensified this outflow as presence of even C_{40+} observed in liquid after the experiment N₅. As result it can be concluded that these shifts toward heavy hydrocarbons are due to limited control on residence time of products in the semi-batch reactor medium caused by high catalyst and intensified at higher temperature.

To further investigate the catalytic cracking, it is worthwhile to establish separate catalytic unit to offset the uncertainty regarding the residence time. On the other hand, due to high yield of catalysis products in C_5 - C_{12} spectrum, the specific component in liquid part should be identified for in depth analysis of the obtained liquid. The GC method (ISO 3924:2016) utilized for detection of condensable products, was more appropriate for large spectrum hydrocarbons. C_{12} hydrocarbon had retention time below 2 min while the whole run time was 30 min (see Appendix E). As result, a dedicated method for analysis of gasoline (C_5 - C_{12}) and diesel ranged products (C_{12} - C_{20}) is necessary to identify different groups of hydrocarbons in liquid obtained from catalytic cracking. Another alternative is to test liquid sample with gas chromatography/mass spectroscopy (GC/MS). This method helps with detailed identification of every single component presented in product.

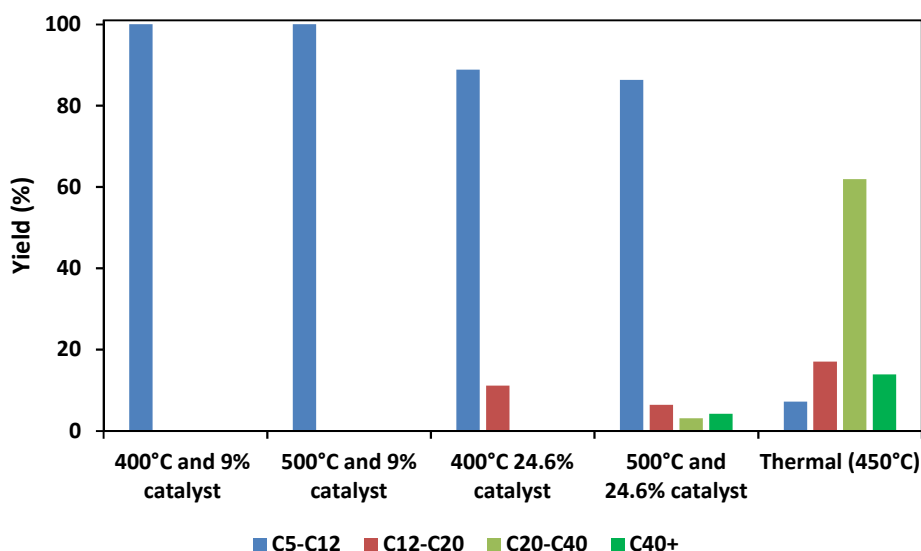


Figure 4.16: Distribution of carbon number of condensable products obtained from thermal and catalytic pyrolysis

4.3.2 Analysis of gaseous products

The analysis of component in gaseous products is discussed in this section. Obtained chromatogram for each gas analysis can be found in Appendix E.

Gaseous products with high yield between 46-63% were one of the noticeable products of catalytic pyrolysis of LDPE over ZSM-5. As result their analysis is valuable in order to gain knowledge about this recently established process and degradation pathway of LDPE in presence of catalyst. Gas collection done with gas bag for 30s while 30 minutes left to the end of experiment. Because of previously mentioned reasons, gas collection performed successfully only for catalytic series. Due to some operational constrains as part of this thesis work, the gas analysis was limited only to ethane, ethylene, propane and propylene components in gas phase.

Figure 4.17 illustrates yield of ethane, ethylene, propane and propylene presented in gas phase during catalytic series. It can be seen from the graph that propane was the most dominant product in gas phase. It reached to its maximal value after catalytic pyrolysis at 400°C with 24.6% wt. catalyst and its minimal value after running at 500°C and 9% wt. catalyst. At the same time ethylene and propylene showed an opposite trend while the yield of propane was highest (23% wt.), ethylene and propylene yields reached to the lowest values of 1 and 7% wt., respectively.

Production of C₂-C₄ olefins is favored by catalytic pyrolysis of polyolefins over ZSM-5 [48, 59, 64]. Higher catalytic temperature and higher catalyst ratios expedites cracking of waxes to intermediate products. Afterwards, aromatization and hydrogen abstraction reactions lead to production of light olefins in gas phase as by products [59].

4 Result and discussion of pyrolysis

The effect of catalytic temperature is obvious as total yield of ethylene and propylene had maximum mean value of around 17.5 wt.% at 500°C. Declination of propane is proof for better catalytic performance at higher temperature as conversion of propane to propylene occurs at presence of ZSM-5 [80]. This fact can be further realized by reminding the high gas yield at 500°C for both catalyst loading level which indicated higher performance of catalytic pyrolysis.

On the other hand, high level of catalyst at each temperature level negatively affected the yield of propylene and favored propane production. It is worthwhile to mention that the gaseous products from pyrolysis with 24.6 wt.% catalyst had shorter resident time in comparison with runs with 9%wt. ZSM-5. Indeed, it clarifies the declination of both propylene and ethylene in gas at high catalyst concentration as less residence time and incomplete contact of products with ZSM-5 resulted less olefins.

On the other hand, between 60-65% of gases were consisted of the C₃₊ gaseous hydrocarbons. Therefore, during future pyrolysis experiment, their mixture should be identified to analysis the trends and product distribution with high level of confidence.

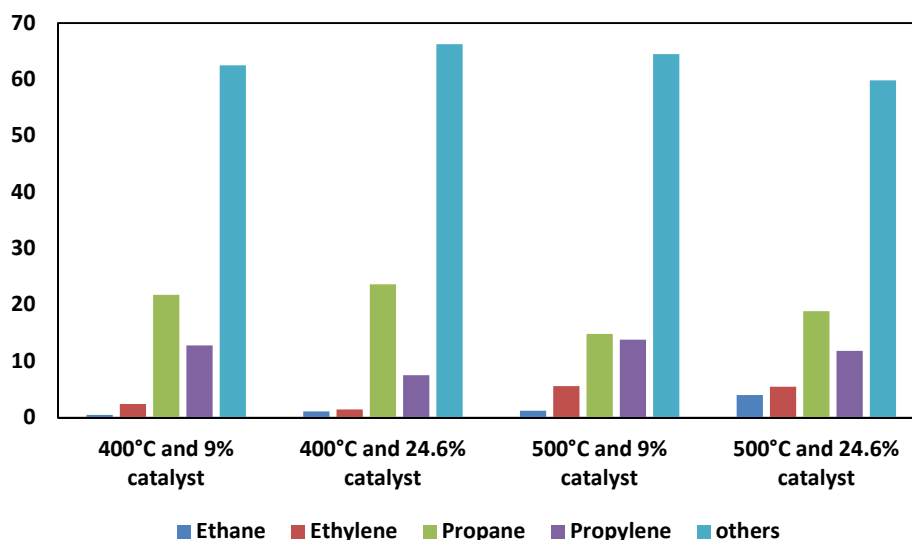


Figure 4.17: Composition of gaseous products obtained from catalytic series during presented work

4.3.3 Identification of functional groups in liquid products

The IR spectrum of obtained liquid/wax products is presented and discussed here. Samples in each series showed a similar peak. Therefore, one sample with strong and detectible peaks, selected for analysis and comparison in this section. IR spectrum of all obtained samples is shown in Appendix F.

Figure 4.18 illustrates the IR spectrum of wax sample obtained from thermal pyrolysis of LDPE. The presence of peaks between 2955, 2920 and 2850 cm⁻¹ is proof for presence of C-H stretch in -CH₃. The peaks at 1464 to 1377 region is an indicator for presence of -CH₂- and C-CH₃ bonds which explain the presence of aliphatic hydrocarbons in molecular structure of wax [40].

4 Result and discussion of pyrolysis

Noticeably, the peaks at 3076, 1641, 909 and 720 cm^{-1} are strong evidence for presence of double bond hydrocarbon in the products. Specifically, the peak at 990 is accounted for -CH=CH- (trans) and peak at 719 for -CH=CH- (cis) bonds. Moreover, peaks at 964 cm^{-1} resulted from the vibration of double carbon bonds at the end of chain (-CH=CH₂) [81]. The obtained result is solid proof for presence of alkadiene and alkene hydrocarbons in wax products. This fact further confirmed by comparing with GC/MS analysis of products obtained by thermal pyrolysis of LDPE. The products were mainly consisted of alkanes, alkene and alkadiene groups [82].

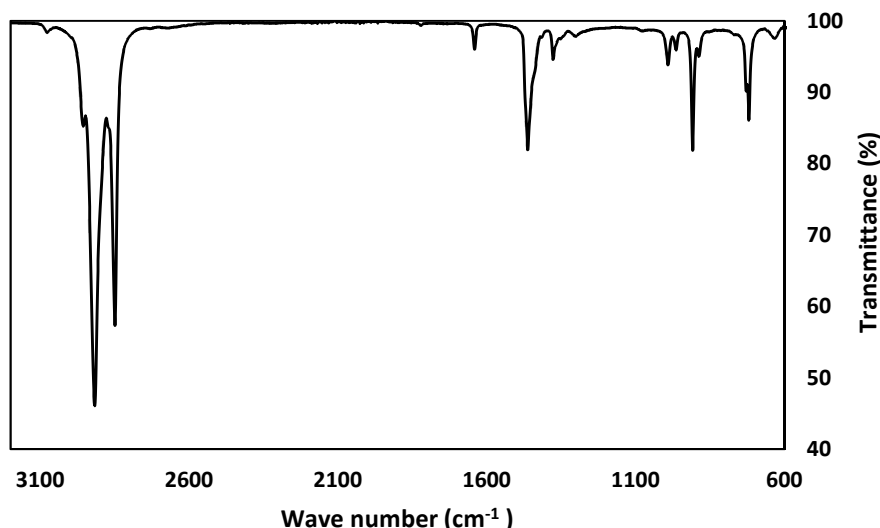


Figure 4.18: IR spectrum of wax sample obtained from thermal pyrolysis of LDPE at 450°C

Figure 4.19 shows the IR spectrum of liquid product obtained from catalytic pyrolysis of LDPE at 500°C and high level of catalyst (24.6%). The peaks at 2957 indicating the presence of C-CH₃ and peak at 2857 and 2929 cm^{-1} is accounted for -CH₂- bonds. The peak at 1456 and 1377 are accounted for -CH₂- and C-CH₃ respectively.

For the rest of spectrum, specially between 600~1050 cm^{-1} numerous peak observed which their detail interpretation would be out of time allocation and scope of this work. However, it is a strong proof of evolution of new functional groups with more complicated molecular structure which resulted more peaks in different wavelength. Zhang et al.[59] concluded that pyrolysis of LDPE over ZSM-5 favors oligomerization, cyclization and aromatization reaction. Knowing this fact helps to identify key peaks that indicates presence of aromatics. The peak at 3025 cm^{-1} is strong evidence of formation of C=C-H bonds in aromatics, as they are expected to occur above 3000 cm^{-1} . This fact is further confirmed by identifying the relatively strong peak at 1604 cm^{-1} which is an indicator for C=C stretch in aromatics [40].

Aforementioned, ZSM-5 shifts pyrolysis products toward gasoline range and hydrocarbon. Thus, comparing this spectrum with available IR spectrum for gasoline mixture reveals appropriate match, as numerous peaks are also observed for gasoline with same intensity between 600~1000 cm^{-1} [83]. However, source of this peak is still unknown as different mono, meta, ortho and para aromatic hydrocarbons can emit wave length with same intensity in mentioned region [81].

4 Result and discussion of pyrolysis

In conclusion presence of unsaturated aromatics are expected in liquid samples obtained from catalytic pyrolysis of LDPE over ZSM-5.

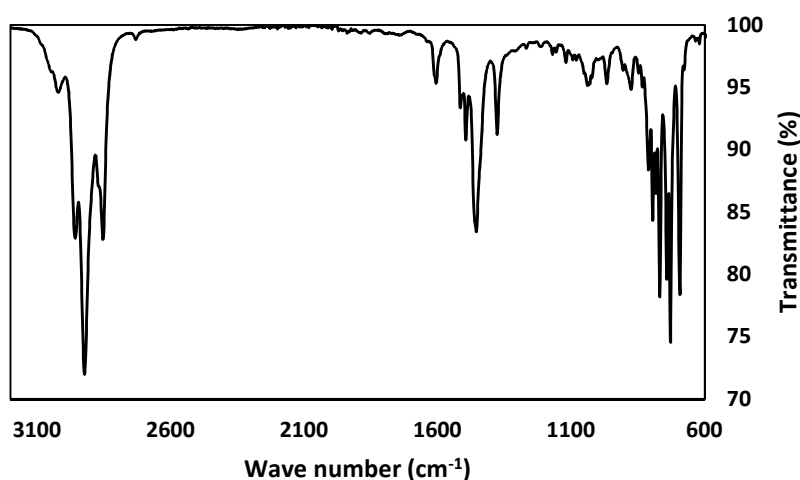


Figure 4.19: IR spectrum of wax sample obtained from thermal pyrolysis of LDPE at 500°C and 24.6 wt.% ZSM-5

4.4 Reproducibility of result and sources of error

Figure 4.20 illustrates Distribution of hydrocarbon with respect to their carbon number in wax product. Aforementioned, thermal series was part of learning process to gain insight into the developed set-up. As there was uncertainty regarding the condensation of wax in reactor outlet pipe, non-measurable nitrogen flow maintained in system to assure continues outflow of volatile product during experiment. Therefore, the residence time of products is associated with high level of uncertainty which can lead to different distribution of secondary products.

As all of test resulted same amount of liquid and gas, it is worthwhile to detect changes that observed in carbon distribution of obtained wax samples.

According to Figure 4.20 run at 550°C resulted a high level of error and it was not utilized for further analysis of pyrolysis results. Compared to thermal run at 450°C, less amount of C₂₀-C₄₀ and more amount of C₄₀₊ resulted for run at 500°C, while the trend should be reversed as 500°C had higher temperature and more cracking to lighter hydrocarbons expected. Therefore, the run at 450°C picked as the most credible pyrolysis run for thermal test.

4 Result and discussion of pyrolysis

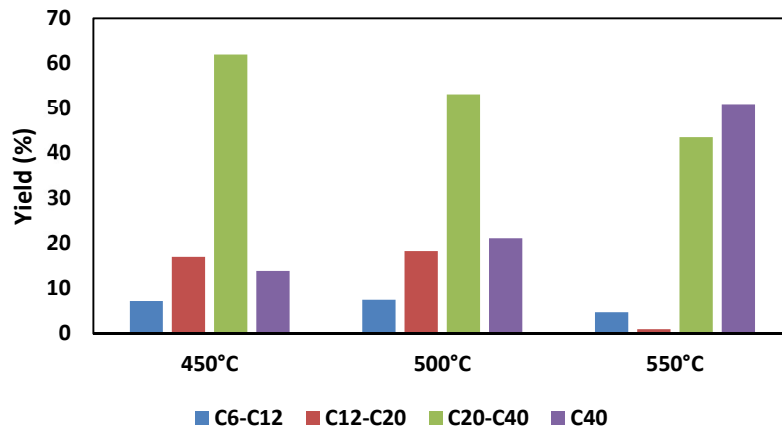


Figure 4.20: Distribution of hydrocarbon with respect to their carbon number in wax product

Figure 4.21 represents the yield of major products obtained from catalytic pyrolysis at mid-level of catalyst loading (17.5 %wt.) and 450°C. Liquid, gas and coke yield showed a perfect match for all runs.

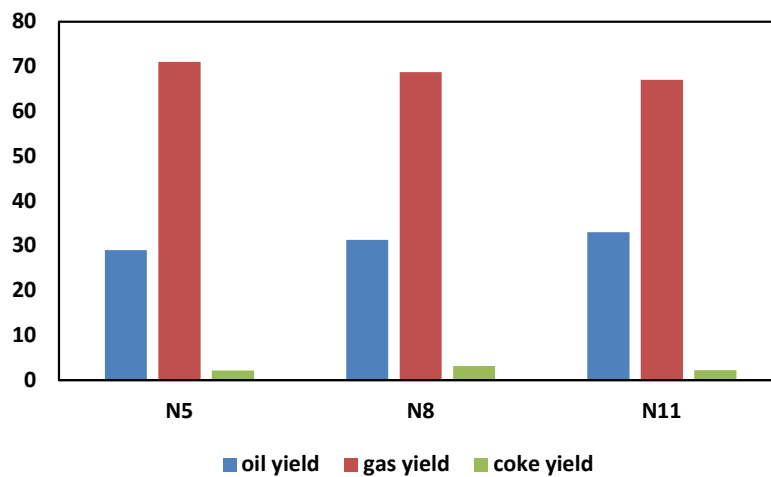


Figure 4.21: yield of major products obtained from catalytic pyrolysis at mid-level of catalyst loading (17.5 wt.%) and 450°C

Figure 4.22 illustrates the yield of different group of hydrocarbons at mid-level of catalyst amount 17.5 wt.% and 450°C. All tests demonstrated same result and presence of very low amount of C₂₀-C₄₀ (below 1% wt.) was negligible.

4 Result and discussion of pyrolysis

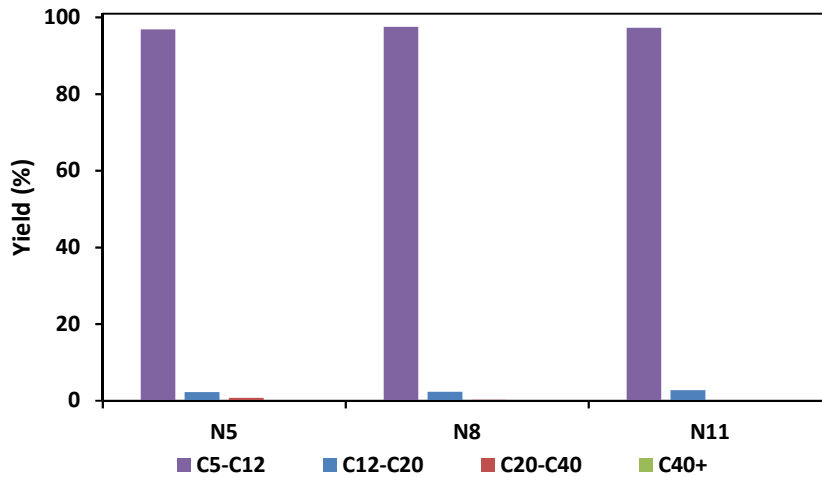


Figure 4.22: Yield of different spectrum of hydrocarbons during experiments at 450°C and 17.5 wt.% catalyst

Figure 4.23 illustrates yield of detectable gas components (ethane, ethylene, propane and propylene) along with yield of other gases for experiments at center point of planned experimental work (Figure 3.5)

Experiment number N₁₁ seems to have highest error for propane and propylene. However, it still reveals that at high yield of alkanes and low yield of alkenes in gas, is expected.

However, yield of all component varied noticeably for same operational condition. With no doubt gas products have lower residence time than formed volatile products as they have higher diffusivity. Unlike liquid sampling which performed from begging to the end of experiment, gas sampling implemented only for 30s of 35 long experiment. As results it is highly recommended to equip the set-up with several and smaller gas bags and perform gas sampling several times from beginning to end of experiment.

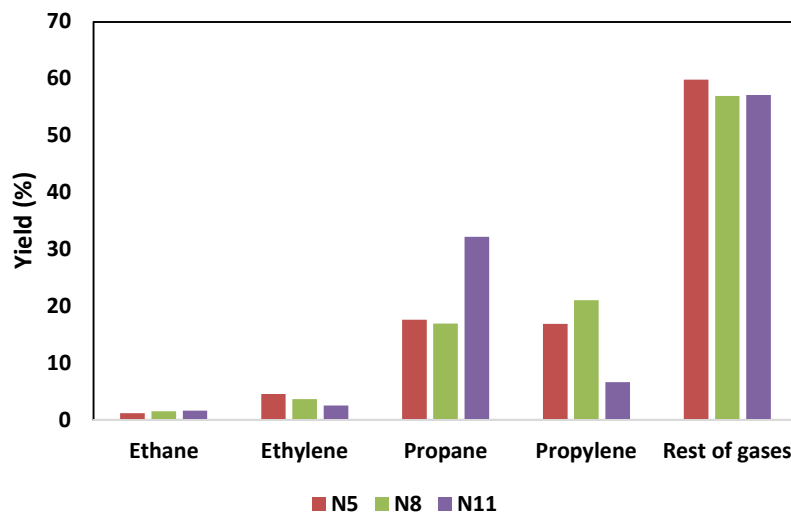


Figure 4.23: Yield of gaseous components during experiments at 450°C and 17.5 wt.% catalyst

5 Conclusion and proposal for future experimental work

In this study, an improved semi-batch bench-scale pyrolysis set-up was utilized to evaluate recovery of valuable hydrocarbons from LDPE through thermal and catalytic pyrolysis using ZSM-5. The impact of temperature and catalyst loading on resulted products discussed by using outcome from different analytical methods.

Induction heating used to heat up the reactor. The method leads to direct heating of reactor body through alternation of magnetic fields results in fast, controllable and energy efficient way of heating.

Preliminary heating tests on reactor body showed that the mid-point at bottom of reactor on external surface is best indicator for melt temperature inside reactor and can be used for control of heating source.

Collection of condensable products can be done effectively, and condensable sample is a good representative of products evolved from start to end of experiment. Addition of heating trace to outlet of reactor prevented any blockage of wax at the outlet of reactor.

The effect of residence time of formed products cannot be investigated in semi-batch reactor as there is no control on outflow of products. Moreover, semi-batch is not appropriate for low heating rates (10-14°C/min) in thermal pyrolysis of LDPE.

Thermal pyrolysis results wax products with high yield of 90 wt.%. Catalytic cracking with ZSM-5 decrease liquid yield up to 70 wt.%. Regardless of ZSM-5 loading, the effect of temperature was dominant and higher temperature favored production of more gaseous products. The ZSM-5 ratio had more impact at lower temperature by favoring gas production. The most optimum liquid yield (54 wt.%) resulted at lowest catalyst ratio (9 wt.%) and lowest pyrolysis temperature (400°C).

According to GC analysis thermal pyrolysis resulted waxy products consisted of 75 wt.% heavy C₂₀₊ hydrocarbons. Addition of ZSM-5 effectively shifts products to gasoline range (C₅-C₁₂) in liquid phase and high yield of gas (46-78 wt.%) with considerable amount of ethylene and propylene close to 20 wt.% of gas.

Identification of hydrocarbons in products was done by using FTIR analysis. Thermal pyrolysis results aliphatic hydrocarbon: alkane, alkene and alkadiene. The results from liquid analysis obtained from catalytic pyrolysis showed that ZSM-5 favors the production of aromatic hydrocarbons in liquid.

TGA experiment at low heating rate is appropriate for simulation of thermal and catalytic degradation of LDPE. According to TGA analysis plastic process do not have effect on degradation behavior of LDPE. However, presence of ZSM-5 decreases the maximum degradation temperature by 60-70°C. TGA analysis showed that ZSM-5 can be regenerated at 550°C to be further utilized for pyrolysis.

This experimental work gave in-depth knowledge about the already existed issues that should be facilitated as part of future experimental work. The improvements are not only related to

5 Conclusion and proposal for future experimental work

set-up but also to analytical methods for analysis of products. The main aspects that be considered are:

- Implementation of a subsequent cracking unit that assure complete contact of catalyst with volatile products formed from thermal pyrolysis
- Implementing gas collection as much as possible from the start to the end of experiments in order to have appropriate gas sampling
- Utilization of GC/MS for further analysis of product presented in fuel
- Replication of experiments at each process condition to further detect variation than can be produced by external source
- More dedicated experimental works for same feed and various catalysts differed by their acidity and pore size

References

- [1] J. R. Jambeck *et al.*, "Plastic waste inputs from land into the ocean," *Science*, 10.1126/science.1260352 vol. 347, no. 6223, p. 768, 2015.
- [2] E. Commission, "A European Strategy for Plastics in a Circular Economy," 2018.
- [3] *Plastics - the Facts 2017*. Available: <https://www.plasticseurope.org/en/resources/market-data>
- [4] D. S. Achilias, C. Roupakias, P. Megalokonomos, A. A. Lappas, and E. V. Antonakou, "Chemical recycling of plastic wastes made from polyethylene (LDPE and HDPE) and polypropylene (PP)," *Journal of Hazardous Materials*, vol. 149, no. 3, pp. 536-542, 2007/11/19/ 2007.
- [5] K. Ragaert, L. Delva, and K. Van Geem, "Mechanical and chemical recycling of solid plastic waste," *Waste Management*, vol. 69, pp. 24-58, 2017/11/01/ 2017.
- [6] M. Gear, J. Sadhukhan, R. Thorpe, R. Clift, J. Seville, and M. Keast, "A life cycle assessment data analysis toolkit for the design of novel processes – A case study for a thermal cracking process for mixed plastic waste," *Journal of Cleaner Production*, vol. 180, pp. 735-747, 2018/04/10/ 2018.
- [7] W. Posch, "3 - Polyolefins A2 - Kutz, Myer," in *Applied Plastics Engineering Handbook* Oxford: William Andrew Publishing, 2011, pp. 23-48.
- [8] P. Sharpe. (2015). *Making Plastics: From Monomer to Polymer*. Available: <https://www.aisce.org/resources/publications/cep/2015/september/making-plastics-monomer-polymer>
- [9] T. C. M. Chung, *Functionalization of Polyolefins*. Elsevier Science, 2002.
- [10] G. Dodbiba, N. Haruki, A. Shibayama, T. Miyazaki, and T. Fujita, "Combination of sink–float separation and flotation technique for purification of shredded PET-bottle from PE or PP flakes," *International Journal of Mineral Processing*, vol. 65, no. 1, pp. 11-29, 2002/05/01/ 2002.
- [11] S. D. Anuar Sharuddin, F. Abnisa, W. M. A. Wan Daud, and M. K. Aroua, "Energy recovery from pyrolysis of plastic waste: Study on non-recycled plastics (NRP) data as the real measure of plastic waste," *Energy Conversion and Management*, vol. 148, pp. 925-934, 2017/09/15/ 2017.
- [12] K. Crombie and O. Mašek, "Investigating the potential for a self-sustaining slow pyrolysis system under varying operating conditions," *Bioresource Technology*, vol. 162, pp. 148-156, 2014/06/01/ 2014.
- [13] V. Chhabra, Y. Shastri, and S. Bhattacharya, "Kinetics of Pyrolysis of Mixed Municipal Solid Waste-A Review," *Procedia Environmental Sciences*, vol. 35, pp. 513-527, 2016/01/01/ 2016.
- [14] *Petroleum Hydrocarbon Ranges*. Available: <http://www.caslab.com/Petroleum-Hydrocarbon-Ranges/>
- [15] D. Almeida and M. d. F. Marques, "Thermal and catalytic pyrolysis of plastic waste," *Polímeros*, vol. 26, pp. 44-51, 2016.

- [16] A. Oasmaa and S. Czernik, "Fuel Oil Quality of Biomass Pyrolysis Oils State of the Art for the End Users," *Energy & Fuels*, vol. 13, no. 4, pp. 914-921, 1999/07/01 1999.
- [17] I. Kalargaris, G. Tian, and S. Gu, "The utilisation of oils produced from plastic waste at different pyrolysis temperatures in a DI diesel engine," *Energy*, vol. 131, pp. 179-185, 2017/07/15/ 2017.
- [18] I. Ahmad *et al.*, "Pyrolysis Study of Polypropylene and Polyethylene Into Premium Oil Products," *International Journal of Green Energy*, vol. 12, no. 7, pp. 663-671, 2015/07/03 2015.
- [19] J. A. Conesa, R. Font, A. Marcilla, and A. N. Garcia, "Pyrolysis of Polyethylene in a Fluidized Bed Reactor," *Energy & Fuels*, vol. 8, no. 6, pp. 1238-1246, 1994/11/01 1994.
- [20] J. Scheirs and W. Kaminsky, *Feedstock recycling and pyrolysis of waste plastics: converting waste plastics into diesel and other fuels*. J. Wiley & Sons, 2006.
- [21] J. P. Mofokeng, A. S. Luyt, T. Tábi, and J. Kovács, "Comparison of injection moulded, natural fibre-reinforced composites with PP and PLA as matrices," *Journal of Thermoplastic Composite Materials*, vol. 25, no. 8, pp. 927-948, 2012/12/01 2011.
- [22] S. Zhou, M. Garcia-Perez, B. Pecha, S. R. A. Kersten, A. G. McDonald, and R. J. M. Westerhof, "Effect of the Fast Pyrolysis Temperature on the Primary and Secondary Products of Lignin," *Energy & Fuels*, vol. 27, no. 10, pp. 5867-5877, 2013/10/17 2013.
- [23] W. Kaminsky, J. Menzel, and H. Sinn, "Recycling of plastics," *Conservation & Recycling*, vol. 1, no. 1, pp. 91-110, 1976/01/01/ 1976.
- [24] N. Kiran Ciliz, E. Ekinci, and C. E. Snape, "Pyrolysis of virgin and waste polypropylene and its mixtures with waste polyethylene and polystyrene," *Waste Management*, vol. 24, no. 2, pp. 173-181, 2004/01/01/ 2004.
- [25] M. Sogancioglu, G. Ahmetli, and E. Yel, "A Comparative Study on Waste Plastics Pyrolysis Liquid Products Quantity and Energy Recovery Potential," *Energy Procedia*, vol. 118, pp. 221-226, 2017/08/01/ 2017.
- [26] D. Czajczyńska *et al.*, "Potential of pyrolysis processes in the waste management sector," *Thermal Science and Engineering Progress*, vol. 3, pp. 171-197, 2017/09/01/ 2017.
- [27] M. Balat, M. Balat, E. Kirtay, and H. Balat, "Main routes for the thermo-conversion of biomass into fuels and chemicals. Part 1: Pyrolysis systems," *Energy Conversion and Management*, vol. 50, no. 12, pp. 3147-3157, 2009/12/01/ 2009.
- [28] L. F. Albright and J. C. Marek, "Coke formation during pyrolysis: roles of residence time, reactor geometry, and time of operation," *Industrial & Engineering Chemistry Research*, vol. 27, no. 5, pp. 743-751, 1988/05/01 1988.
- [29] G. Duman, C. Okutucu, S. Ucar, R. Stahl, and J. Yanik, "The slow and fast pyrolysis of cherry seed," *Bioresource Technology*, vol. 102, no. 2, pp. 1869-1878, 2011/01/01/ 2011.
- [30] J. A. Onwudili, N. Insura, and P. T. Williams, "Composition of products from the pyrolysis of polyethylene and polystyrene in a closed batch reactor: Effects of temperature and residence time," *Journal of Analytical and Applied Pyrolysis*, vol. 86, no. 2, pp. 293-303, 2009/11/01/ 2009.

- [31] S. Khedri and S. Elyasi, "Kinetic analysis for thermal cracking of HDPE: A new isoconversional approach," *Polymer Degradation and Stability*, vol. 129, pp. 306-318, 2016/07/01/ 2016.
- [32] U. Hujuri, A. K. Ghoshal, and S. Gumma, "Modeling pyrolysis kinetics of plastic mixtures," *Polymer Degradation and Stability*, vol. 93, no. 10, pp. 1832-1837, 2008/10/01/ 2008.
- [33] T. Ozawa, "A New Method of Analyzing Thermogravimetric Data," *Bulletin of the Chemical Society of Japan*, vol. 38, no. 11, pp. 1881-1886, 1965/11/01 1965.
- [34] D. F. García, B. García, J. C. Burgos, and N. García-Hernando, "Determination of moisture diffusion coefficient in transformer paper using thermogravimetric analysis," *International Journal of Heat and Mass Transfer*, vol. 55, no. 4, pp. 1066-1075, 2012/01/31/ 2012.
- [35] N. M. a. P. Cherntongchai, "Cherntongchai Kinetic Analysis of Thermal Degradation of Polyolefin Mixtures," *International Journal of Chemical Engineering and Applications*, vol. 5, no. 2, pp. 169-175, 2014.
- [36] S. Singh, C. Wu, and P. T. Williams, "Pyrolysis of waste materials using TGA-MS and TGA-FTIR as complementary characterisation techniques," *Journal of Analytical and Applied Pyrolysis*, vol. 94, pp. 99-107, 2012/03/01/ 2012.
- [37] M. Ischia, C. Perazzolli, R. DalMaschio, and R. Campostrini, "Pyrolysis study of sewage sludge by TG-MS and TG-GC-MS coupled analyses," *Journal of Thermal Analysis and Calorimetry*, vol. 87, no. 2, pp. 567-574, 2007/01/01 2007.
- [38] K. Miteva, A. Slavcho, and G. Bogoeva-Gaceva, "Kinetic Analysis of Pyrolysis of Waste Polyolefin Mixture," *Arabian Journal for Science and Engineering*, vol. 41, no. 7, pp. 2601-2609, 2016/07/01 2016.
- [39] G. Elordi, G. Lopez, M. Olazar, R. Aguado, and J. Bilbao, "Product distribution modelling in the thermal pyrolysis of high density polyethylene," *Journal of Hazardous Materials*, vol. 144, no. 3, pp. 708-714, 2007/06/18/ 2007.
- [40] X. Jing, G. Yan, Y. Zhao, H. Wen, and Z. Xu, "Study on mild cracking of polyolefins to liquid hydrocarbons in a closed batch reactor for subsequent olefin recovery," *Polymer Degradation and Stability*, vol. 109, pp. 79-91, 2014/11/01/ 2014.
- [41] J. Aguado, D. P. Serrano, and J. M. Escola, "Catalytic Upgrading of Plastic Wastes," *Feedstock Recycling and Pyrolysis of Waste Plastics*, 2006.
- [42] W. Kaminsky and I.-J. N. Zorriquetta, "Catalytical and thermal pyrolysis of polyolefins," *Journal of Analytical and Applied Pyrolysis*, vol. 79, no. 1, pp. 368-374, 2007/05/01/ 2007.
- [43] D. P. Serrano, J. Aguado, and J. M. Escola, "Developing Advanced Catalysts for the Conversion of Polyolefinic Waste Plastics into Fuels and Chemicals," *ACS Catalysis*, vol. 2, no. 9, pp. 1924-1941, 2012/09/07 2012.
- [44] K. Iisa *et al.*, "In Situ and ex Situ Catalytic Pyrolysis of Pine in a Bench-Scale Fluidized Bed Reactor System," *Energy & Fuels*, vol. 30, no. 3, pp. 2144-2157, 2016/03/17 2016.
- [45] D. K. Ratnasari, M. A. Nahil, and P. T. Williams, "Catalytic pyrolysis of waste plastics using staged catalysis for production of gasoline range hydrocarbon oils," *Journal of Analytical and Applied Pyrolysis*, vol. 124, pp. 631-637, 2017/03/01/ 2017.

- [46] J. F. Mastral, C. Berruero, M. Gea, and J. Ceamanos, "Catalytic degradation of high density polyethylene over nanocrystalline HZSM-5 zeolite," *Polymer Degradation and Stability*, vol. 91, no. 12, pp. 3330-3338, 2006/12/01/ 2006.
- [47] G. Elordi *et al.*, "Catalytic pyrolysis of HDPE in continuous mode over zeolite catalysts in a conical spouted bed reactor," *Journal of Analytical and Applied Pyrolysis*, vol. 85, no. 1, pp. 345-351, 2009/05/01/ 2009.
- [48] A. Marcilla, M. I. Beltrán, and R. Navarro, "Thermal and catalytic pyrolysis of polyethylene over HZSM5 and HUSY zeolites in a batch reactor under dynamic conditions," *Applied Catalysis B: Environmental*, vol. 86, no. 1, pp. 78-86, 2009/02/02/ 2009.
- [49] D. P. Serrano, J. Aguado, and J. M. Escola, "Catalytic Cracking of a Polyolefin Mixture over Different Acid Solid Catalysts," *Industrial & Engineering Chemistry Research*, vol. 39, no. 5, pp. 1177-1184, 2000/05/01 2000.
- [50] R. van Grieken, D. P. Serrano, J. Aguado, R. García, and C. Rojo, "Thermal and catalytic cracking of polyethylene under mild conditions," *Journal of Analytical and Applied Pyrolysis*, vol. 58-59, pp. 127-142, 2001/04/01/ 2001.
- [51] M. Olazar, G. Lopez, M. Amutio, G. Elordi, R. Aguado, and J. Bilbao, "Influence of FCC catalyst steaming on HDPE pyrolysis product distribution," *Journal of Analytical and Applied Pyrolysis*, vol. 85, no. 1, pp. 359-365, 2009/05/01/ 2009.
- [52] G. Lopez, M. Artetxe, M. Amutio, J. Bilbao, and M. Olazar, "Thermochemical routes for the valorization of waste polyolefinic plastics to produce fuels and chemicals. A review," *Renewable and Sustainable Energy Reviews*, vol. 73, pp. 346-368, 2017/06/01/ 2017.
- [53] S. Eser. *Bronsted and Lewis Acid Sites*. Available: <https://www.e-education.psu.edu/fsc432/content/bronsted-and-lewis-acid-sites>
- [54] G. Manos, A. Garforth, and J. Dwyer, "Catalytic Degradation of High-Density Polyethylene over Different Zeolitic Structures," *Industrial & Engineering Chemistry Research*, vol. 39, no. 5, pp. 1198-1202, 2000/05/01 2000.
- [55] J. Aguado, D. P. Serrano, J. L. Sotelo, R. Van Grieken, and J. M. Escola, "Influence of the Operating Variables on the Catalytic Conversion of a Polyolefin Mixture over HMCM-41 and Nanosized HZSM-5," *Industrial & Engineering Chemistry Research*, vol. 40, no. 24, pp. 5696-5704, 2001/11/01 2001.
- [56] P. J. Donaj, W. Kaminsky, F. Buzeto, and W. Yang, "Pyrolysis of polyolefins for increasing the yield of monomers' recovery," *Waste Management*, vol. 32, no. 5, pp. 840-846, 2012/05/01/ 2012.
- [57] A. López, I. de Marco, B. M. Caballero, A. Adrados, and M. F. Laresgoiti, "Deactivation and regeneration of ZSM-5 zeolite in catalytic pyrolysis of plastic wastes," *Waste Management*, vol. 31, no. 8, pp. 1852-1858, 2011/08/01/ 2011.
- [58] K. Akubo, M. A. Nahil, and P. T. Williams, "Aromatic fuel oils produced from the pyrolysis-catalysis of polyethylene plastic with metal-impregnated zeolite catalysts," *Journal of the Energy Institute*, 2017/10/19/ 2017.
- [59] X. Zhang, H. Lei, G. Yadavalli, L. Zhu, Y. Wei, and Y. Liu, "Gasoline-range hydrocarbons produced from microwave-induced pyrolysis of low-density polyethylene over ZSM-5," *Fuel*, vol. 144, pp. 33-42, 2015/03/15/ 2015.

- [60] X. Zhang *et al.*, "From plastics to jet fuel range alkanes via combined catalytic conversions," *Fuel*, vol. 188, pp. 28-38, 2017/01/15/ 2017.
- [61] M. Artetxe, G. Lopez, G. Elordi, M. Amutio, J. Bilbao, and M. Olazar, "Production of Light Olefins from Polyethylene in a Two-Step Process: Pyrolysis in a Conical Spouted Bed and Downstream High-Temperature Thermal Cracking," *Industrial & Engineering Chemistry Research*, vol. 51, no. 43, pp. 13915-13923, 2012/10/31 2012.
- [62] X. Jing, Y. Zhao, H. Wen, and Z. Xu, "High Olefin Yield in Pyrolysis of Heavier Hydrocarbon Liquids Using Microwave as Heat Supplier," *Energy & Fuels*, vol. 31, no. 2, pp. 2052-2062, 2017/02/16 2017.
- [63] T. Ren, M. Patel, and K. Blok, "Olefins from conventional and heavy feedstocks: Energy use in steam cracking and alternative processes," *Energy*, vol. 31, no. 4, pp. 425-451, 2006/03/01/ 2006.
- [64] G. Elordi, M. Olazar, G. Lopez, M. Artetxe, and J. Bilbao, "Continuous Polyolefin Cracking on an HZSM-5 Zeolite Catalyst in a Conical Spouted Bed Reactor," *Industrial & Engineering Chemistry Research*, vol. 50, no. 10, pp. 6061-6070, 2011/05/18 2011.
- [65] D. P. Serrano, J. Aguado, J. M. Escola, J. M. Rodríguez, L. Morselli, and R. Orsi, "Thermal and catalytic cracking of a LDPE-EVA copolymer mixture," *Journal of Analytical and Applied Pyrolysis*, vol. 68-69, pp. 481-494, 2003/08/01/ 2003.
- [66] A. Adrados, I. de Marco, B. M. Caballero, A. López, M. F. Laresgoiti, and A. Torres, "Pyrolysis of plastic packaging waste: A comparison of plastic residuals from material recovery facilities with simulated plastic waste," *Waste Management*, vol. 32, no. 5, pp. 826-832, 2012/05/01/ 2012.
- [67] A. F. Azubuiké, "Experimental Study of Catalysis in Plastic Pyrolysis," Faculty of Technology, Natural sciences and Maritime Sciences, University of South-Eastern Norway, Porsgrunn, 2017.
- [68] K. Nakanoh, S. Hayashi, and K. Kida, "Waste treatment using induction-heated pyrolysis," *Fuji Electric Review*, vol. 47, no. 3, pp. 69-73, 2001.
- [69] J. Davies, *Conduction and induction heating*. P. Peregrinus Ltd. on behalf of the Institution of Electrical Engineers, 1990.
- [70] E. García-Pérez *et al.*, "A computational study of CO₂, N₂, and CH₄ adsorption in zeolites," *Adsorption*, vol. 13, no. 5, pp. 469-476, 2007/12/01 2007.
- [71] D. H. Olson, W. O. Haag, and W. S. Borghard, "Use of water as a probe of zeolitic properties: interaction of water with HZSM-5," *Microporous and Mesoporous Materials*, vol. 35-36, pp. 435-446, 2000/04/01/ 2000.
- [72] L. Ohlin, P. Bazin, F. Thibault-Starzyk, J. Hedlund, and M. Grahm, "Adsorption of CO₂, CH₄, and H₂O in Zeolite ZSM-5 Studied Using In Situ ATR-FTIR Spectroscopy," *The Journal of Physical Chemistry C*, vol. 117, no. 33, pp. 16972-16982, 2013/08/22 2013.
- [73] S. G. Hill and D. Seddon, "The hygroscopic nature of H-ZSM—5," *Zeolites*, vol. 5, no. 3, pp. 173-178, 1985/05/01/ 1985.
- [74] S. Du, D. P. Gamliel, M. V. Giotto, J. A. Valla, and G. M. Bollas, "Coke formation of model compounds relevant to pyrolysis bio-oil over ZSM-5," *Applied Catalysis A: General*, vol. 513, pp. 67-81, 2016/03/05/ 2016.

- [75] C. Henriques, J. Monteiro, P. Magnoux, and M. Guisnet, *Characterization of the Coke Formed During o-Xylene Isomerization over Mordenites at Various Temperatures*. 1997, pp. 436-445.
- [76] R. Bagri and P. T. Williams, "Catalytic pyrolysis of polyethylene," *Journal of Analytical and Applied Pyrolysis*, vol. 63, no. 1, pp. 29-41, 2002/03/01/ 2002.
- [77] G. Kanojia, G.-J. Willems, H. W. Frijlink, G. F. A. Kersten, P. C. Soema, and J.-P. Amorij, "A Design of Experiment approach to predict product and process parameters for a spray dried influenza vaccine," *International Journal of Pharmaceutics*, vol. 511, no. 2, pp. 1098-1111, 2016/09/25/ 2016.
- [78] S. J. Miller, N. Shah, and G. P. Huffman, "Conversion of Waste Plastic to Lubricating Base Oil," *Energy & Fuels*, vol. 19, no. 4, pp. 1580-1586, 2005/07/01 2005.
- [79] D. Kubička and R. Černý, "Upgrading of Fischer–Tropsch Waxes by Fluid Catalytic Cracking," *Industrial & Engineering Chemistry Research*, vol. 51, no. 26, pp. 8849-8857, 2012/07/04 2012.
- [80] G. J. Buckles and G. J. Hutchings, "Conversion of Propane Using H-ZSM-5 and Ga H-ZSM-5 in the Presence of Ga-H-ZSM-5 in the Presence of Co-fed Nitric Oxide, Oxygen, and Hydrogen," *Journal of Catalysis*, vol. 151, no. 1, pp. 33-43, 1995/01/01/ 1995.
- [81] P. Beauchamp. *IR, ¹H NMR, ¹³C NMR & MS Data Tables for spectroscopy*. Available: <http://www.cpp.edu/~psbeauchamp/courses.html>
- [82] P. T. Williams and E. A. Williams, "Fluidised bed pyrolysis of low density polyethylene to produce petrochemical feedstock," *Journal of Analytical and Applied Pyrolysis*, vol. 51, no. 1, pp. 107-126, 1999/07/01/ 1999.
- [83] K. Brudzewski, A. Kesik, K. Kołodziejczyk, U. Zborowska, and J. Ulaczyk, "Gasoline quality prediction using gas chromatography and FTIR spectroscopy: An artificial intelligence approach," *Fuel*, vol. 85, no. 4, pp. 553-558, 2006/03/01/ 2006.

Appendices

Appendix A: Task description

Appendix B: Unreacted polymer and wax obtained from heat test with 7.4 g of LDPE

Appendix C: Obtained products from thermal and catalytic cracking of LDPE using ZSM-5

Appendix D: Visualized contours based on predictive linear models

Appendix E: GC chromatogram for gas and liquid samples

Appendix F: FTIR spectrum of obtained liquid and wax products

Appendix A: Task description

HSN University College
of Southeast Norway
Faculty of Technology, Natural Sciences and Maritime Sciences, Campus Porsgrunn

FMH606 Master's Thesis

Title: Pyrolysis of plastic waste into green fuels – experimental study

USN supervisor: Prof. Lars-André Tokheim

External partner: Norner AS (Dr. Siw Fredriksen, Dr. Muhammad Bashir and Kai Arne Sætre)

Task background:

“Plastic has become the most common material since the beginning of the 20th century and modern life is unthinkable without it. Unfortunately, what makes it so useful, such as its durability, light weight and low cost, also makes it problematic when it comes to its end of life phase.” (European Commission, 2016).

Norner is a global provider of R&D services in polymers for the industry, located in Telemark. Norner has a comprehensive scientific laboratory, and the company competence and equipment covers a wide range of key technologies in the polymer and materials industry. Norner is expanding business and employees with 10% each year, and in 2018/2019, Norner will move to the new Telemark Powerhouse in Porsgrunn.



The European Commission has adopted an ambitious new Circular Economy Package to help European businesses and consumers to make the transition to a stronger and more circular economy where resources are used in a more sustainable way. The targets for plastic waste recycling in EU may be as high as 80 % in 2030. However, plastics packaging are often complex materials composed of several different materials that makes materials recycling challenging.

An alternative could be chemical recycling of plastic waste by thermal methods – pyrolysis – to produce hydrocarbon oils that in turn may be further cracked to provide ethylene and propylene, the building blocks for the most important plastic packaging polymers; polyethylene (PE) and polypropylene (PP).

In this project, the student will identify/screen catalyst(s) for pyrolysis of PE and PP. The student will carry out experimental work in Norner comprising pyrolysis of PE, PP as well as relevant mixed plastics packaging to map and, thereafter, suggest the process conditions and catalyst providing optimal product composition.

Task description:

The aim of the project is to study experimentally the process of plastic pyrolysis in order to improve pyrolysis selectivity by the use of catalyst and reaction conditions, in order to produce hydrocarbon oils suitable for production of ethylene and propylene in a second step.

Address: Kjølnes ring 56, NO-3918 Porsgrunn, Norway. **Phone:** 35 57 50 00. **Fax:** 35 55 75 47.

Appendix A: Task description

The specific tasks are:

1. A literature review on relevant catalysts for PE and PP pyrolysis
2. An experimental study of pyrolysis of PE, PP and plastics packaging (mixed plastics) with at least one commercial catalyst to investigate the effect of different catalyst properties on the liquid product composition. The properties of catalysts in focus will be either physical or chemical.
3. A complete report documenting the findings

References

Azubuikwe, F.A., Experimental study of catalysis in plastic pyrolysis, Master's thesis, University College of Southeast Norway, 2017

Ding *et al.*, Kinetic study of low temperature conversion of plastic mixtures to value added products, *Journal of Analytical and Applied Pyrolysis*, 2012, **94**; 83–90, https://www.researchgate.net/publication/256995981_Kinetic_study_of_low-temperature_conversion_of_plastic_mixtures_to_value_added_products

European Commission (2016), http://ec.europa.eu/environment/waste/plastic_waste.htm (accessed 7. November 2017)

Kunwar *et al.* Plastic to fuel: A review, *Renewable and Sustainable Energy Reviews*, 2016, **54**, 421-428, https://www.researchgate.net/publication/284131362_Plastics_to_fuel_a_review

Lopez *et al.*, Thermochemical routes for the valorization of waste polyolefinic plastics to produce fuels and chemicals. A review, *Renewable and Sustainable Energy Reviews* 73 (2017) 346–368.

Miandad *et al.* Catalytic pyrolysis of plastic waste: A review, *Process Safety and Environmental Protection* 2016, **102** (2016) 822–838, [http://www.jbiomech.com/article/S0957-5820\(16\)30108-2/pdf](http://www.jbiomech.com/article/S0957-5820(16)30108-2/pdf)

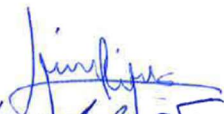
Serrano *et al.*, Developing Advanced Catalysts for the Conversion of Polyolefinic Waste Plastics into Fuels and Chemicals, *ACS Catalysis*. 2012, **2**, 1924–1941

Student category: PT or EET

Practical arrangements:

Practical work is planned to be carried out at USN and at Norner. From Porsgrunn, Norner can be reached by bus. Option 1: Route M1 from Porsgrunn to Stathelle, then P8 from Stathelle to Asdal. Option 2: Route P5 to Herre, then P8 from Herre to Asdal. The P5 and P8 routes are not very frequent. (Access to a car would make it easier to travel between Norner and USN, but is not a must.)

Signatures:

Student (date and signature): 30.01.2018 

Supervisor (date and signature): 30.01.2018 

Appendix B: Unreacted polymer and wax obtained from heat test with 7.4 g of LDPE

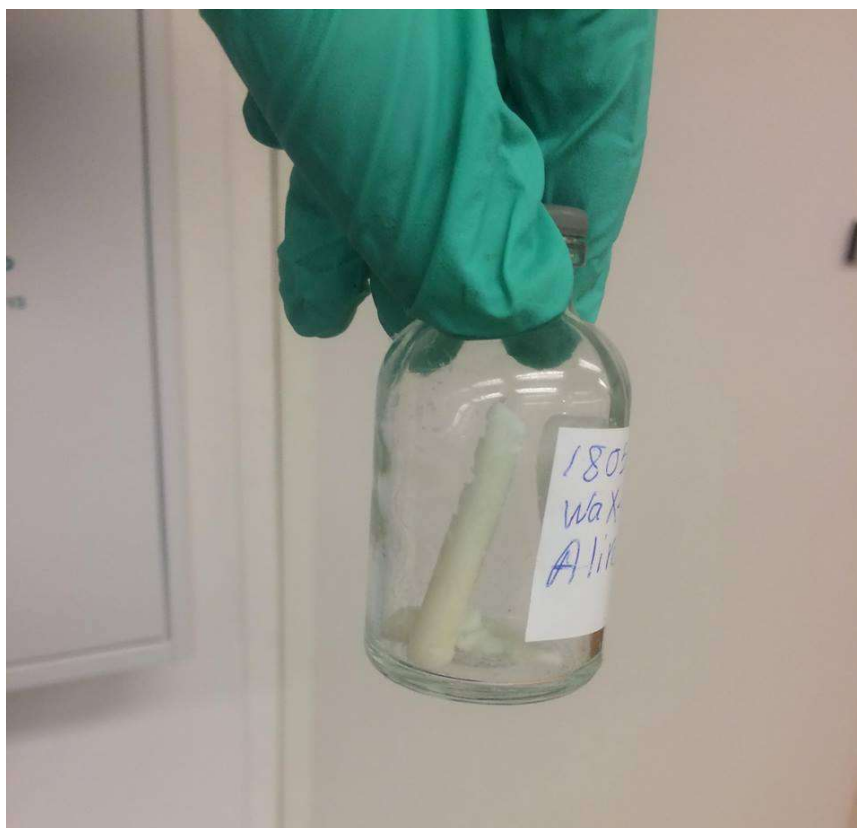


Figure B1: Obtained wax from heating test



Figure B2: Unreacted polymer obtained from heating test

Appendix C: Obtained products from thermal and catalytic cracking of LDPE using ZSM-5



Figure C1: from right to left: wax obtained from experiments number N1, N2 and N3

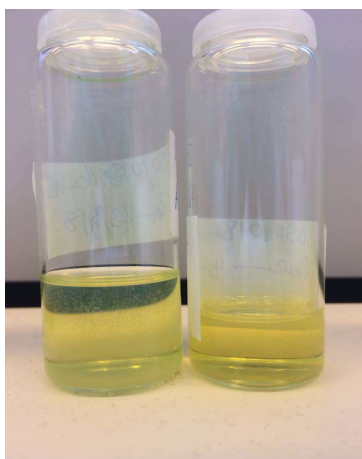


Figure C2: From right to left: liquid fuel obtained from experiment N9 and N6

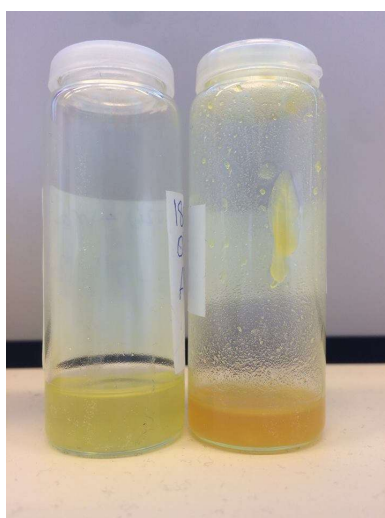


Figure C3: From right to left: liquid obtained from experiment N5 and N8



Figure C4: From right to left: liquid obtained from experiments N10, N7 and N4



Figure C5: residue left from experiment N8 inside the reactor

Appendix D: Visualized contours based on predictive linear models

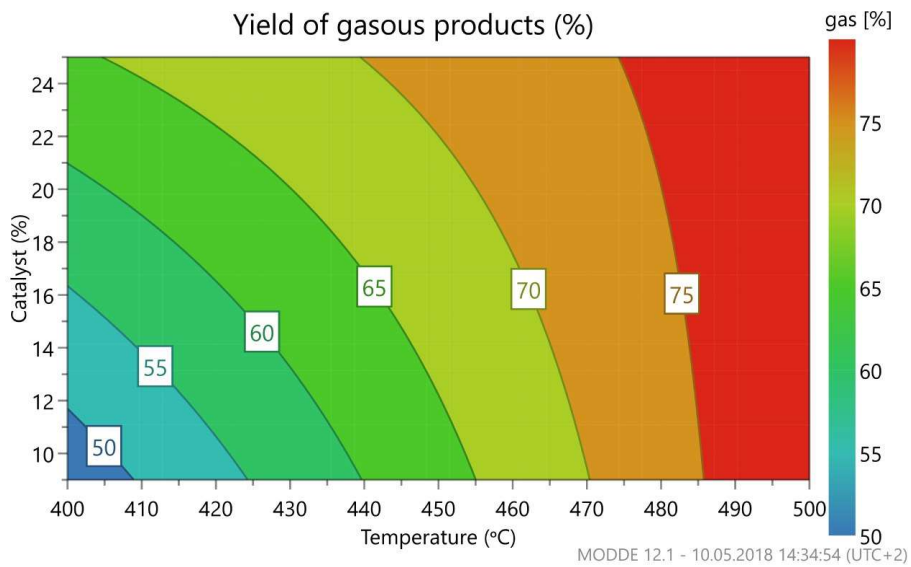


Figure D1: Visualized contour for gas yield response

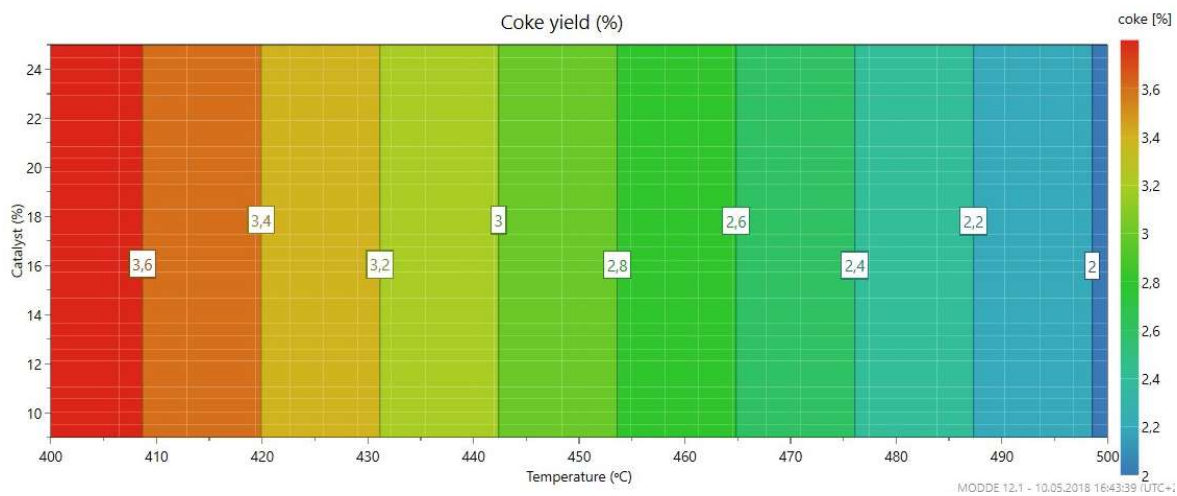


Figure D2: Visualized contour for coke yield response

Appendix E: GC chromatogram for gas and liquid samples

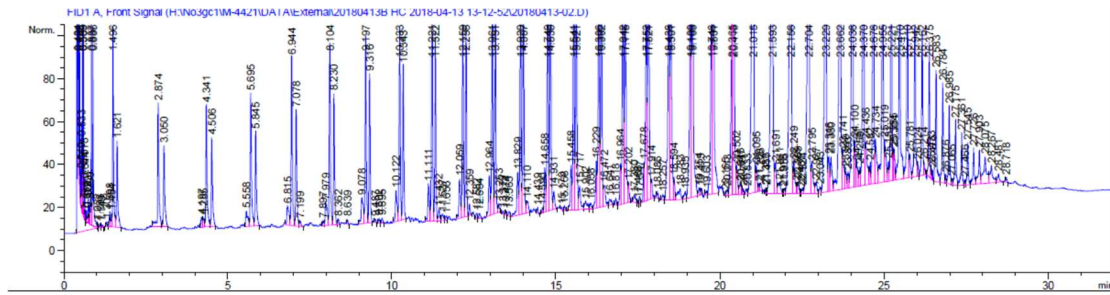


Figure D1: GC chromatogram of wax sample obtained from experiment N1

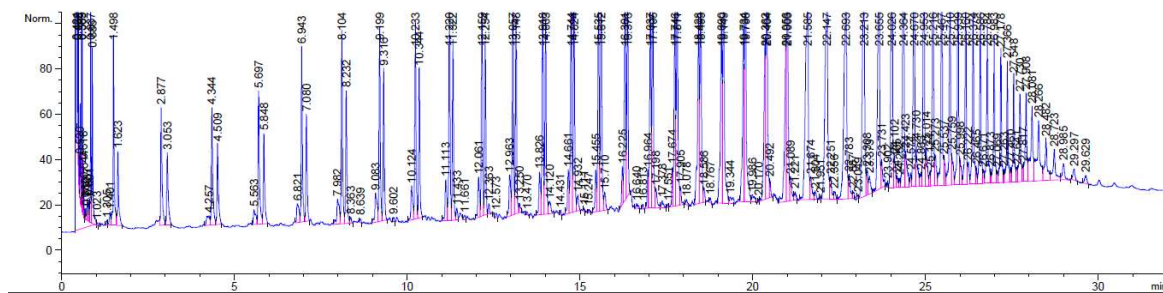


Figure D2: GC chromatogram of wax sample obtained from experiment N2

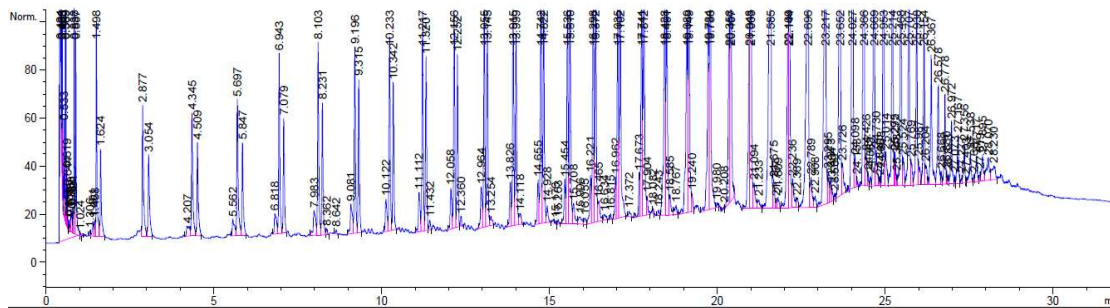


Figure D3: GC chromatogram of wax sample obtained from experiment N3

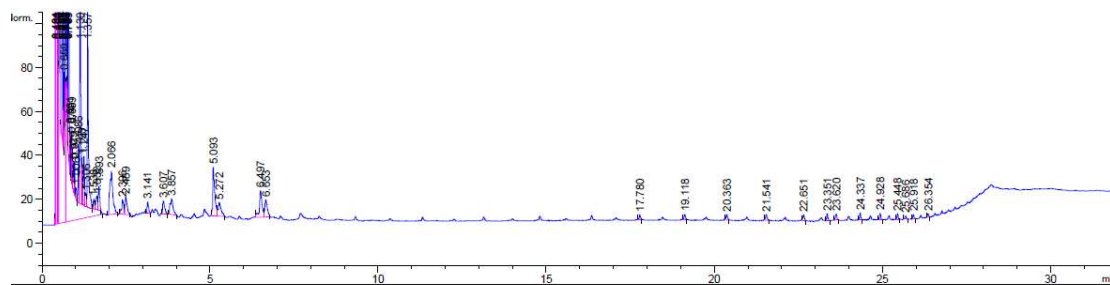


Figure D4: GC chromatogram of liquid sample obtained after experiment N5

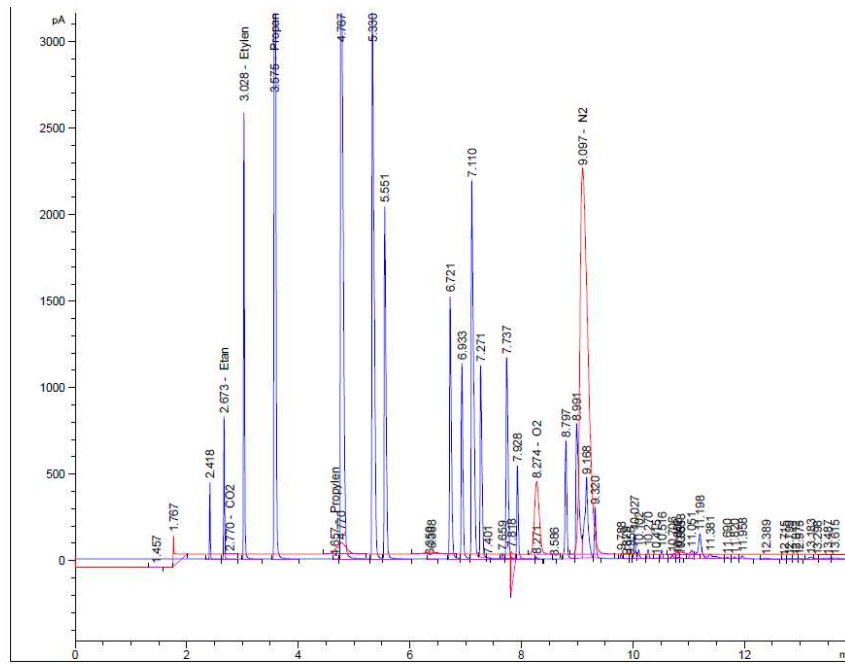


Figure D5: GC chromatogram of gas sample obtained from experiment N5

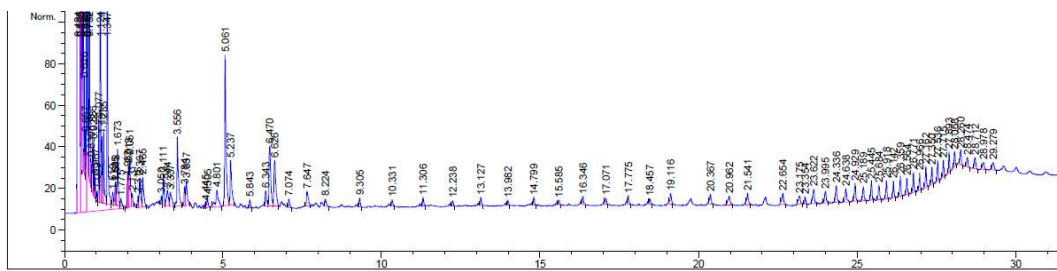


Figure D6: GC chromatogram of liquid sample obtained from experiment N6

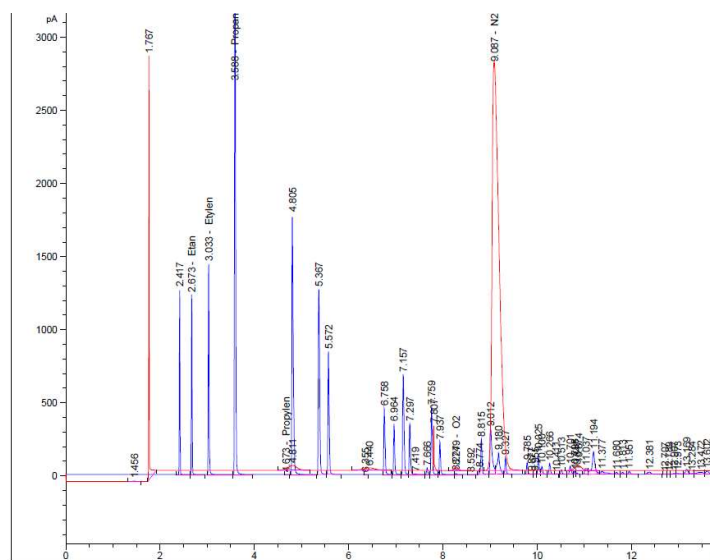


Figure D7: GC chromatogram of gas sample obtained from experiment N6

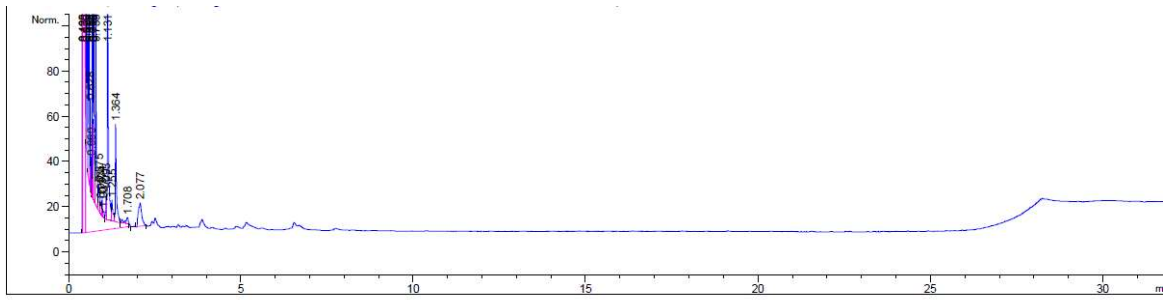


Figure D8: GC chromatogram of liquid sample obtained from N7

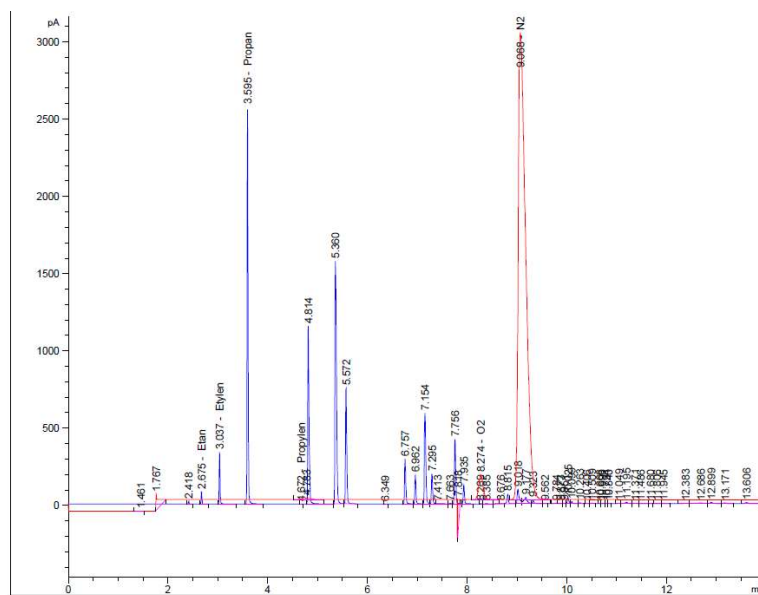


Figure D9: GC chromatogram of gas sample obtained from experiment N7

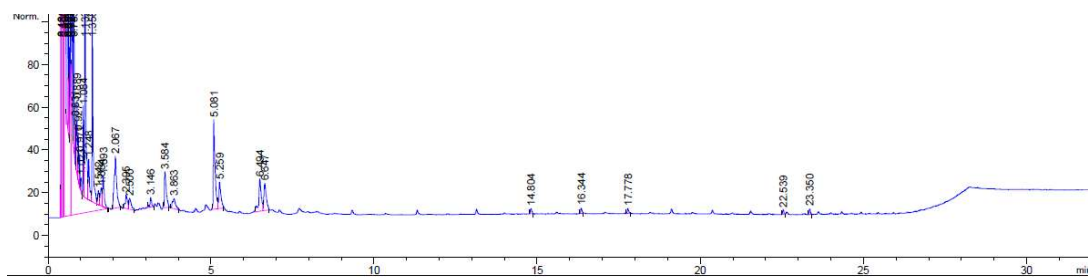


Figure D10: GC chromatogram of liquid sample obtained from experiment N8

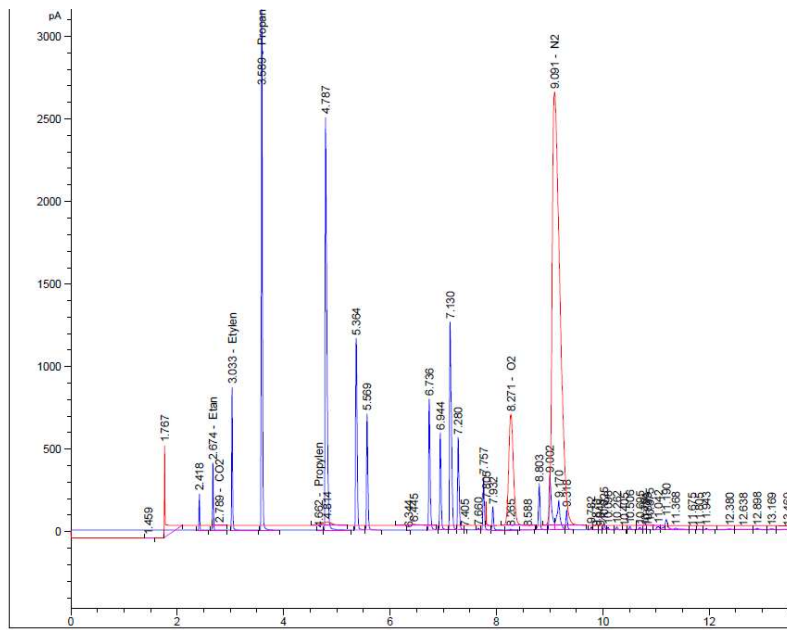


Figure D11: GC chromatogram of gas sample obtained from experiment N8

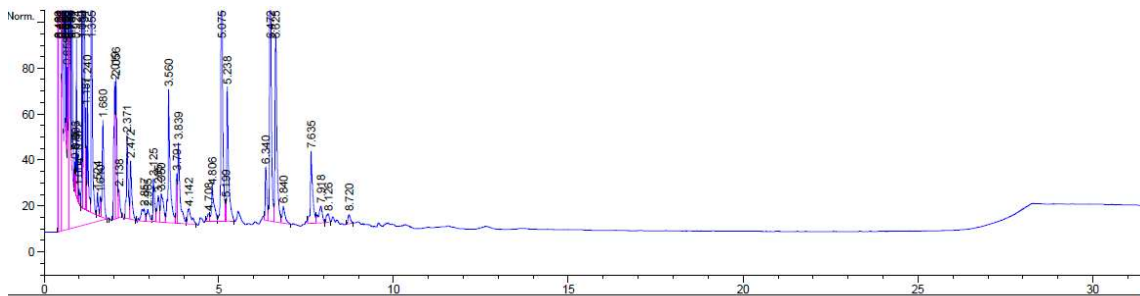


Figure D12: GC chromatogram of liquid sample obtained from experiment N9

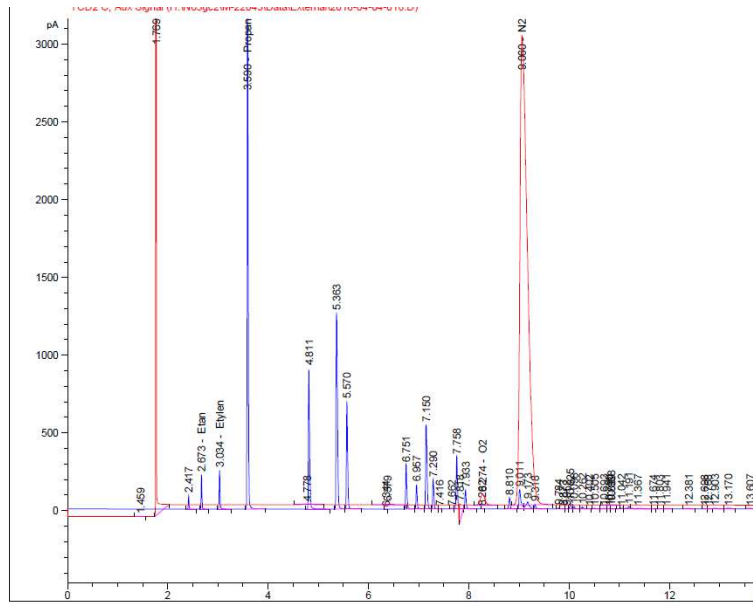


Figure D13: GC chromatogram of gas sample obtained from experiment N9

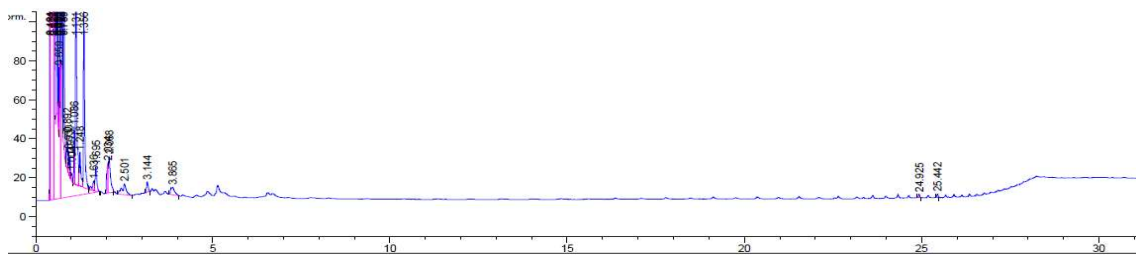


Figure D14: GC chromatogram of liquid sample obtained from experiment N10

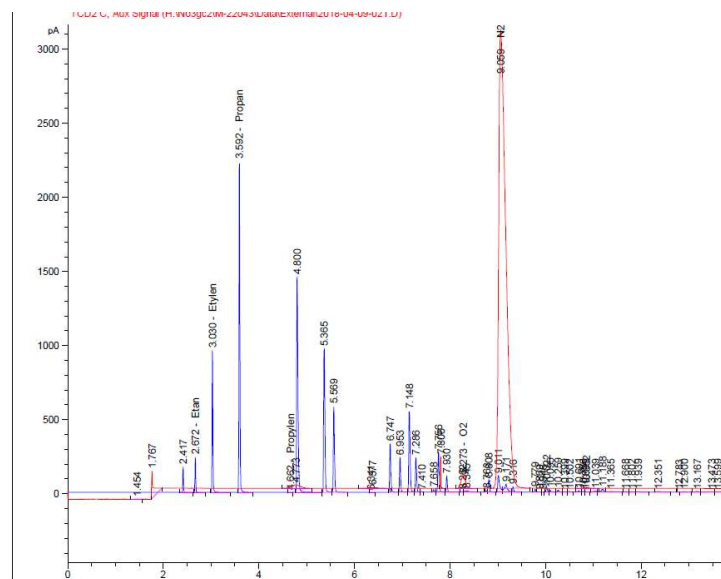


Figure D15: GC chromatogram of gas sample obtained from N10

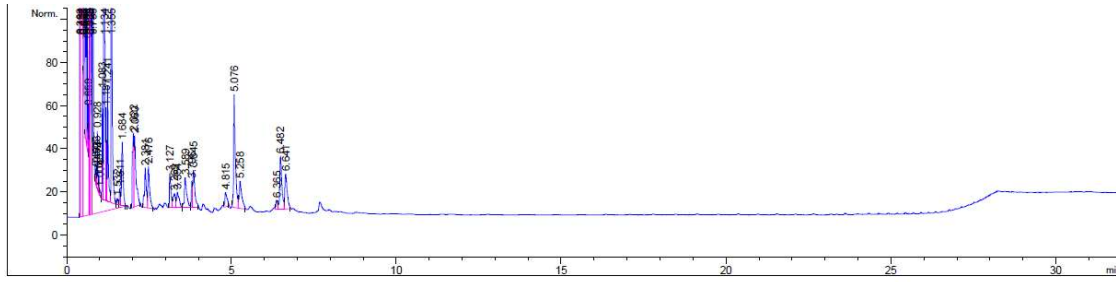


Figure D16: Chromatogram of liquid sample obtained from N11

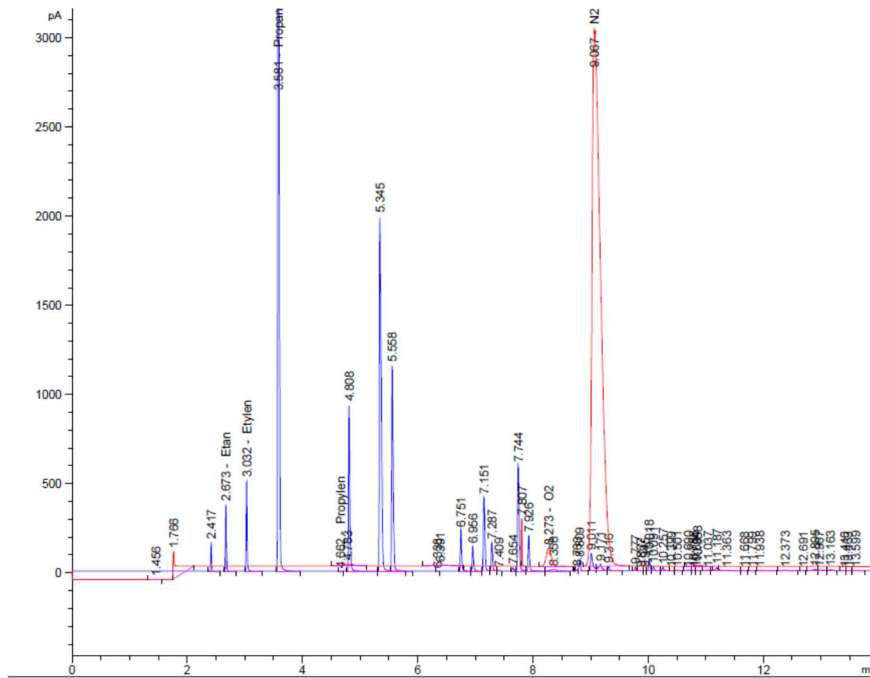


Figure D17: GC chromatogram of gas sample obtained from N11

Appendix F: FTIR spectrum of obtained liquid and wax products

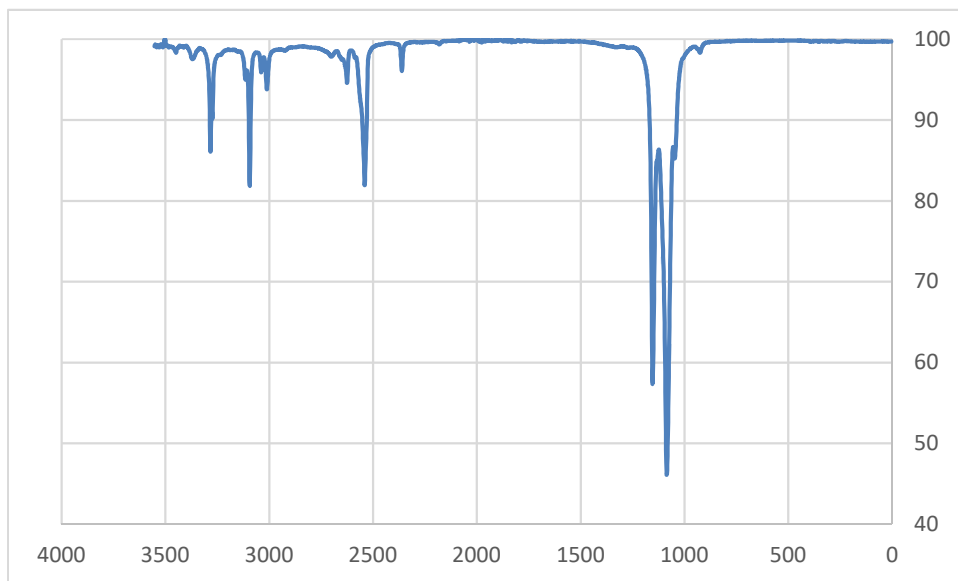


Figure F1: FTIR spectrum of obtained wax products after experiment N2

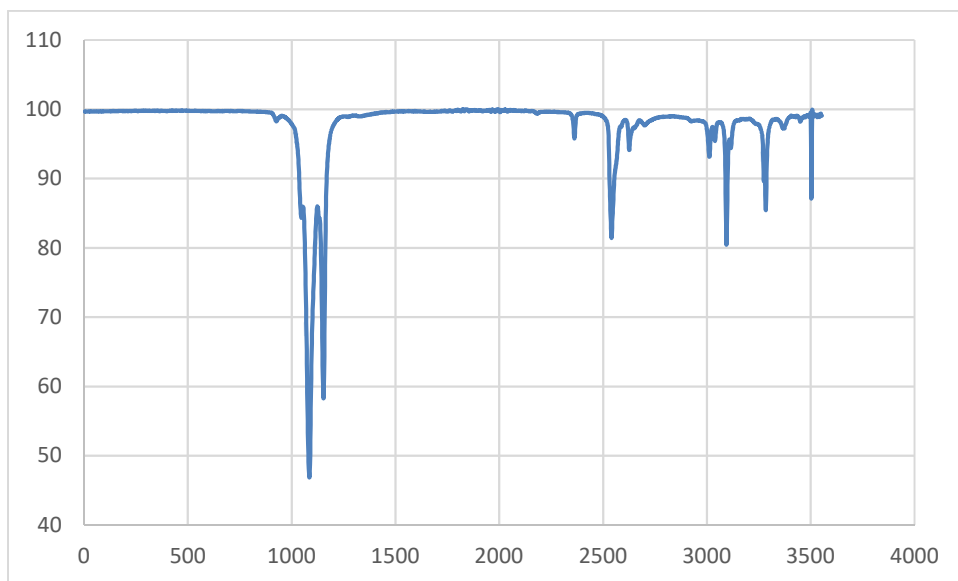


Figure F2: FTIR spectrum of obtained wax products after experiment N3

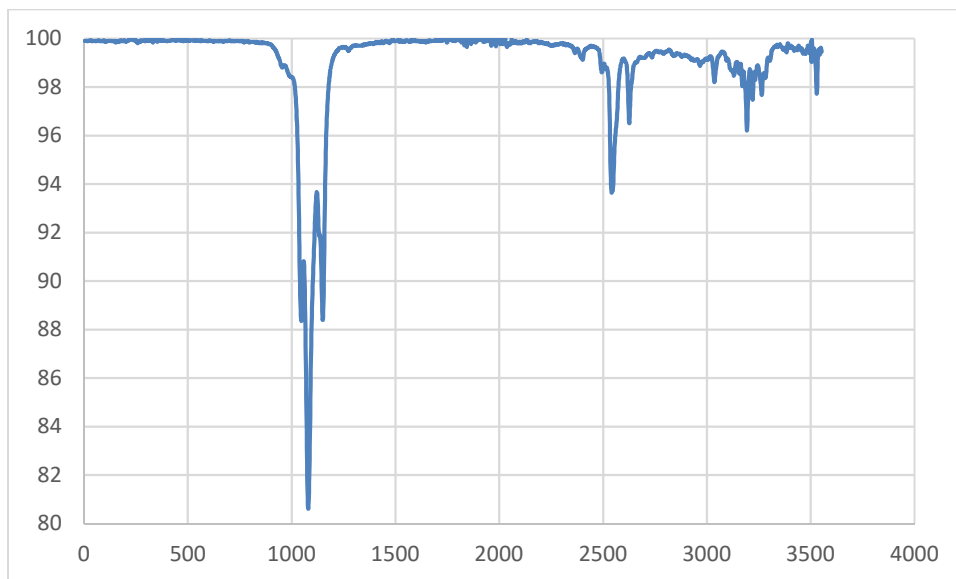


Figure F3: FTIR spectrum of obtained liquid products after experiment N4

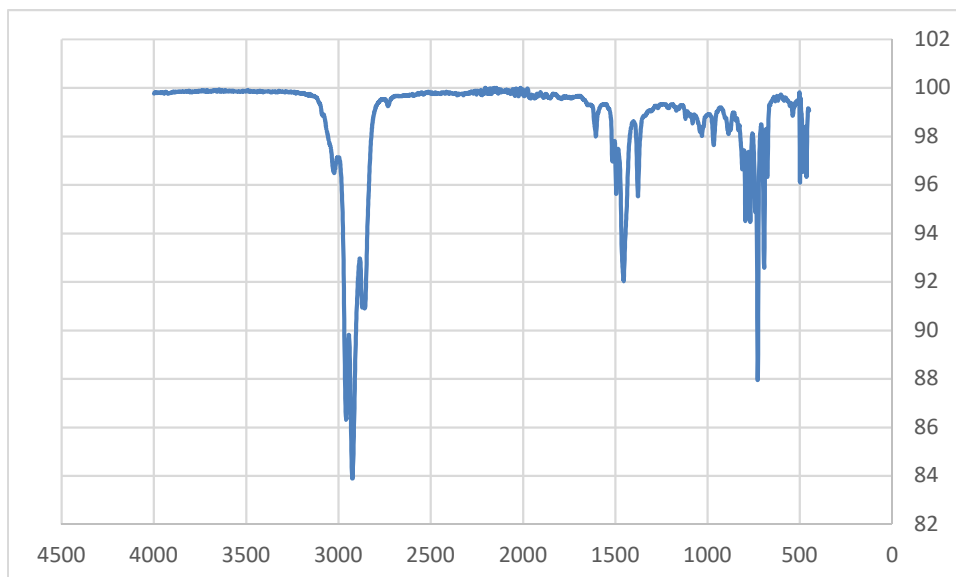


Figure F4: FTIR spectrum of obtained liquid products after experiment N7

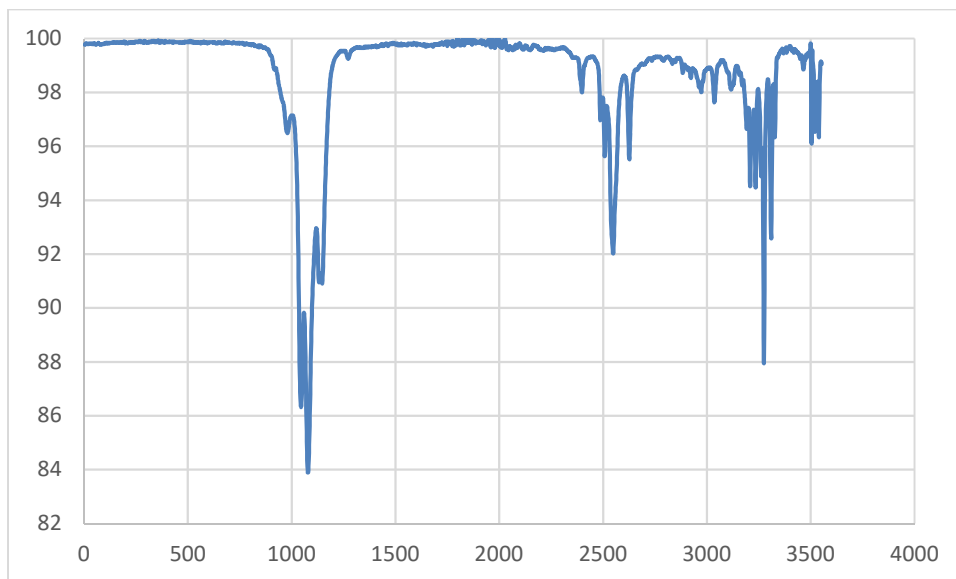


Figure F5: FTIR spectrum of obtained liquid products after experiment N8

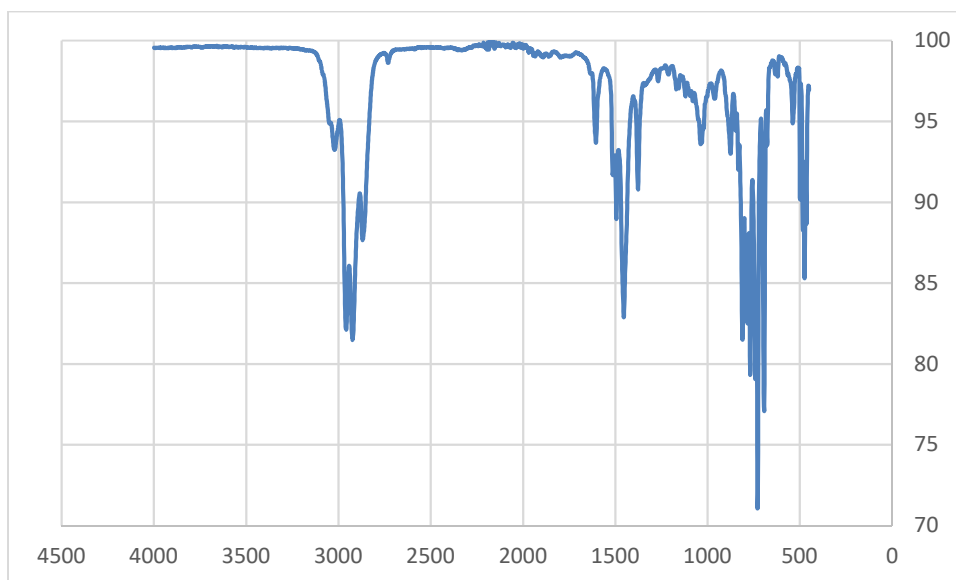


Figure F6: FTIR spectrum of obtained liquid products after experiment N9

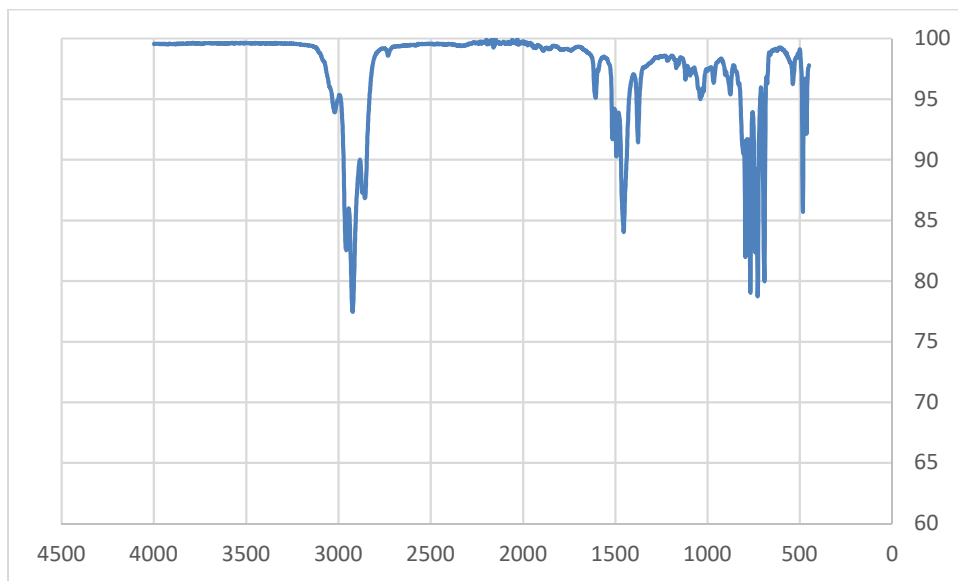


Figure F7: FTIR spectrum of obtained liquid products after experiment N10

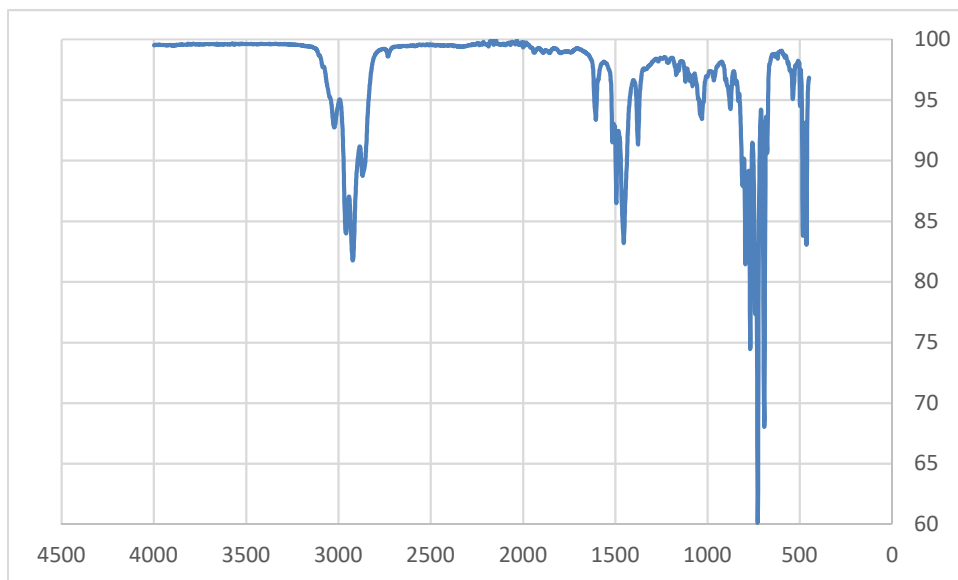


Figure F8: FTIR spectrum of obtained liquid products after experiment N11